1871
ИнБЮМ – IBSS

ISSN 2499-9768 print

МОРСКОЙ БИОЛОГИЧЕСКИЙ ЖУРНАЛ

MARINE BIOLOGICAL JOURNAL

Vol. 8 No. 3
2023

300 years
Russian Academy of Sciences

МОРСКОЙ БИОЛОГИЧЕСКИЙ ЖУРНАЛ
MARINE BIOLOGICAL JOURNAL
Выпуск посвящён 300-летию Российской академии наук.
Журнал включён в перечень рецензируемых научных изданий, рекомендованных ВАК Российской Федерации, а также в базу данных Russian Science Citation Index (RSCI).
Журнал реферируется международной библиографической и реферативной базой данных Scopus (Elsevier), международной информационной системой по водным наукам и рыболовству ASFA (ProQuest), Всероссийским институтом научно-технической информации (ВИНИТИ), а также Российским индексом научного цитирования (РИНЦ) на базе Научной электронной библиотеки elibrary.ru.
Все материалы проходят независимое двойное слепое рецензирование.

Адрес учредителя, издателя и редакции:
ФИЦ «Институт биологии южных морей имени А. О. Ковалевского РАН».
Пр-т Нахимова, 2, Севастополь, 299011, РФ.
Тел.: +7 8692 54-41-10. E-mail: *mbj@imbr-ras.ru*.
Сайт журнала: https://marine-biology.ru.
Адрес соиздателя:
Зоологический институт РАН.
Университетская наб., 1, Санкт-Петербург, 199034, РФ.

Founder, Publisher, and Editorial Office address:
A. O. Kovalevsky Institute of Biology of the Southern Seas of Russian Academy of Sciences.
2 Nakhimov ave., Sevastopol, 299011, Russia.
Tel.: +7 8692 54-41-10. E-mail: *mbj@imbr-ras.ru*.
Journal website: https://marine-biology.ru.
Co-publisher address:
Zoological Institute Russian Academy of Sciences.
1 Universitetskaya emb., Saint Petersburg, 199034, Russia.

A. O. KOVALEVSKY INSTITUTE OF BIOLOGY OF THE SOUTHERN SEAS OF RAS
ZOOLOGICAL INSTITUTE OF RAS

МОРСКОЙ БИОЛОГИЧЕСКИЙ ЖУРНАЛ

MARINE BIOLOGICAL JOURNAL

2023 Vol. 8 no. 3

Established in February 2016 SCIENTIFIC JOURNAL *4 issues per year*

CONTENTS

Scientific communications

Gorbunova S. Yu. and Chekushkin A. A.
Technology of cultivation of the marine microalga *Tetraselmis viridis* under natural light and at minimum technical cost 3–11

Egorov V. N., Mirzoyeva N. Yu., Artemov Yu. G., Proskurnin V. Yu., Stetsiuk A. P., Marchenko Yu. G., Evtushenko D. B., Moseichenko I. N., and Chuzhikova-Proskurnina O. D.
The possibility of implementation of the sustainable development concept for the recreational coastline of Yalta city regarding biogenic elements, radionuclides, heavy metals, and organochlorine compounds (Crimea, Black Sea) 12–32

Lebedeva D. I., Zaitsev D. O., Alekseeva Ja. I., and Makhrov A. A.
Metazoan parasites of two stickleback species at the Solovetsky Archipelago (White Sea) 33–46

Markina Zh. V. and Popik A. Yu.
Interactions of the diatom algae *Pseudo-nitzschia hasleana* and *Thalassiosira pseudonana* in the mixed culture 47–61

Prazukin A. V., Lee R. I., Balycheva D. S., Firsov Yu. K., and Kholodov V. V.
Cladophora (Chlorophyta) as an ecological engineer in hypersaline lake Chersonesskoye: Distribution of diatom algae in the structured space of plant mats 62–86

Chekalov V. P.
Relationship of the processes of aerobic oxidation and anaerobic destruction of organic matter in the bottom sediments of coastal waters of Crimea (Black Sea) 87–96

Aydemir-Çil E., Birinci-Özdemir Z., and Özdemir S.
First find of the starfish, *Asterias rubens* Linnaeus, 1758, off the Anatolian coast of the Black Sea (Sinop) 97–101

Notes

Kuznetsov A. V. and Bobko N. I.
Discoordination of *Hoilungia hongkongensis* (Placozoa) movements in the presence of Zn^{2+} ions 102–107

Sadogurskiy S. Ye., Belich T. V., and Sadogurskaya S. A.
Floristic finds in the coastal marine water area of the nature reserve “Cape Martyan” (Crimea, Black Sea) 108–110

Chronicle and information

In memoriam: Alexander Trapeznikov (29.01.1951 – 29.06.2023) 111–112

1871
ИнБЮМ – IBSS

Морской биологический журнал
Marine Biological Journal
2023, vol. 8, no. 3, pp. 3–11
https://marine-biology.ru

SCIENTIFIC COMMUNICATIONS

UDC 582.263:57.083.13

TECHNOLOGY OF CULTIVATION OF THE MARINE MICROALGA *TETRASELMIS VIRIDIS* UNDER NATURAL LIGHT AND AT MINIMUM TECHNICAL COST

© 2023 **S. Yu. Gorbunova[1] and A. A. Chekushkin**

[1] A. O. Kovalevsky Institute of Biology of the Southern Seas of RAS, Sevastopol, Russian Federation
E-mail: *svetlana_8423@mail.ru*

Received by the Editor 28.12.2020; after reviewing 23.03.2021;
accepted for publication 04.08.2023; published online 21.09.2023.

The main reason for slow implementation of scientific developments of marine algotechnology into industrial practice is the lack of systems that allow obtaining microalgae biomass in quantities that are necessary for practical study of potential products and development of industrial technology for their production. Such systems can significantly reduce the economic cost of creating and maintaining favorable abiotic conditions for growing microalgae on an industrial scale, since solar energy is used as a light source. The article proposes a method for growing marine microalgae *Tetraselmis viridis* in natural light and at minimum technical cost. The authors developed a mobile unit for cultivating marine microalgae and studying their growth characteristics in natural light. This unit is proposed to be used in the transition from laboratory cultivation to cultivation on an industrial scale. The basic requirements for the mobile unit for industrial cultivation of algologically pure *T. viridis* are specified. The technology ensuring the organization of *T. viridis* cultivation process with a maximum productivity of 5.7 $g \cdot m^{-2} \cdot day^{-1}$ and a maximum culture density of 271.6 billion $cells \cdot m^{-2}$ ($R^2 = 0.99$) has been developed. The authors provide a comparative assessment of the biochemical composition and kinetic growth characteristics of *T. viridis* depending on growing conditions using either the mobile unit in natural light or the laboratory photobioreactor in constant artificial light.

Keywords: marine microalgae, *Tetraselmis viridis*, batch culture, productivity, industrial cultivation

Intensive cultivation of microalgae in open water bodies is aimed mainly at obtaining biomass and using it as a food supplement [Benemann, 1992; Chaumont, 1993; Gudvilovich, Borovkov, 2012], as a source of raw materials in producing chemicals for their further use in the pharmaceutical industry [Demmig-Adams, Adams, 2002; Zhondareva, Trenkenshu, 2019], and for wastewater treatment [de la Noüe et al., 1992; Dobrojan, 2010; Markou, 2015]. The main reason for slow implementation of scientific developments of algotechnology into practice is the lack of industrial systems that allow obtaining microalgae biomass in quantities necessary for study of potential products and development of technologies for their production.

In most cases, the technology of microalgae mass cultivation involves the use of open systems in natural light, consisting of pools and ponds. Mostly, these are shallow film-lined pools; sometimes, these are cemented trenches, trays of various shape, or tanks. Such systems can significantly reduce

the economic cost of creating and maintaining favorable conditions for microalgae cultivation on an industrial scale, since solar energy is used as a light source. However, when using open systems, there is a danger of biomass contamination by bacteria and other invasive organisms. Moreover, it is reasonable to place production facilities in areas with few cloudy and rainy days and small diurnal temperature fluctuations. One of such areas is the south of Russia; this is due to favorable climatic conditions which allow growing microalgae using only solar energy continuously for two–three seasons during the year [Abdulagatov et al., 2018; Borovkov et al., 2020; Peel et al., 2007].

The objective of this work was to develop a low-cost version of mobile unit, the conditions in which are close to industrial conditions for growing marine microalgae on the example of *Tetraselmis viridis* (Rouchijajnen) R. E. Norris, Hori & Chihara, 1980, and to compare the biochemical composition and kinetic characteristics of algae growth when cultivated in laboratory conditions under constant artificial light and in the mobile unit under natural light.

MATERIAL AND METHODS

The green microalga *T. viridis*, strain IBSS-25 from IBSS collection, served as a study object. A nutrient medium was prepared based on non-sterile Black Sea water with a salinity of 1.4–1.8‰. The composition of the medium for *T. viridis* cultivation in dense culture was given earlier [Trenkenshu et al., 1981]. To preserve the algologically pure culture of the microalga, the salinity level in the medium was increased to the Mediterranean one by adding 15 g·L^{-1} NaCl [Gorbunova, Trenkenshu, 2020]. To obtain an inoculum, *T. viridis* was grown for 5 days in laboratory conditions by the batch method in 3-L photobioreactors under 10 klx illuminance on the Trenkenshu nutrient medium. The pool was filled with an actively dividing culture with an initial density of 0.08 g·L^{-1} of dry matter.

The unit for the microalga cultivation was placed on the pier of IBSS laboratory building from 26 August to 7 September, 2020. It was a pool 1 × 1 m in size and 0.1 m in height (Fig. 1). Since the unit was in the open air 24 h a day, it was necessary to maintain the temperature there within optimum for *T. viridis* cultivation. For this purpose, a cooling system was connected. A foam sheet was fixed throughout the perimeter of the pool bottom, with a polyurethane tube placed on it, through which seawater continuously circulated. The tube was covered with sand, and the pool bottom was lined with plastic film.

Fig. 1. The pool with a cooling system

Using a water pump Air Pump ACO-008, with a power of 120 W and a pressure of less than 0.032 MPa, water was supplied from the sea to the pier. The daytime temperature of the suspension in the pool was lower than the air temperature by 3–7 °C. Throughout the experiment, the daily temperature in the unit was maintained within the range of +23…+28 °C. Without a cooling system, the culture overheated and died within 36–48 h. To protect the pool from debris and possible precipitation, a sloping roof covered with plastic film was installed (Fig. 1); this ensured natural ventilation of the unit. The working volume of the pool was 70 L. To compensate for water evaporation, this volume was maintained throughout the experiment by adding distilled water before measurements to the level of 7 cm.

Continuous mixing of the microalga in the pool was carried out by the water pump, with a suspension pumping rate of 2,800 $L \cdot h^{-1}$, which ensured round-the-clock gas exchange of the culture and uniform cell illumination throughout the unit. On the pool surface, illumination was monitored twice a day with a Yu-116 luxmeter. *Prior* to the pool launch, the culture was kept under different light conditions: in the laboratory, the illumination was constant, and its intensity was more than 6 times lower than the natural maximum daily light. During the first three days, while the culture density was low, the pool roof was shaded with a net. Otherwise, under cloudless conditions, *T. viridis* cells became completely discolored. On average, during the experiment, the maximum daily illumination in the area of photosynthetically active radiation was 300 $W \cdot m^{-2}$; for calculations, the data presented in [Chekushkin et al., 2020] were used. The value of illumination is given taking into account the absorption of 25% of solar energy by the pool roof.

At the same time, *T. viridis* was grown in the laboratory photobioreactor under the same conditions as the pool inoculum. The optical density was calculated by the formula $D = -\lg(T)$, where T is the transmission value determined using Unico 2100 (United Products & Instruments, the USA) at a wavelength of 750 nm, in cuvettes with a working length of 0.5 cm. Absolute error did not exceed 1.0%.

For the convenience of comparing the obtained results with the data presented in the publication [Zhondareva, Trenkenshu, 2019], the optical density of the suspension layer (7 cm) was determined by multiplying the density values in the cuvette (0.5 cm) by 14.

When calculating optical density units (o. d. u.) in terms of the microalga dry weight (hereinafter DW), an empirically determined coefficient k was used, equal to 0.8 $g \cdot L^{-1} \cdot o.\,d.\,u.^{-1}$: $DW = k \times D_{750}$ [Borovkov, Gevorgiz, 2005]. The cell concentration was determined by direct counting in the Goryaev chamber under a microscope in eight replications. Microscopic control of the culture was carried our under a light microscope Carl Zeiss Axiostar Plus (Germany).

Pigments (chlorophyll *a*, chlorophyll *b*, and carotenoids) were extracted from the microalga cells with acetone (100%) [Kopytov et al., 2015]. The absorption spectra of acetone extracts were recorded in the range 400–800 nm in quartz cuvettes with a 1-cm optical path. The pigment composition was estimated from the absorption spectrum of acetone extract in three replications according to the standard method, using linear equations for three points in the absorption spectrum of the extract [Wellburn, 1994]. All calculations were performed for the significance level $a = 0.05$. Mathematical processing and modeling of the experimental data were carried out using computer programs Grapher 3, MS Excel, and MATLAB.

RESULTS AND DISCUSSION

The growth of *T. viridis* culture in the pool with constant illumination was monitored for 12 days. Linear growth of the culture was recorded from the 2nd to the 10th day of the experiment (Fig. 2A). During this time, the culture density increased by 7.5 times.

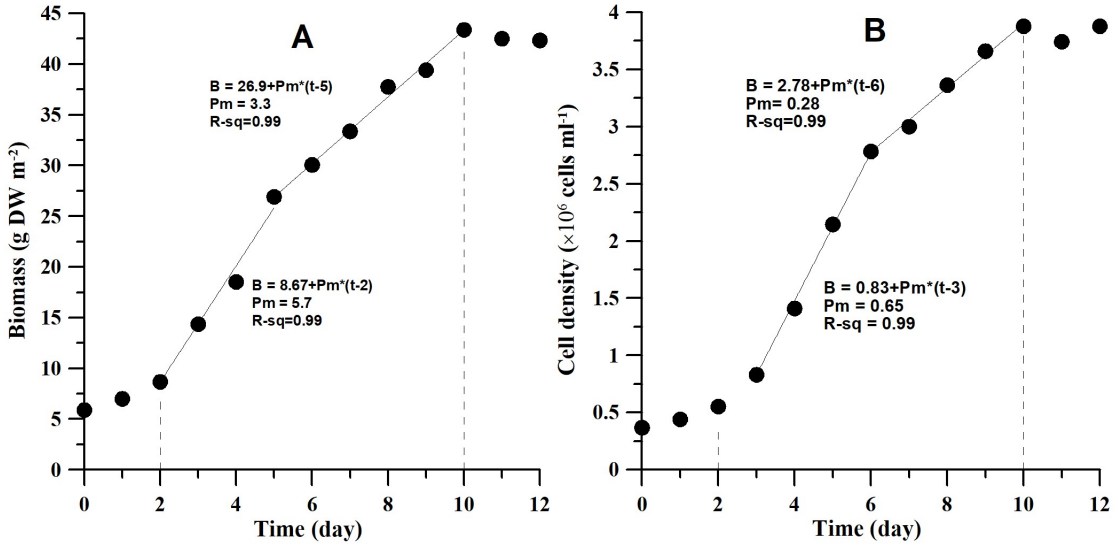

Fig. 2. Dynamics of *Tetraselmis viridis* density (A) and growth (B) in the pool under natural light

On the 5th day, the productivity of the culture by biomass (Pm) decreased from 5.7 to 3.3 g DW·m^{-2} (R^2 = 0.99). Apparently, this results from the beginning of limiting the microalga growth by carbon or light conditions, since in the linear plot, the growth rate is determined by the magnitude of the external flux (light or carbon dioxide), which is completely absorbed by the culture and limits its productivity [Trenkenshu, 2005]. On the 11th day, *T. viridis* growth stopped. The end of the linear growth phase indicates a change in the limiting factor [Lelekov, Trenkenshu, 2007], and both light and mineral medium conditions can limit the microalga growth. In our experiment, the mineral component cannot be a limiting factor, since the Trenkenshu nutrient medium, on which *T. viridis* was grown, is designed to achieve a culture density of 4–6 g DW *per* L [Trenkenshu et al., 1981]. Thus, we can assume that culture growth was limited by light conditions.

The obtained characteristics were compared with the results presented in [Zhondareva, Trenkenshu, 2019]. In that work, the linear growth phase of *T. viridis* was two times shorter than that according to our data and was recorded only from the 1st to the 5th day. Starting from the 6th day, the microalga growth stopped, while in our experiment, the linear growth phase was recorded from the 5th to the 10th day, on which the maximum productivity was 3.3 g DW·m^{-2}. Thus, we obtained the microalga yield of 43.4 g DW·m^{-2}, and this value is 2 times higher than in [Zhondareva, Trenkenshu, 2019]. This can be explained by providing optimal conditions for *T. viridis* cultivation: the presence of a cooling system, an increase in the salinity of the culture medium to the Mediterranean level, a 7-cm layer of the microalga in the pool, and an effective mixing system. A similar pattern was observed for the concentration dynamics of *T. viridis* cells in the culture (Fig. 2B).

As established, the linear growth of the culture occurs from the 3rd to the 10th day of the experiment, with a change in the curve slope on the 6th day, which confirms the theory about the beginning of the microalga growth limitation by carbon or light conditions. *T. viridis* productivity in the first part of the linear growth phase was 650 thousand cells·day^{-1}; in the second part (6th–10th days), the value was 280 thousand cells·day^{-1}. During the experiment, the cell concentration almost reached the value of 4 million cells·mL^{-1}. Fig. 3 shows the appearance of the pool at the beginning of the experiment and at the end (in 12 days).

Fig. 3. The pool with *Tetraselmis viridis* culture at the beginning of the experiment (left) and at the end (right)

As shown, with easy-to-use equipment and minimal capital investments, it is possible to organize *T. viridis* cultivation with a productivity of up to 5.7 g DW·m^{-2}·day^{-1}. When microalgae are grown in large volumes in natural light, productivity values are higher than theoretical maximum; also, the values may differ from those determined in laboratory conditions [Béchet et al., 2017; Bonnefond et al., 2016].

Data on the biochemical composition and kinetic characteristics of *T. viridis* grown in the laboratory photobioreactor under constant illumination and in a pool under natural light are given in Table 1.

Table 1. Biochemical composition and kinetic characteristics of the microalga *Tetraselmis viridis* growth (the end of the linear growth phase)

Parameter	*Tetraselmis viridis* in the laboratory photobioreactor	*Tetraselmis viridis* in the pool
Chlorophyll *a*, %	1.05 ± 0.05	1.01 ± 0.01
Chlorophyll *b*, %	0.58 ± 0.07	0.52 ± 0.01
Total carotenoids, %	0.23 ± 0.01	0.21 ± 0.004
Maximum density, g DW·L^{-1}	1.00 ± 0.05	0.62 ± 0.03
Maximum productivity, g DW·L^{-1}·day^{-1} (R^2 = 0.99)	0.122	0.08

In both cases, the culture was grown on the same nutrient medium and without additional carbon sources used. Sampling for the analysis was carried out at the same time. Fig. 4 shows the appearance of the laboratory photobioreactor at the beginning of the experiment and in 12 days.

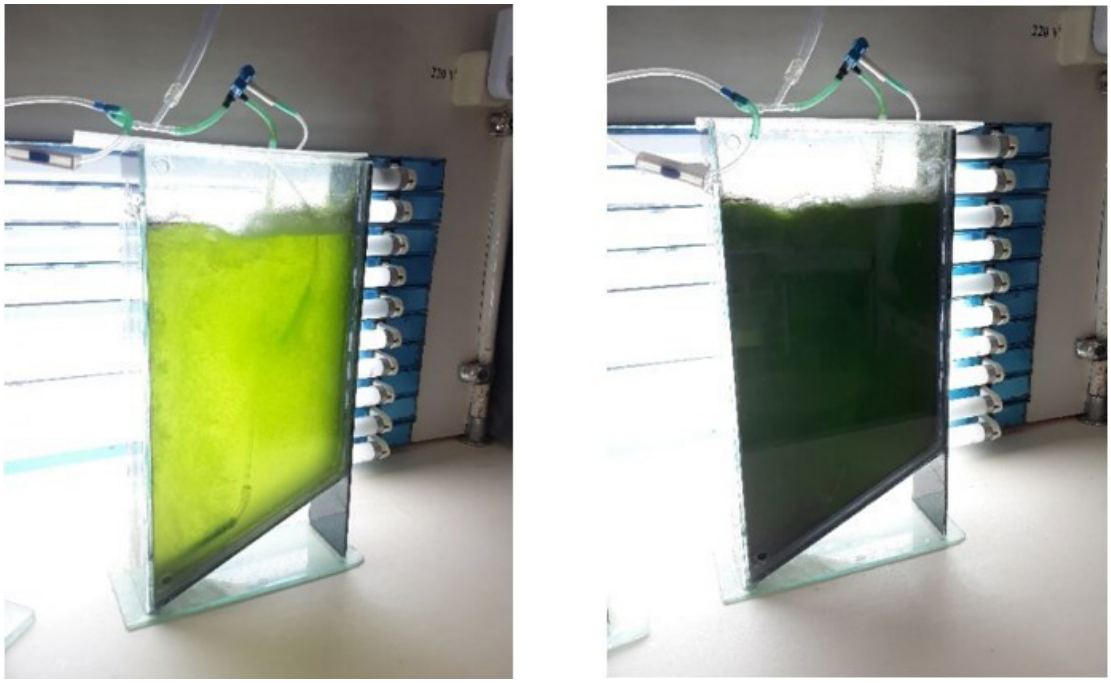

Fig. 4. Photo of the laboratory photobioreactor with the microalga *Tetraselmis viridis* at the beginning of the experiment (left) and after 12 days (right)

Models of native forms of chlorophyll *a*, chlorophyll *b*, and total carotenoids were used to assess the biological value of the obtained microalga and quickly calculate the concentrations of pigments in the culture [Chernyshev et al., 2020]. Our results on the chemical composition of *T. viridis* grown in laboratory conditions are in good agreement with the data of [Kharchuk, Beregovaya, 2019]. No significant differences in the microalga biochemical composition depending on the growing conditions were found. However, there was a trend towards a decrease in concentration of biochemical components in *T. viridis* cells when grown in the pool in natural light. This results from the shift in physicochemical parameters, the inability to maintain sterile conditions due to large volumes of pools, and diurnal changes in the illumination, accompanied by the reduction of some microalga biomass during the dark period [Avsiyan, 2018; Bonnefond et al., 2016; Xu et al., 2016].

Conclusion. A mobile unit for marine microalgae cultivation was developed. Microalgae growth characteristics in natural light were studied. This unit is proposed to be used in the transition from laboratory scales of marine microalgae cultivation to industrial ones. It was experimentally shown that the minimization of capital investments is ensured by the presence of easy-to-use equipment, the use of a cooling system, an increase in the salinity of the culture medium to the Mediterranean level, the choice of the optimal layer of the microalga in the pool, the absence of additional carbon sources, the use of an efficient mixing system, and the use of solar energy as a light source. The proposed approach allows *Tetraselmis viridis* cultivating with a maximum productivity of 5.7 $g \cdot m^{-2} \cdot day^{-1}$ and a culture density of 271.6 billion $cells \cdot m^{-2}$. Comparative assessment revealed no differences between biochemical and kinetic characteristics of *T. viridis* growth when cultivated in the mobile unit under natural light and in the laboratory photobioreactor under constant artificial light.

This work was carried out within the framework of IBSS state research assignment "Investigation of mechanisms of controlling production processes in biotechnological complexes with the aim of developing scientific foundations for production of biologically active substances and technical products of marine genesis" (No. 121030300149-0).

REFERENCES

1. Abdulagatov I. M., Alkhasov A. B., Dogeev G. D., Tumalaev N. R., Aliev R. M., Badavov G. B., Aliev A. M., Salikhova A. S. Technological application of microalgae in power industry and environmental protection. *Yug Rossii: ekologiya, razvitie*, 2018, vol. 1, no. 13, pp. 166–183. (in Russ.). https://doi.org/10.18470/1992-1098-2018-1-166-183
2. Avsiyan A. L. Influence of diurnal light regimen on *Arthrospira platensis* Gomont culture productivity. *Voprosy sovremennoi algologii*, 2018, no. 3 (18). (in Russ.). http://algology.ru/1374
3. Borovkov A. B., Gevorgiz R. G. Production of *Spirulina platensis* and *Tetraselmis viridis* by different methods of cultivation. *Ekologiya morya*, 2005, iss. 70, pp. 9–13. (in Russ.). https://repository.marine-research.ru/handle/299011/4698
4. Gorbunova S. Yu., Trenkenshu R. P. Experiment on obtaining an algologically pure culture of *Tetraselmis viridis* in non-sterile conditions. *Voprosy sovremennoi algologii*, 2020, no. 1 (22), pp. 94–100. (in Russ.). https://doi.org/10.33624/2311-0147-2020-1(22)-94-100
5. Gudvilovich I. N., Borovkov A. B. Biological value of BAS on the base of *Spirulina* supplements. *Byulleten' Gosudarstvennogo Nikitskogo botanicheskogo sada*, 2012, iss. 105, pp. 130–133. (in Russ.)
6. Zhondareva Ya. D., Trenkenshu R. P. Growth of *Tetraselmis viridis* (Rouchijajnen) R. E. Norris, Hori & Chihara, 1980 in the greenhouse pool under natural light and aeration. *Voprosy sovremennoi algologii*, 2019, no. 3 (21), pp. 76–87. (in Russ.). https://doi.org/10.33624/2311-0147-2019-3(21)-76-87
7. Kopytov Yu. P., Lelekov A. S., Gevorgiz R. G., Nekhoroshev M. V., Novikova T. M. Method of complex analysis of biochemical composition of microalgae. *Al'gologiya*, 2015, vol. 25, no. 1, pp. 35–40. (in Russ.). https://doi.org/10.1615/InterJAlgae.v17.i4.70
8. Lelekov A. S., Trenkenshu R. P. Simplest models of microalgae growth. 4. Exponential and linear growth phases of microalgae culture. *Ekologiya morya*, 2007, iss. 74, pp. 47–49. (in Russ.). https://repository.marine-research.ru/handle/299011/4780
9. Trenkenshu R. P., Terskov I. A., Sidko F. Ya. Plotnye kul'tury morskikh mikrovodoroslei. *Izvestiya Sibirskogo otdeleniya Akademii nauk SSSR. Seriya biologicheskikh nauk*, 1981, no. 15, iss. 3, pp. 75–82. (in Russ.)
10. Trenkenshu R. P. Simplest models of microalgae growth. 1. Batch culture. *Ekologiya morya*, 2005, iss. 67, pp. 89–97. (in Russ.). https://repository.marine-research.ru/handle/299011/4658
11. Kharchuk I. A., Beregovaya N. M. The content of biochemical components in the marine microalgae *Tetraselmis viridis* during long-term storage in a state of cold hibernation. *Voprosy sovremennoi algologii*, 2019, no. 1 (19), pp. 88–95. (in Russ.). https://doi.org/10.33624/2311-0147-2019-1(19)-88-95
12. Chekushkin A. A., Lelekov A. S., Gevorgiz R. G. Seasonal dynamics of limit productivity in a horizontal photobioreactor. *Aktual'nye voprosy biologicheskoi fiziki i khimii*, 2020, vol. 5, no. 3, pp. 405–411. (in Russ.)
13. Chernyshev D. N., Gorbunova S. Yu., Trenkenshu R. P. Decomposition of cultural absorption spectra and the acetone extract of microalgae *Tetraselmis viridis* into spectrum of individual pigments. *Aktual'nye voprosy biologicheskoi fiziki i khimii*, 2020, vol. 5, no. 2, pp. 232–238. (in Russ.)
14. Béchet Q., Moussion P., Bernard O. Calibration of a productivity model for the microalgae *Dunaliella salina* accounting for light and temperature. *Algal Research*, 2017, vol. 21, pp. 156–160. https://doi.org/10.1016/j.algal.2016.11.001
15. Benemann J. R. Microalgae aquaculture feeds. *Journal of Applied Phycology*, 1992, vol. 4, iss. 3, pp. 233–245. https://doi.org/10.1007/BF02161209
16. Bonnefond H., Moelants N., Talec A., Bernard O., Sciandra A. Concomitant effects of light

and temperature diel variations on the growth rate and lipid production of *Dunaliella salina*. *Algal Research*, 2016, vol. 14, pp. 72–78. https://doi.org/10.1016/j.algal.2015.12.018
17. Borovkov A. B., Gudvilovich I. N., Avsiyan A. L. Scale-up of *Dunaliella salina* cultivation: From strain selection to open ponds. *Journal of Applied Phycology*, 2020, vol. 32, iss. 3, pp. 1545–1558. https://doi.org/10.1007/s10811-020-02104-5
18. Chaumont D. Biotechnology of algal biomass production: A review of systems for outdoor mass culture. *Journal of Applied Phycology*, 1993, vol. 5, iss. 6, pp. 593–604. https://doi.org/10.1007/BF02184638
19. de la Noüe J., Laliberté G., Proulx D. Algae and waste water. *Journal of Applied Phycology*, 1992, vol. 4, iss. 3, pp. 247–254. https://doi.org/10.1007/BF02161210
20. Demmig-Adams B., Adams W. Antioxidants in photosynthesis and human nutrition. *Science*, 2002, vol. 298, no. 5601, pp. 2149–2153. https://doi.org/10.1126/science.1078002
21. Dobrojan S. Obţinerea substanţelor biologic active din biomasa microalgei *Spirulina platensis* (Nordst.) Geitl crescută pe ape reziduale. *Mediul Ambiant [Scientific Journal of Information and Ecological Culture]*, 2010, no. 2 (50), pp. 24–28. (in Moldavian).
22. Markou G. Fed-batch cultivation of *Arthrospira* and *Chlorella* in ammonia-rich wastewater: Optimization of nutrient removal and biomass production. *Bioresource Technology*, 2015, vol. 193, pp. 35–41. https://doi.org/10.1016/j.biortech.2015.06.071
23. Peel M. C., Finlayson B., McMahon T. A. Updated world map of the Köppen–Geiger climate classification. *Hydrology and Earth System Sciences*, 2007, vol. 11, iss. 5, pp. 1633–1644. https://doi.org/10.5194/hess-11-1633-2007
24. Wellburn R. W. The spectral determination of chlorophylls *a* and *b*, as well as total carotenoids, using various solvents with spectrophotometers of different resolution. *Journal of Plant Physiology*, 1994, vol. 144, iss. 3, pp. 307–313. http://dx.doi.org/10.1016/S0176-1617(11)81192-2
25. Xu Y., Ibrahim I. M., Harvey P. J. The influence of photoperiod and light intensity on the growth and photosynthesis of *Dunaliella salina* (Chlorophyta) CCAP 19/30. *Plant Physiology and Biochemistry*, 2016, vol. 106, pp. 305–315. https://doi.org/10.1016/j.plaphy.2016.05.021

ТЕХНОЛОГИЯ ВЫРАЩИВАНИЯ МОРСКОЙ МИКРОВОДОРОСЛИ *TETRASELMIS VIRIDIS* ПРИ ЕСТЕСТВЕННОМ ОСВЕЩЕНИИ И МИНИМАЛЬНЫХ ТЕХНИЧЕСКИХ ЗАТРАТАХ

С. Ю. Горбунова[1], А. А. Чекушкин

[1]ФГБУН ФИЦ «Институт биологии южных морей имени А. О. Ковалевского РАН»,
Севастополь, Российская Федерация
E-mail: *svetlana_8423@mail.ru*

Главной причиной медленного внедрения научных разработок морской альготехнологии в промышленную практику является отсутствие систем, позволяющих получать биомассу микроводорослей в количествах, которые необходимы для исследования потенциальных продуктов и для отработки промышленной технологии их производства. Такие системы позволяют значительно снизить экономические затраты на создание и поддержание благоприятных абиотических условий для выращивания микроводорослей в промышленных масштабах, поскольку в качестве источника освещения используется энергия солнца. В статье предложен способ

выращивания морской микроводоросли *Tetraselmis viridis* при естественном освещении и минимальных технических затратах. Авторами разработана мобильная установка для культивирования морских микроводорослей и для исследования их ростовых характеристик в условиях естественного освещения. Данную установку предлагается использовать при переходе от лабораторных масштабов культивирования микроводорослей к промышленным. Приведены основные требования, которым должна удовлетворять мобильная установка, и обоснование её конструкции для промышленного выращивания альгологически чистой культуры *T. viridis*. Разработана технология, позволяющая обеспечить организацию процесса культивирования *T. viridis* с максимальной производительностью культуры 5,7 г·м$^{-2}$·сут$^{-1}$ и плотностью 271,6 млрд кл.·м$^{-2}$ (R^2 = 0,99). Дана сравнительная оценка биохимического состава и кинетических характеристик роста *T. viridis* при выращивании в мобильной установке в условиях естественного освещения и в лабораторных культиваторах при постоянном искусственном освещении.

Ключевые слова: микроводоросли, *Tetraselmis viridis*, накопительная культура, продуктивность, промышленное культивирование

1871
ИнБЮМ – IBSS

Морской биологический журнал
Marine Biological Journal
2023, vol. 8, no. 3, pp. 12–32
https://marine-biology.ru

UDC [502.1:556.545](292.471-75)

THE POSSIBILITY OF IMPLEMENTATION OF THE SUSTAINABLE DEVELOPMENT CONCEPT FOR THE RECREATIONAL COASTLINE OF YALTA CITY REGARDING BIOGENIC ELEMENTS, RADIONUCLIDES, HEAVY METALS, AND ORGANOCHLORINE COMPOUNDS (CRIMEA, BLACK SEA)

© 2023 **V. N. Egorov, N. Yu. Mirzoyeva, Yu. G. Artemov, V. Yu. Proskurnin, A. P. Stetsiuk, Yu. G. Marchenko, D. B. Evtushenko, I. N. Moseichenko, and O. D. Chuzhikova-Proskurnina**

A. O. Kovalevsky Institute of Biology of the Southern Seas of RAS, Sevastopol, Russian Federation
E-mail: *egorov.ibss@yandex.ru*

Received by the Editor 10.05.2023; after reviewing 10.05.2023;
accepted for publication 04.08.2023; published online 21.09.2023.

In the Yalta city water area (Crimea, Black Sea), hydroacoustic sounding was carried out, and area and volume of waters of the Vodopadnaya River estuarine zone were determined down to a depth of 40 m. Concentration of biogenic elements (NO_2, NO_3, NH_4, and PO_4) and heavy metals (Cu, Zn, Fe, Co, Ni, Mo, Cd, Pb, and Hg) in freshwater of the river estuary exceeds their content in coastal seawater by 3–64 times. The effect of the river discharge on seawater eutrophication was assessed. Using post-Chernobyl radioisotopes ^{90}Sr and ^{137}Cs, bottom sediments dating was carried out, and the sedimentation rate in the studied water area was determined. Fluxes of pollutants with the Vodopadnaya River runoff and the periods of their turnover in the Yalta city recreational coastline were calculated. The obtained results were used to substantiate the sustainable development concept for the Yalta city recreational zone in terms of the factors of pollution of its marine environment.

Keywords: Black Sea, Crimea, water, biogenic elements, strontium-90, cesium-137, heavy metals, organochlorine compounds, bottom sediments dating

The water area of Yalta city (Crimea) is one of the critical zones of the Black Sea [Zaitsev, Polikarpov, 2002], where pollutant content in the marine environment can exceed natural levels or reach maximum permissible concentrations (hereinafter MPC) for the population and biotic components of ecosystems. The main coastal recreational area of the city, located in the southwestern Yalta Bay, is affected by the seaport, by recreational, touristic, municipal, and agricultural activities on the coast, and by the Vodopadnaya River (Uchan-su), with its flood flow regime. The river originates at the foot of Ai-Petri peak. The river length is 7.0 km; the catchment area is 28.9 km^2; and the slope is 94.3 $m \cdot km^{-1}$. There are certain environmental problems in this area, and the most significant ones are hypereutrophication caused by nutrients [Egorov et al., 2021] and water contamination with heavy metals and organochlorine compounds [Egorov et al., 2018]. The need for minimizing negative consequences of anthropogenic load on the Yalta city recreational coastline requires the development and application of measures aimed at implementation of sustainable development.

The aim of these studies was to standardize maximum permissible fluxes of pollutants into the Yalta city recreational area (Crimea, Black Sea) in terms of biogeochemical criteria and to substantiate the sustainable development concept based on contamination factors for the marine environment of the area analyzed. Accordingly, the following tasks were solved:

- determination of biogenic element concentrations in water and assessment of the limitation of phytoplankton primary production in the Vodopadnaya River estuarine zone;
- bottom sediments dating in terms of the peaks of ^{90}Sr and ^{137}Cs radioactive fallout maximums on the sea surface and determination of sediment fluxes of pollutants into the thickness of the bottom sediments in the Yalta city recreational zone;
- assessment of contamination for freshwater of the river estuary and seawater of the city area with radionuclides and heavy metals, as well as determination, based on the results of our own observations, of biogeochemical characteristics of self-purification of the Yalta city recreational zone from ∑6PCB and ∑DDT according to data given in [Malakhova, Lobko, 2022] and from radionuclides and heavy metals.

MATERIAL AND METHODS

The Yalta city recreational zone is located on the southwestern coast of the Yalta Bay (Crimea, Black Sea) (Fig. 1). To the north, there are marina, berths for coasters serving tourist routes, and the seaport. From the east and the west, the recreational zone borders the open Black Sea area.

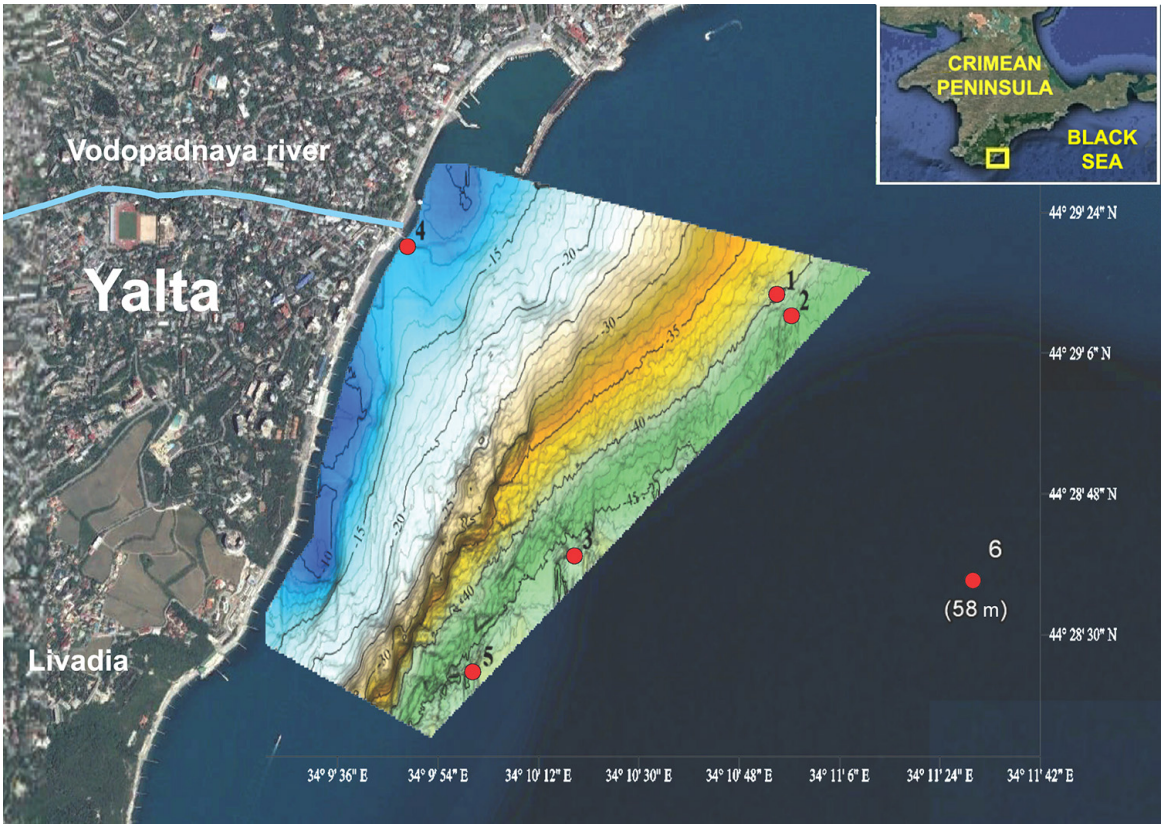

Fig. 1. Bathymetric map of the Yalta city water area and the Vodopadnaya River estuarine zone. Red circles denote the sampling stations. The coastline from the Vodopadnaya River estuary to Livadia settlement is occupied by a city beach, which is included in the Yalta city recreational zone

Methodology of oceanographic works. For hydroacoustic observations, we used boats equipped with Lowrance Elite-7 Ti chartplotter with a built-in GPS receiver. Water was sampled with a 10-L bathometer; sediments were sampled with a manual gravity corer. For geochronological analysis, sediment cores were sampled at stations 5 and 6. Sta. 6 was located outside the polygon, and its research material was used for comparative purposes. A bathymetric map of the Yalta city water area and the Vodopadnaya River estuarine zone is shown in Fig. 1. Sampling metadata are presented in Table 1.

Table 1. Dates, coordinates, and depths of water and sediment sampling stations in the Yalta Bay

Number of the sampling station	Date	Coordinates		Depth, m
		N	E	
1	19.07.2019	44°29.2234′	34°10.9130′	35
2	19.07.2019	44°29.1806′	34°10.9530′	37
3	19.07.2019	44°28.6701′	34°10.3051′	40
4	19.04.2017 28.06.2017 19.07.2019 22.06.2020	44°29.3294′	34°09.8040′	1
5	19.07.2019	44°28.4208′	34°10.0072′	41
6	15.10.2020	44°28.565′	34°11.512′	58

Concentrations of nitrites, nitrates, and ammonium in freshwater of the Vodopadnaya River estuary and in seawater of its estuarine zone were determined by the standard method [Rukovodstvo, 1977]. The absorption of biogenic elements during biosynthesis was established from the ratio [Hutchinson, 1969; Redfield, 1958]:

$$1P : 7N : 40C\,, \tag{1}$$

from which it followed that the absorption coefficient of phosphorus in relation to carbon is 0.025, and the absorption coefficient of nitrogen is 0.175. The degree of limitation of phytoplankton production by biogenic elements was assessed from the stoichiometric ratio N : P = 16 : 1 by molar concentration or 7 : 1 by weight concentration. To determine the biogenic factor limiting production processes, the Redfield stoichiometry (PR_{at}) was used. This ratio, with the dimensions of its parameters expressed in $\mu g \cdot L^{-1}$, had the form as follows [Redfield, 1958]:

$$PR_{at}(N/P) = 1.53(1.35NO_2 + NO_3 + 3.44NH_4)/PO_4\,. \tag{2}$$

At $PR_{at} > 16$, phosphorus is a limiting nutrient; at $PR_{at} < 16$, nitrogen.

For geochronological studies, the bottom sediment cores were sampled using a manual gravity corer (inner diameter of 58 mm) with a vacuum seal. The resulting cores were cut into layers 1 cm thick with a screw extruder described in [Papucci, 1997]. Immediately after cutting, the samples were weighed, dried at a temperature of +40…+50 °C, and then weighed again to determine the amount of evaporated water. To estimate the initial moisture content of the bottom sediments, the concentration of salts dissolved in pore water was calculated [Schafer et al., 1980]. Artificial radionuclides ^{90}Sr and ^{137}Cs were used as radioactive tracers for bottom sediments dating [Gulin et al., 1994; Mirzoeva et al., 2005; Radioekologicheskii otklik, 2008]. Concentrations of ^{90}Sr and ^{137}Cs were determined separately for each layer of the bottom sediment cores.

^{90}Sr activity was measured by the Cherenkov radiation of its daughter product ^{90}Y with a low background liquid scintillation counter (LSC) LKB Quantulus 1220 [Harvey et al., 1989; Radioekologicheskii otklik, 2008]. The lower limit of detection (LLD) is 0.01–0.04 Bq·kg^{-1} or Bq·m^{-3} of the sample. The relative error of the obtained results did not exceed 20%. The results were subjected to mathematical processing of radiospectrometric data [Radioekologicheskii otklik, 2008]. The correctness of the methodology used and the reliability of the results obtained were controlled *via* constant participation in international intercalibration under the auspices of the IAEA (Vienna, Austria) and the National Laboratory (Risø, Denmark). The data on the intercalibration of the determination techniques obtained from the measurement results for reference samples and field parallel determinations between IBSS and other institutes indicated as follows. The used methodological base made it possible to assess, with the necessary and sufficient degree of reliability, the contamination of the studied ecosystems with the long-lived radionuclide ^{90}Sr [Radioekologicheskii otklik, 2008]. In dried samples, ^{137}Cs content was determined using a NaI(Tl) scintillation detector. It was calibrated with standard samples of bottom sediments IAEA-306 and IAEA-315 supplied by the IAEA [Radioekologicheskii otklik, 2008]; their shape and dimensions were similar to those of the bottom sediment samples studied by us. The mean relative error in the samples did not exceed 27%.

Heavy metals (hereinafter HM) were isolated from seawater by extraction/preconcentration in accordance with the guidance document 52.10.243-92 [1993]. This technique is based on the extraction of the complexes of the elements to be determined with carbon tetrachloride using sodium diethyldithiocarbamate (NaDDC); it is followed by the destruction of the complexes with concentrated nitric acid and the re-extraction of the elements into an aqueous solution of a smaller volume. In this case, the quantitative extraction is achieved for Fe, Co, Ni, Cu, Zn, Mo, Cd, and Pb [Mirzoeva et al., 2022]. HM extraction from samples of the bottom sediments was carried out in accordance with environmental regulatory document 16.2.2:2.3.71-2011 [2011]. This technique is based on the acid mineralization of sediment dry matter and leaching of the elements to be determined into the solution.

In extracts from seawater and mineralizates of the bottom sediments, HM were determined in IBSS core facility "Spectrometry and Chromatography" by inductively coupled plasma mass spectrometry on a PlasmaQuant MS Elite mass spectrometer (Analytik Jena AG, Germany) according to the international technical standard 56219-2014 [2015] and the operating manual [PlasmaQuant MS, 2014]. For the elements to be determined, the machine was calibrated with a multi-element standard solution IV-28 (Inorganic Ventures, the USA). The error of HM determination in the water samples and the bottom sediments for all elements did not exceed 10% at their concentration in water > 0.01 μg·L^{-1} and in bottom sediments > 0.1 mg·kg^{-1}. At lower content, the error reached 60%.

Water and bottom sediments to determine mercury content were sampled simultaneously. To separate dissolved and particulate mercury, seawater was fixed immediately after sampling with concentrated nitric acid (10 mL HNO_3 *per* 1 L of water). Then, in the laboratory, those were filtered through pre-weighed nuclepore filters with a pore diameter of 0.45 μm. Mercury concentration in suspended matter samples was determined in accordance with the international technical standard 26927-86 [2002]. The measurements were carried out by atomic absorption spectrophotometry using a Hiranuma-1 mercury analyzer. To calibrate it and to control the quality of the analysis, certified mercury standard samples were used. The measurement error did not exceed 2%.

The mean sedimentation rate was calculated using the following formula [Gulin et al., 1994]:

$$S = h/(T_0 - T)\,, \tag{3}$$

where S is the mean sedimentation rate, cm·year^{-1};

T is the absolute age of the layer, years;

T_0 is the year of sampling;

h is the mean layer depth, cm.

The age of bottom sediment layers in the cores was determined by the formula [Gulin et al., 1997]:

$$T = T_0 - h/S\,, \tag{4}$$

where T (the age of the layer) is the year of accumulation of the bottom sediment layer;

T_0 is the year of sampling;

h is the mean depth of the bottom sediment layer, cm;

S is the mean sedimentation rate, cm·year^{-1}.

The method for determining the sedimentation rate in weight units (g·m^{-2}·year^{-1}) is described in [Gulin et al., 1994]. Theoretical analysis of the results of observations was carried out based on modern ideas about the radioisotopic and chemical homeostasis of marine ecosystems [Egorov et al., 2021].

RESULTS

Echo sounding data were processed with WaveLens program [Artemov, 2006]. According to these data, the area (S) of the Yalta water area in the Vodopadnaya River estuarine zone down to a depth of 40 m (Fig. 1) is 2.82 km^2, and water volume (V) is 0.08 km^3. As *per* regular measurements of the Yalta stream gauging station, the mean river flow at its estuary (V_r) is 0.384 m^3·s^{-1}, or 12.11×10^6 m^3·year^{-1}.

Bottom sediments dating. Primary data on bottom sediments dating are presented in Tables 2 and 3.

Table 2. ^{90}Sr and ^{137}Cs activity concentration in different layers of the bottom sediment core at station 5

Bottom sediment layer, cm	Layer weight, g		^{90}Sr concentration, Bq·kg^{-1} dry weight		^{137}Cs concentration, Bq·kg^{-1} dry weight	
	wet	dry	^{90}Sr	±	^{137}Cs	±
0–1	46.0	30.5	b. d.	b. d.	26.6	3.0
1–2	56.5	41.0	b. d.	b. d.	14.6	1.5
2–3	42.5	32.0	b. d.	b. d.	15.6	2.2
3–4	22.0	16.5	b. d.	b. d.	0	0
4–5	62.0	52.5	b. d.	b. d.	0	0
5–6	27.0	18.5	1.91	0.52	0	0
6–7	33.5	23.0	5.99	0.87	26.0	4.0
7–8	36.0	25.0	b. d.	b. d.	0	0
8–9	45.0	31.5	2.19	0.51	0	0
9–10	44.5	31.0	1.97	0.43	0	0
10–11	45.5	31.0	b. d.	b. d.	19.3	3.1

Continue on the next page…

Bottom sediment layer, cm	Layer weight, g		^{90}Sr concentration, Bq·kg^{-1} dry weight		^{137}Cs concentration, Bq·kg^{-1} dry weight	
	wet	dry	^{90}Sr	±	^{137}Cs	±
11–12	45.5	29.5	5.18	0.64	17.2	1.9
12–13	35.0	22.0	4.6	1.0	0	0
13–14	39.0	23.0	b. d.	b. d.	0	0
14–15	39.0	22.5	3.13	0.87	13.5	3.3
15–16	38.0	22.0	7.86	1.26	31.8	2.5
16–17	41.5	24.5	13.17	1.41	22.7	1.8
17–18	43.0	27.5	10.67	1.48	12.1	0
18–19	42.5	28.5	6.7	0.95	0	0
19–20	55.5	37.5	b. d.	b. d.	17.5	1.7
21–22	44.5	29.0	3.22	0.69	0	0
22–23	41.5	27.0	b. d.	b. d.	0	0

Note: b. d. denotes values below the detection limit.

Table 3. ^{137}Cs activity concentration in different layers of the bottom sediment core at station 6

Bottom sediment layer, cm	Layer weight, g		^{137}Cs concentration, Bq·kg^{-1} dry weight	
	wet	dry	^{137}Cs	±
0–1	64.0	42.3	12.0	1.5
1–2	49.5	31.4	11.0	1.0
2–3	45.5	28.6	0	0
3–4	50.0	34.4	0	0
4–5	36.0	23.2	5.0	0.7
5–6	50.5	31.1	0	0
6–7	42.5	25.9	2.5	0.25
7–8	45.0	28.8	32.5	1.6
8–9	45.5	30.3	12.5	1.0
9–10	44.5	29.6	0	0
10–11	51.0	34.0	0	0
11–12	44.5	29.0	0	0
12–13	47.0	30.7	0	0
13–14	41.5	26.1	0	0
14–15	42.5	25.5	0	0
15–16	44.5	27.0	23.0	1.6
16–17	46.5	28.5	14.0	2.1
17–18	43.0	26.5	0	0
18–19	45.0	28.0	0	0
19–20	45.0	29.0	0	0

A graphic representation of the method for bottom sediments dating is given in Fig. 2.

Horizons are identified (Fig. 2), to which layers are linked, related to the period of the prohibition of nuclear weapons tests in open environments (1963) and to the year of the accident at the Chernobyl Nuclear Power Plant (1986). Linking to these dates allows estimating the sedimentation rate and using the “radio-geochemical clock” for bottom sediments dating. The same as in all cases of experimental and natural measurements, the results of observations are always burdened with errors. In this case,

the main errors are determined by inaccuracy in cutting the cores into layers, non-considering the change in sediment density in the core (in terms of depth), and the fact that the dates are linked to certain years, although each identified layer can refer to several years of sedimentation.

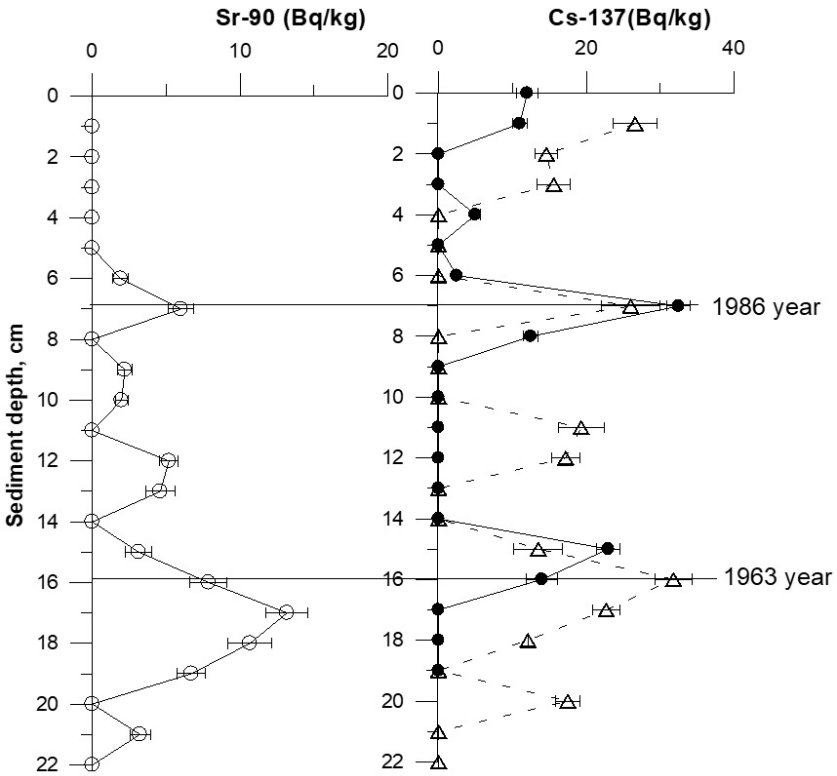

Fig. 2. Bottom sediment vertical distribution profiles of ^{90}Sr (○) at station 5 and ^{137}Cs at stations 5 (Δ) and 6 (●)

In the vertical distribution profiles of ^{90}Sr and ^{137}Cs in the bottom sediments, all three upper peaks almost coincided, and the layer at a 7-cm depth in the core can be dated to 1986 (Fig. 2). At the same time, the sedimentation rate, determined from the upper peak, for 1986–2019 is 70 mm / 33 years = 2.12 mm·year^{-1}. The lower peaks in the vertical distribution profiles of ^{90}Sr and ^{137}Cs in the bottom sediment cores were close to coinciding. If each of them is linked to 1963, then we get that the sedimentation rate, estimated from the vertical distribution profile for ^{137}Cs at sta. 6, will be for 1963–2020 150 mm / 57 years = 2.63 mm·year^{-1}; for ^{137}Cs profile at sta. 5 for 1963–2019, the value will be 160 mm / 56 years = 2.86 mm·year^{-1}; and for ^{90}Sr profile for 1963–2019, the value will be 170 mm / 56 years = 3.036 mm·year^{-1}. The mean sedimentation rate is 10.646 / 4 = 2.66 mm·year^{-1}, with a range from 2.12 to 3.036 mm·year^{-1}. Therefore, it is equally probable that the true value of the sedimentation rate falls within a range of 2.12–3.036 mm·year^{-1}. Specifically, if the mean sedimentation rate is 2.66 mm·year^{-1}, then practically each layer corresponded to four years of sedimentation, and the peak related, for example, to 1986, could fall anywhere within this layer.

It is worth noting that ^{90}Sr and ^{137}Cs occurred in the deeper layers of the cores as well (Fig. 2). Knowing that the Atomic Age began in July 1945, it is possible to verify that the age of these layers corresponds to the dating made. To do this, it is enough to correlate the depth of the layers with the minimum and maximum values of sedimentation rates. ^{90}Sr was found in the core in the 21-cm layer;

^{137}Cs, in the 20-cm layer. This allows assessing the time intervals, to which their localization can be attributed, taking into account the measurement errors. Estimate for ^{90}Sr: at the maximum sedimentation rate Tb(max) = 210 / 3.036 = 69 years, and at the minimum Tb(min) = 210 / 2.12 = 99 years. Thus, in terms of ^{90}Sr, the age of this layer corresponds to Tb interval 1920–1950. Estimate for ^{137}Cs: at the maximum sedimentation rate, Tb(max) = 200 / 3.036 = 66 years, and at the minimum Tb(min) = 200 / 2.12 = 94 years. Thus, in terms of ^{137}Cs, the age of this layer corresponds to Tb interval 1925–1953.

Obviously, all unaccounted errors occur within ranges of intervals of estimates for Tb values. Therefore, as follows from the presented material, these intervals also include the year of the beginning of the Atomic Age (1945). In general, the analysis of vertical distribution profiles for ^{90}Sr and ^{137}Cs in the bottom sediment cores showed that the chosen linking to the peaks of concentration maximums of 1986 and 1963 unambiguously corresponds to the sedimentation rate Vsed, lying in the range of 2.12–3.036 mm·year^{-1} (mean value is 2.66 mm·year^{-1}). Moreover, age estimates for the lowest sediment layers containing non-zero concentrations of measured radionuclides cover the beginning of the Atomic Age.

In general, using radioisotope dating, it was determined that in the Vodopadnaya River estuarine zone at sta. 5 and 6, sedimentation rate is 2.120–3.036 mm·year^{-1}, averaging 2.66 mm·year^{-1}. The specific value MAR_{sp} is 3,072.3 g·m^{-2}·year^{-1}, or 8,663.9 t·year^{-1} for the entire water area down to a depth of 40 m (MAR_{Σ}).

Biogenic elements. The results of determining the concentration of biogenic elements and calculating the parameters of the Redfield equations are given in Table 4 [Egorov et al., 2021].

Table 4. Concentration of nitrogen in form of ammonium (NH_4), nitrites (NO_2), and nitrates (NO_3); concentration of total mineral nitrogen compounds ($\sum N$); concentration of phosphorus (PO_4); and Redfield factor (R_{at}) in 2020 in the Vodopadnaya River estuarine zone [Egorov et al., 2021]

No.	Date	Seawater in the estuarine zone (station 4)						Freshwater in the estuary (44°29′22.0″N, 34°09′46.6″E)				
		NH_4 ± *SD*, μg·L^{-1}	NO_2 ± *SD*, μg·L^{-1}	NO_3 ± *SD*, μg·L^{-1}	$\sum N$, μg·L^{-1}	PO_4 ± *SD*, μg·L^{-1}	R_{at}	NH_4 ± *SD*, μg·L^{-1}	NO_2 ± *SD*, μg·L^{-1}	NO_3 ± *SD*, μg·L^{-1}	$\sum N$, μg·L^{-1}	PO_4 ± *SD*, μg·L^{-1}
1	16.01.2020	11.50 ± 0.60	2.70 ± 0.04	32.00 ± 0.96	46.2	17.00 ± 0.26	6.77	72.50 ± 3.74	19.50 ± 0.29	1,860 ± 56	1,952	44.50 ± 0.67
2	05.03.2020	9.10 ± 0.44	2.90 ± 0.04	20.30 ± 0.61	32.3	12.20 ± 0.18	6.96	23.10 ± 1.20	10.40 ± 0.16	960 ± 29	994	31.30 ± 0.47
3	23.06.2020	24.30 ± 1.17	1.60 ± 0.02	8.30 ± 0.25	34.2	3.40 ± 0.05	42.32	147.20 ± 7.07	43.80 ± 0.66	586 ± 18	777	53.40 ± 0.80
4	14.08.2020	19.10 ± 0.92	4.60 ± 0.07	10.50 ± 0.32	32.2	9.70 ± 0.15	13.00	9.40 ± 0.35	16.50 ± 0.25	690 ± 21	716	86.30 ± 1.50
5	02.10.2020	6.80 ± 0.33	1.90 ± 0.03	10.50 ± 0.32	19.2	10.90 ± 0.16	5.12	23.00 ± 1.0	21.30 ± 0.32	755 ± 22	799	92.80 ± 1.40
6	15.10.2020	11.90 ± 0.36	2.90 ± 0.04	12.80 ± 0.38	27.6	6.10 ± 0.09	14.46	12.70 ± 0.61	10.30 ± 0.15	1,005 ± 30	1,028	70.00 ± 1.05
7	26.11.2020	14.00 ± 1.58	2.30 ± 0.03	11.60 ± 0.35	27.9	6.50 ± 0.10	14.80	24.00 ± 1.1	11.32 ± 0.17	555 ± 17	590	43.90 ± 0.66
8	17.12.2020	10.00 ± 0.48	2.00 ± 0.03	8.00 ± 0.24	20.0	7.50 ± 0.11	9.20	22.00 ± 1.06	16.40 ± 0.25	766 ± 23	792	74.80 ± 1.12
Mean		13.34	2.61	14.25	30.2	9.16	14.08	40.24	18.69	897.12	956	62.12

Heavy metals and trace elements. The results of analytical determinations of HM concentrations in freshwater of the Vodopadnaya River estuary and in seawater of its estuarine zone are presented in Table 5.

Table 5. Concentration of heavy metals and trace elements in water (C_w) and relative (considering MPC [Ob utverzhdenii, 2016]) contamination of waters

No.	Date	Sampling area	Component	Component concentration, $C_w \pm SD$, $\mu g \cdot L^{-1}$	MPC, $\mu g \cdot L^{-1}$	C_w / MPC, %
1	22.06.2020	Yalta, the Vodopadnaya River, freshwater in the estuary, C_{fw}	Fe	5.220 ± 0.230	100	5.22
			Co	0.015 ± 0.001	5	0.30
			Ni	0.596 ± 0.020	10	5.96
			Cu	1.728 ± 0.044	5	34.56
			Zn	23.408 ± 0.593	50	4.68
			Mo	0.067 ± 0.005	1	6.70
			Cd	< 0.025	10	< 0.25
			Pb	0.157 ± 0.007	10	1.57
2	22.06.2020	Yalta, seawater in the estuarine zone, C_{sw}	Fe	2.453 ± 0.158	100	2.45
			Co	0.001 ± 0.001	5	0.02
			Ni	0.518 ± 0.024	10	5.18
			Cu	0.628 ± 0.028	5	12.56
			Zn	5.818 ± 0.206	50	11.64
			Mo	1.312 ± 0.047	1 (300)	131.20 (0.44)
			Cd	0.123 ± 0.005	10	1.23
			Pb	0.097 ± 0.004	10	0.97

Note: in parentheses, MPC values for seawater are given according to [Warmer, van Dokkum, 2002].

The results of analytical determinations of HM in the bottom sediments are shown in Table 6.

Table 6. Concentrations of heavy metals in the bottom sediments at station 5 (Table 1)

No.	Bottom sediment layer, cm	Layer dating, year	Heavy metal concentration in the bottom sediments, $C_{bs} \pm SD$, $mg \cdot kg^{-1}$ dry weight							
			Cr	Co	Ni	Cu	Zn	Mo	Cd	Pb
1	0.0–0.5	2019	19.39 ± 0.51	7.37 ± 0.09	25.9 ± 0.51	17.28 ± 0.26	63.35 ± 1.22	0.35 ± 0.05	1.35 ± 0.04	12.77 ± 0.36
2	1.5–2.0	2013	23.07 ± 0.90	8.09 ± 0.07	28.88 ± 0.37	17.73 ± 0.15	58.06 ± 1.57	0.30 ± 0.01	0.03 ± 0.02	13.86 ± 0.17
3	4.0–4.5	2003	22.58 ± 0.47	8.06 ± 0.09	32.75 ± 0.23	14.82 ± 0.09	54.46 ± 0.43	0.25 ± 0.02	< 0.01	13.96 ± 0.17
4	8.5–9.0	1989	26.67 ± 0.43	9.41 ± 0.09	33.19 ± 0.29	19.24 ± 0.09	57.94 ± 0.91	0.57 ± 0.01	0.02 ± 0.01	11.68 ± 0.38
5	11.0–11.5	1977	25.94 ± 0.29	8.71 ± 0.08	31.83 ± 0.29	17.76 ± 0.25	56.08 ± 1.03	0.25 ± 0.01	0.02 ± 0.01	11.15 ± 0.29
6	14.5–15.0	1964	19.30 ± 0.44	6.75 ± 0.09	24.67 ± 0.44	13.89 ± 0.19	45.83 ± 0.99	0.35 ± 0.05	< 0.01	7.49 ± 0.19
7	18.5–19.0	1949	23.51 ± 0.23	7.80 ± 0.08	27.47 ± 0.25	13.65 ± 0.07	43.22 ± 0.41	0.24 ± 0.01	< 0.01	7.61 ± 0.20
8	23.5–24.0	1930	25.25 ± 0.27	9.56 ± 0.10	30.36 ± 0.17	16.01 ± 0.14	48.32 ± 0.59	0.12 ± 0.01	< 0.01	9.10 ± 0.22

Mercury. Estimates of the concentrating ability of suspensions in relation to mercury in the Yalta city water area are given in Table 7.

Table 7. Results of mercury concentration measurement in water (C_w) and suspended matter (C_s) and mercury concentration factor (C_f) for suspended matter in the Yalta city water area

No.	Sampling site	Sampling date	Suspended matter concentration, $g \cdot m^{-3}$	C_w, $ng \cdot L^{-1}$			C_{tot} / MPC, %	C_s, $ng \cdot g^{-1}$ dry weight	C_f, $\times 10^5$
				Dissolved	Particulate	Total, C_{tot}			
1	Seawater (surface)	22.06.2020	1.3	40	5	45	45	3,846.15	0.96
2	Seawater (bottom)	15.10.2020	6.9	60	8	68	68	1,159.42	0.19
3	Seawater (surface)	28.04.2021	4	30	24	54	54	6,000.00	2.00
4		09.07.2021	40.7	30	5	35	35	122.85	0.04
5		07.10.2021	31.7	30	120	150	150	3,785.49	1.26
	Mean					60	60		
6	Freshwater in the estuary	22.06.2020	3.1	53	10	63	63	3,225.81	0.61
7		28.04.2021	2.2	20	100	120	120	45,454.55	22.73
8		09.07.2021	546.8	40	230	270	270	420.63	0.11
9		07.10.2021	1.8	35	70	105	105	38,888.89	11.11
	Mean					140	140		

The results of analytical determinations of mercury in the bottom sediments are presented in Table 8.

Table 8. Mercury concentration in bottom sediment layers (C_{bs}) at station 6 (Table 1)

No.	Bottom sediment layer, cm	Layer dating, year	C_{bs}, $\mu g \cdot kg^{-1}$ dry weight	Mercury specific flux into the bottom sediments, $F_{sp} = MAR \cdot C_{bs}$, $\mu g \cdot m^{-2} \cdot year^{-1}$	Mercury flux into the bottom sediments, $F_{Hg} = F_{sp} \cdot S$, $kg \cdot year^{-1}$
1	0–1	2020	62	264.2	0.75
2	1–2	2018	68	289.8	0.82
3	2–3	2014	66	281.2	0.79
4	3–4	2011	53	225.8	0.64
5	4–5	2007	63	268.5	0.76
6	5–6	2003	141	600.8	1.69
7	6–7	1999	63	268.5	0.76
8	7–8	1996	67	285.5	0.81
9	8–9	1992	80	340.9	0.96

The third column in Table 8 shows the age of the layers. The fifth column contains estimates of Hg flux into the bottom sediments of the Yalta city water area at sta. 6.

DISCUSSION

Biogenic elements. Graphic material presented in Fig. 3 reflects the patterns of changes in biogenic element concentration in the Vodopadnaya River estuary and estuarine zone. Freshwater of the estuary is characterized by an increased content of nitrogen in composition of nitrites (by 7.2 times), ammonium (by 3.0 times), nitrates (by 62.9 times), and mineral phosphorus (by 13.2 times) in comparison with their concentrations in seawater of the estuarine zone. These data indicate a statistically significant effect of the river runoff on the shift in concentrations of the total content of nitrogen compounds, as well as mineral phosphorus in seawater of the estuarine zone. The flux of biogenic elements from the river in summer can change the limiting nutrient for primary production from nitrogen to phosphorus.

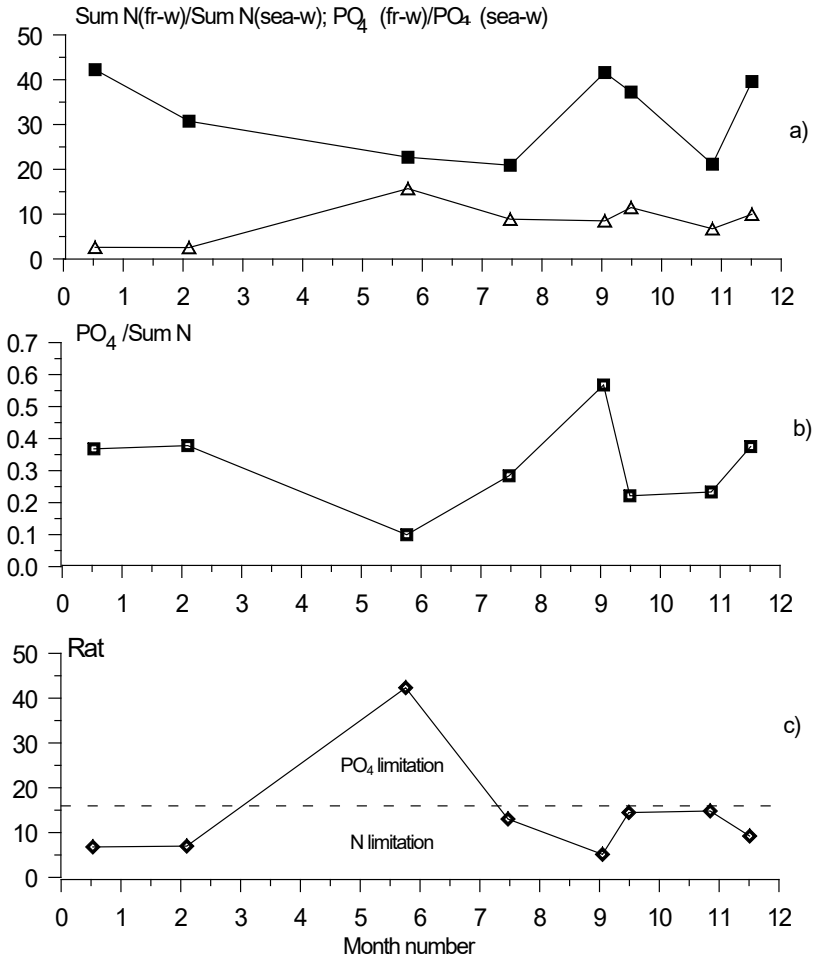

Fig. 3. Ratio of total nitrogen (■) and mineral phosphorus (Δ) concentrations in freshwater of the Vodopadnaya River estuary to the values in seawater of its estuarine zone (a); ratio of mineral phosphorus concentration to the total nitrogen concentration in seawater in the Vodopadnaya River estuarine zone (b); calculated values of the Redfield factor for the sea area of the Vodopadnaya River estuarine zone (c)

In 2019, concentration of biogenic elements in the river estuary at sta. 4 was 14–16 times higher than their content in the estuarine zone in terms of total nitrogen compounds, while the concentration of phosphates could be of the same order of magnitude or up to 25 times higher. This indicated the eutrophic effect of the river runoff on coastal waters of the Yalta city area. That year, with the river runoff,

330.66 kg·day^{-1} of nitrogen compounds and 7.35 kg·day^{-1} of mineral phosphorus entered the city estuarine water area daily. With nitrogen limitation of production processes, the flux of biogenic elements with the river runoff could lead to water hypertrophy on the area of 531,000 m^2, and with phosphorus limitation, on the area of 88,000 m^2 [Egorov, 2021].

In 2020, with a mean annual river flow of 33.18 m^3·day^{-1}, the concentration of total nitrogen compounds ($\sum N_i$) in freshwater was 956 μg·L^{-1}, and mineral phosphorus (PO_4), 62.12 μg·L^{-1} (Table 4). At the same time, the daily flux of $\sum N_i$ into the Yalta city estuarine zone amounted to about 31.717 kg·day^{-1}, and for mineral phosphorus, the value was up to 2.060 kg·day^{-1}. As known, the synthesis of 1,000 g of organic matter in terms of mass requires 80 g of carbon, 2 g of phosphorus, and 14 g of nitrogen [Zilov, 2009]. Accordingly, with nitrogen limitation of production processes, new production can be (31.717 / 14) · 80 = 181.240 kg C_{org}·day^{-1}; with phosphorus limitation, (2.060 / 2) · 80 = 82.400 kg C_{org}·day^{-1}. These data indicate as follows: under water eutrophication by phytoplankton, equal to 100 mg C_{org}·m^{-3}·day^{-1}, and the location of the summer core of primary production in the 0–10-m layer, due to the flux of nitrogen compounds, water hypereutrophication will spread to the area of 181,240 m^2; with phosphorus limitation, the area will be 82,400 m^2. Taking into account the previously published data for 2019 [Egorov, 2021], with prevailing nitrogen limitation of primary production processes, the daily growth rate of water hypereutrophicated by biogenic elements in the Yalta city water area in different years can be 6–18% *per* day of the polygon area.

Water masses of the polygon are exchanged with the open sea through liquid boundaries, especially from the northeast to the southwest [Egorov et al., 2018], along the main coastal recreational zone of Yalta city. This can result in an increase in the primary production of the water area, outbreaks of gelatinous plankton [*Rhizostoma pulmo* (Macri, 1778) and *Aurelia aurita* (Linnaeus, 1758)], and water bloom. Therefore, the flux of biogenic elements with the river runoff is a significant factor in reducing sanitary and hygienic water quality in the city recreational zone.

Heavy metals and mercury. In freshwater of the river estuary, Fe, Co, Ni, Cu, Zn, and Cd concentrations did not exceed MPC. In seawater of the estuarine zone, Mo content in some years could surpass MPC (Tables 5, 7) established for fishery basins [Ob utverzhdenii, 2016]. However, Mo concentration was still two orders of magnitude lower than MPC recommended for marine waters [Chuzhikova-Proskurnina et al., 2022; Warmer, van Dokkum, 2002]. In the Yalta city water area, content of the dissolved form of mercury in freshwater and seawater of the estuarine zone did not exceed MPC (Table 7). At the same time, the concentration of particulate mercury in freshwater and seawater was usually higher and could surpass MPC. High levels of mercury accumulation by suspended matter were established: accumulation coefficients from 0.11×10^5 to 22.73×10^5; this indicated a high significance of suspended matter in Hg migration in the aquatic environment.

HM distribution in the bottom sediments, taking into account the radioactive tracer dating (Fig. 2) of their age from 1930 to 2020 at sta. 5 and 6, is presented in Fig. 4.

Between 1930 and 2020 (Fig. 4), the content of Cr, Fe (after 2000), and Cu (after 1990), under data variability, nevertheless showed a tendency to decrease in the bottom sediments. At the same time, concentrations of Co (since 1990), Mo (since 2000), Cd (after 2010), and Hg (since 2010) in the bottom sediments increased. The trends of rising contamination of the bottom sediments with Zn and Pb from the 1950s to the present time, assessed by the coefficients of determination, had a high degree of statistical significance ($R^2 = 0.715$ and $R^2 = 0.729$, respectively).

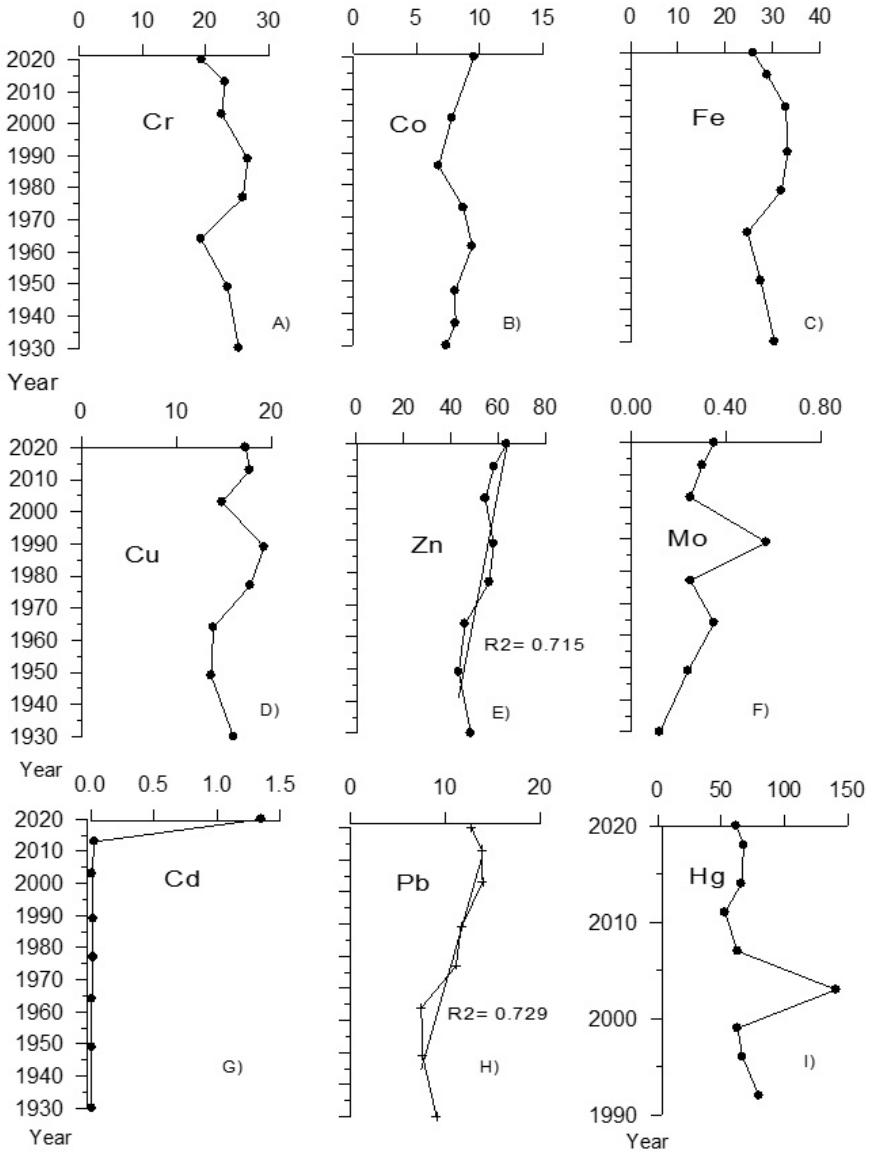

Fig. 4. Vertical distribution profiles for Cr (A), Co (B), Fe (C), Cu (D), Zn (E), Mo (F), Cd (G), Pb (H), and Hg (I), mg·kg^{-1} dry weight, in the thickness of the bottom sediments in the Yalta city water area

Intensity of biogeochemical processes for migration of heavy metals and organochlorine compounds in the Yalta city recreational water area. Indicators of the intensity of biogeochemical processes in the Yalta water area are given in Table 9.

The second and fourth columns in Table 9 present data on the concentration of pollutants in seawater and in the upper layer of the bottom sediments in the Yalta water area. The second column contains the results of calculations of pollutant pools in the water area with a volume of $80 \cdot 10^6$ m^3. In the fifth and sixth columns, there are estimates of the total sedimentation flux and periods of pollutant deposition into the thickness of the bottom sediments. The eighth and ninth columns present the results of calculations of pollutant flux into the water area with the river runoff and estimates of the periods of their turnover in the Yalta water area due to the river runoff. In general, those testify to a high significance of contamination factors of the analyzed water area with the river runoff and its sedimentary self-purification due to biogeochemical processes. The data show (Table 9) that the turnover of pollutants in the Yalta

city water area, resulting from the effect of sedimentation processes, occurs on time scales from daily to synoptic, and due to the river runoff, from annual to long-term. At the same time, periods of turnover for these elements due to processes of sedimentary self-purification are 1–2 orders of magnitude lower than due to the river runoff.

Table 9. Biogeochemical characteristics of turnover of pollutants (P) in the Vodopadnaya River estuarine zone and in the Yalta city water area

P	Concentration of P in seawater of the Yalta city water area, C_{sw}, $\mu g \cdot L^{-1}$	Pool of P in the Yalta city water area, $Q_{wa} = C_{sw} \cdot V$, kg	Concentration of P in the upper layer of the bottom sediments, C_{bs}, $mg \cdot kg^{-1}$ dry weight	Sedimentation flux of P into the bottom sediments, $F_{sed} = C_{bs} \cdot MAR \cdot S$, $kg \cdot year^{-1}$	Period of sedimentation turnover of P in the Yalta city water area, $T_{sed} = Q_{wa} / F_{sed}$, days	Concentration of P in freshwater of the Vodopadnaya River, C_{rw}, $\mu g \cdot L^{-1}$	Flux of P with the Vodopadnaya River runoff, $I_r = C_{rw} \cdot V_r$, $kg \cdot year^{-1}$	Period of turnover of P due to the Vodopadnaya River runoff, $T_r = Q_{wa} / I_r$, days
Cu	0.628	50.240	17.280	149.712	122.5	1.728	8.23	$2.2 \cdot 10^3$
Zn	5.818	465.440	63.350	548.857	309.5	23.408	111.47	$1.5 \cdot 10^3$
Fe	2.453	196.240	n. d.	n. d.*	n. d.	5.220	24.86	$2.9 \cdot 10^3$
Co	0.001	0.080	7.370	63.853	0.5	0.015	0.07	408.8
Ni	0.518	41.440	25.900	224.395	67.4	0.596	2.84	$5.3 \cdot 10^3$
Mo	1.312	104.960	0.350	3.032	$1.2 \cdot 10^4$	0.067	0.32	$1.2 \cdot 10^5$
Cd	1.123	9.840	1.350	11.696	307.0	< 0.025	< 0.12	$> 3.0 \cdot 10^4$
Pb	0.097	7.760	12.770	110.638	25.6	0.157	0.75	$3.8 \cdot 10^3$
Hg	0.071	5.700	0.063	0.546	$2.9 \cdot 10^{-2}$	0.14	1.689	$9.2 \cdot 10^{-3}$
^{90}Sr	8.5 $Bq \cdot m^{-3}$	680.0 MBq	1.6 $Bq \cdot kg^{-1}$	13.9 $MBq \cdot year^{-1}$	$1.8 \cdot 10^4$	n. d.	n. d.	n. d.
∑DDT*	$1.42 \cdot 10^{-3}$	0.114	0.036	0.312	132.9	$0.32 \cdot 10^{-3}$	0.002	$2.7 \cdot 10^4$
∑6PCB*	$6.80 \cdot 10^{-3}$	0.544	0.010	0.088	2,244.7	$1.09 \cdot 10^{-3}$	0.005	$3.8 \cdot 10^4$

Note: n. d. denotes no data; * denotes data according to [Malakhova, Lobko, 2022].

In general, consideration of the presented material on HM distribution in the Yalta city water area (Table 5) showed that Fe, Co, Ni, Cu, Zn, Mo, Cd, and Pb concentrations in freshwater of the river estuarine zone ranged from 0.25 to 34.5 % of MPC for respective elements. In seawater of the estuarine zone, Mo content could exceed MPC established for fishery basins [Ob utverzhdenii, 2016], reaching the values of up to 131.2% of MPC, while the concentration of other HM ranged from 0.02 to 12.56% of MPC. However, it should be noted as follows: in the Russian environmental law, there is no MPC for Mo in seawater. At the same time, the values of Mo concentrations measured by us in the Yalta marine area were at the lower limit of values typical for the World Ocean waters [Mirzoeva et al., 2022] and also 2 orders of magnitude lower than MPC recommended for marine waters by the document [Warmer, van Dokkum, 2002]. The data on mercury distribution in the Yalta water area (Table 7) indicated that the content of its dissolved form in freshwater and seawater of the estuarine zone during the observation period did not exceed MPC [Ob utverzhdenii, 2016]. At the same time, the concentration of the particulate form of mercury in freshwater and seawater, as a rule, is higher, and the total content of mercury in water reached 140% of MPC.

It is worth noting that the estimates (Table 9) of maximum permissible fluxes are normalized to the average annual level of the Vodopadnaya River runoff (Fig. 5).

Fig. 5. The Vodopadnaya River estuary at the average annual discharge intensity

However, the Vodopadnaya River has flood flow regime as well. Specifically, on 18.06.2021, 84 mm of precipitation fell at the river source on Ai-Petri peak, and this exceeded the monthly rate of 72 mm. As a result, the water discharge in the river reached 9.9 $m^3 \cdot s^{-1}$, which is almost 28 times higher than the average level. The plume from high water spread far beyond the Yalta city recreational zone, deteriorating water quality on the beaches of the Southern Coast of Crimea (Fig. 6). Apparently, to deflect the plume from the coast, in addition to construction of coastal protection piers (Fig. 1), construction of appropriate hydraulic structures is required.

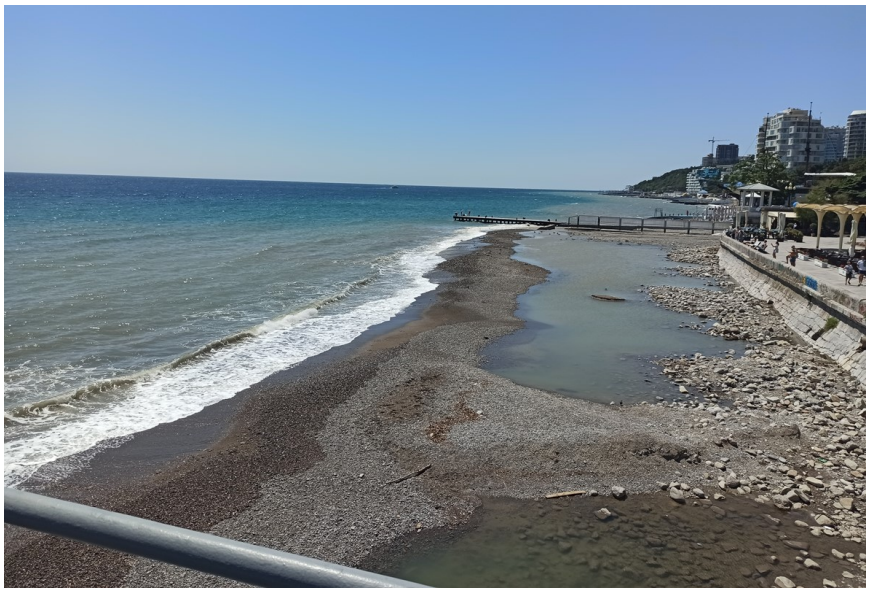

Fig. 6. Estuary and marine estuarine zone in the Yalta city water area during the high water in the Vodopadnaya River

As known, the optimal strategy for nature management is the implementation of the sustainable development concept; its core is to maintain a balance between consumption and reproduction of natural resources of the regions. In the present work, as criteria for consumption and reproduction of water quality resources in relation to pollutants, we used the results of studying the patterns of interaction between living and inert matter with radioactive and chemical components of the marine environment; also, we used modern theoretical ideas about biogeochemical mechanisms of radioisotopic and chemical homeostasis of marine ecosystems [Egorov et al., 2021]. MPC of a pollutant in the aquatic environment is known to serve as an indicator of water quality. In accordance with its dimension, MPC is only a diagnostic assessment. Obviously, the analysis of the ratio C_w / MPC (%) makes it possible to determine the relative environmental hazard from water pollution by various contaminants. On a certain time scale, monitoring of this ratio can characterize trends in changes in sanitary and hygienic water quality, since with a decrease in C_w / MPC value, the ecological situation in the water area in relation to the considered pollutant will improve, while with an increase, it will deteriorate. Obviously, in order to manage the ecological situation of water areas in terms of radioactive and chemical pollution, it is necessary to develop an indicator of consumption and reproduction of water quality, which has the dimension of fluxes.

As follows from the data presented (Table 9), under conditions of stationarity of the ecosystem state in the Yalta city recreational zone, the flux of pollutants into the water area with the Vodopadnaya River runoff on an annual time scale was an indicator of a deterioration (*i. e.*, consumption) in water quality. With such an interpretation of the mechanisms of ecosystem stationarity formation, the sedimentation flow that compensates for pollution due to biogeochemical processes is obviously a measure of natural reproduction of water quality, and the data on the periods of pollutant turnover in the water area due to sedimentation processes (the sixth column in Table 9) reflect its relative intensity. Naturally, the data given in the eighth and ninth columns, within the accepted assumptions, evidence for relative intensity of the deterioration in water quality of the Yalta city recreational zone because of the river runoff.

CONCLUSION

Water self-purification from conservative pollutants, which results from the effect of biogeochemical processes, is necessarily associated with the depot of their elimination. Adjacent water areas and underlying water layers can act as water depots, while the bottom sediments can act as geological depots. Living, inert, and terrigenous matter can serve as a source of sediments. The coefficients of pollutant accumulation by various components of sediments (K_{sed}) differ and may depend on pollutant concentration in the aquatic environment. For radionuclides, K_{sed} = const in the range of radioactive contamination of water up to $10^{-6}…10^{-3}$ mol·L^{-1} [Polikarpov, 1964]. For other pollutants, K_{sed} values depend on the size spectra of sediment particles, as well as on their sorption, metabolic, and trophic characteristics, which are described by the patterns of Michaelis–Menten, Langmuir, or Freundlich. If K_{sed} = const, then the maximum permissible flux of water self-purification due to entering the depot, equal to the ecological capacity of a water area, can be determined as the result of the product of the maximum permissible concentration of pollutants in the aquatic environment (MPC) by K_{sed} value and the intensity of the sedimentation flux. At the same time, if pollutants enter the thickness of the bottom sediments, then the flux of their elimination, called the assimilation capacity of the marine environment, also depends on the degree of saturation of the adsorption capacity for sediments in relation to the studied pollutant [Egorov, 2021]. Therefore, the sorption properties of bottom sediments should be studied and taken into account when setting maximum permissible anthropogenic load on marine ecosystems.

The presented data indicate a statistically significant effect of the river runoff on the shift in the concentrations of the total content of nitrogen compounds, as well as mineral phosphorus in seawater of the river estuarine zone. The flux of biogenic elements from the river in summer could change the regime of limitation of primary production from nitrogen to phosphorus. As a result of the river runoff, Co and Zn turnover in the Yalta city water area occurs on time scales from hourly to synoptic, and periods of Ni, Cu, ∑6PCB, Pb, Hg, and Mo turnover are estimated at $81.8 \div 17.2 \cdot 10^3$ days. The processes of sedimentation turnover for Co and Hg occur on time scales from daily to monthly, while for Cu, Pb, Cd, ^{90}Sr, and Mo, those are in the range from $1.1 \cdot 10^3$ to $185.2 \cdot 10^3$ days.

An analysis of the distribution profiles for pollutants in the bottom sediments showed as follows: between 1930 and 2020, in the content of Cr, Fe (after 2000), and Cu (after 1990), under data variability, there was a tendency to a decrease in concentrations of these heavy metals in the bottom sediments. At the same time, the content of Co (since 1990), Mo (since 2000), Cd (after 2010), and Hg (since 2010) in the bottom sediments increased. Trends in rising contamination of the bottom sediments with Zn and Pb from 1950s to the present time had a high degree of statistical significance. In total, the results of observations and analytical assessments testified as follows: against the backdrop of generally favorable environmental situation in terms of water contamination with heavy metals, the content of various pollutants in some years could exceed MPC and significantly worsen the quality of the Yalta city recreational water area. In this regard, it is required to develop standards for regulating water quality in recreational areas.

Highlights:

1. The specific sedimentation of the water area of the coastal and marine recreational zone of Yalta city is estimated at 2.120–3.036 mm·year^{-1}, averaging 2.66 mm·year^{-1}. In terms of mass, the value is 3,072.3 g·m^{-2}·year^{-1}, or 8,663.9 t·year^{-1} for the entire water area down to a depth of 40 m.
2. Freshwater of the Vodopadnaya River estuary is characterized by an increased content of nitrogen in composition of nitrites (by 7.2 times), ammonium (by 3.0 times), nitrates (by 62.9 times), and mineral phosphorus (by 13.2 times) compared to their concentrations in seawater of the estuarine zone. In the coastal recreational zone of the Yalta city, nitrogen limitation of phytoplankton primary production prevails. The flux of biogenic elements from the river can change the regime of limitation of phytoplankton primary production from nitrogen to phosphorus. Due to the flux of biogenic elements with the river runoff, new production in the Yalta water area under nitrogen limitation of production processes can amount to 181.240 kg C_{org}·day^{-1}; under phosphorus limitation, 82.400 kg C_{org}·day^{-1}. With nitrogen limitation of production processes, the growth rate of hypereutrophicated water in summer can be 6–18% *per* day of the Yalta city recreational water area.
3. In freshwater of the river estuarine zone, concentrations of Fe, Co, Ni, Cu, Zn, Mo, Cd, and Pb ranged from 0.25 to 34.5% of MPC. In seawater of the estuarine zone, relative content of heavy metals varied from 0.02 to 12.56% of MPC. In freshwater, the total concentration of mercury averaged 60% of MPC, and in seawater, 140%.
4. As a result of the river runoff, Co and Zn turnover in waters of the Yalta city area occurs on time scales from hourly to synoptic; periods of Ni, Cu, Pb, Hg, and Mo turnover are estimated at $81.8 \div 17.2 \cdot 10^3$ days. The processes of sedimentation turnover for Co and Hg occur on time scales from daily to monthly, while for Cu, Pb, Cd, ^{90}Sr, and Mo, those are in the range from $1.1 \cdot 10^3$ to $185.2 \cdot 10^3$ days.

5. Over the period from 1930 to 2020, the content of Cr, Fe (after 2000), and Cu (after 1990) in the bottom sediments had a decreasing trend. Concentrations of Co (since 1990), Mo (since 2000), Cd (after 2010), and Hg (since 2010) in more recent bottom sediments increased.
6. On the example of the Vodopadnaya River estuarine zone, the development of a methodology for implementation of the sustainable development concept is shown for water areas under conditions when the consumption of water quality in relation to pollutants does not exceed their reproduction resulting from biogeochemical processes. To implement the sustainable development of the Yalta water area, in terms of the current level of marine pollution, the permissible flux into its estuarine zone should not exceed: for Cu, 149.7 kg·year^{-1}; Zn, 548.9 kg·year^{-1}; Co, 63.9 kg·year^{-1}; Ni, 224.4 kg·year^{-1}; Mo, 3.0 kg·year^{-1}; Cd, 11.7 kg·year^{-1}; Pb, 110.6 kg·year^{-1}; Hg, 0.546 kg·year^{-1}; ∑DDT, 0.3 kg·year^{-1}; and ∑6PCB, 0.1 kg·year^{-1}.

This work was carried out within the framework of IBSS state research assignment "Molismological and biogeochemical fundamentals of marine ecosystems homeostasis" (No. 121031500515-8).

REFERENCES

1. Gulin S. B., Polikarpov G. G., Egorov V. N., Stokozov N. A. Ispol'zovanie prirodnykh i iskusstvennykh radiotrasserov dlya izucheniya biogeokhimicheskikh protsessov perenosa i deponirovaniya radioaktivnykh i khimicheskikh zagryaznenii v usloviyakh okislitel'no-vosstanovitel'noi vodnoi tolshchi Chernogo morya. In: *Radioekologiya: uspekhi i perspektivy* : materialy nauchnogo seminara, Sevastopol, 3–7 Oct., 1994. Sevastopol : [s. n.], 1994, pp. 103–104. (in Russ.)
2. GOST R 56219-2014. *Voda. Opredelenie soderzhaniya 62 elementov metodom mass-spektrometrii s induktivno-svyazannoi plazmoi.* Moscow : Standartinform, 2015, 36 p. (in Russ.)
3. GOST 26927-86. *Syr'e i produkty pishchevye. Metody opredeleniya rtuti.* Moscow : IPK Izd-vo standartov, 2002, 12 p. (in Russ.)
4. Egorov V. N., Bobko N. I., Marchenko Yu. G., Sadogurskiy S. Ye. Nutrient content and limitation of the phytoplankton primary production in the estuary area of the Vodopadnaya River (south coast of Crimea). *Ekologicheskaya bezopasnost' pribrezhnoi i shel'fovoi zon morya*, 2021, no. 3, pp. 37–51. (in Russ.). https://doi.org/10.22449/2413-5577-2021-3-37-51
5. Egorov V. N., Plugatar Yu. V., Malakhova L. V., Mirzoeva N. Yu., Gulin S. B., Popovichev V. N., Sadogurskiy S. E., Malakhova T. V., Shchurov S. V., Proskurnin V. Yu., Bobko N. I., Marchenko Yu. G., Stetsyuk A. P. Ekologicheskoe sostoyanie akvatorii osobo okhranyaemoi prirodnoi territorii "Mys Mart'yan" i problema realizatsii ee ustoichivogo razvitiya po faktoram evtrofikatsii, radioaktivnogo i khimicheskogo zagryazneniya vod. In: *Sokhranenie biologicheskogo raznoobraziya i zapovednoe delo v Krymu* : materialy nauch.-prakt. konf. s mezhdunar. uchastiem, Yalta, 23–26 Oct., 2018. Yalta : NBG – NSC, 2018, pp. 36–40. (Nauchnye zapiski prirodnogo zapovednika "Mys Mart'yan" ; iss. 9). (in Russ.). https://doi.org/10.25684/NBG.scnote.009.2018.04
6. Zaitsev Ju. P., Polikarpov G. G. Ecological processes in critical zones of the Black Sea (results synthesis of two research directions, middle of the XX – beginning of the XXI cen-

tury). *Morskoj ekologicheskij zhurnal*, 2002, vol. 1, no. 1, pp. 35–55. (in Russ.). https://repository.marine-research.ru/handle/299011/686

7. Zilov E. A. *Gidrobiologiya i vodnaya ekologiya (organizatsiya, funktsionirovanie i zagryaznenie vodnykh ekosistem).* Irkutsk : Izd-vo Irkutskogo gos. un-ta, 2009, 147 p. (in Russ.)
8. Malakhova L. V., Lobko V. V. Assessment of pollution of the Yalta Bay ecosystem components with organochlorine xenobiotics. *Ekologicheskaya bezopasnost' pribrezhnoi i shel'fovoi zon morya*, 2022, no. 3, pp. 104–116. (in Russ.)
9. Mirzoeva N. Yu., Egorov V. N., Polikarpov G. G. Soderzhanie ^{90}Sr v donnykh otlozheniyakh Chernogo morya posle avarii na Chernobyl'skoi AES i ego ispol'zovanie v kachestve radiotrassera dlya otsenki skorosti osadkonakopleniya. In: *Sistemy kontrolya okruzhayushchei sredy: sredstva i monitoring*. Sevastopol : EKOSI-Gidrofizika, 2005, iss. 8, pp. 276–282. (in Russ.)
10. *Ob utverzhdenii normativov kachestva vody vodnykh ob"ektov rybokhozyaistvennogo znacheniya, v tom chisle normativov predel'no dopustimykh kontsentratsii vrednykh veshchestv v vodakh vodnykh ob"ektov rybokhozyaistvennogo znacheniya* : prikaz Minsel'khoza Rossii ot 13.12.2016 no. 552 [v red. ot 10.03.2020]. (in Russ.). URL: https://docs.cntd.ru/document/420389120 [accessed: 04.05.2023].
11. PND F 16.2.2:2.3.71-2011. *Metodika izmerenii massovykh dolei metallov v osadkakh stochnykh vod, donnykh otlozheniyakh, obraztsakh rastitel'nogo proiskhozhdeniya spektral'nymi metodami.* Moscow : Federal'naya sluzhba po nadzoru v sfere prirodopol'zovaniya, 2011, 45 p. (in Russ.)
12. Polikarpov G. G. *Radioekologiya morskikh organizmov.* Moscow : Atomizdat, 1964, 295 p. (in Russ.). https://repository.marine-research.ru/handle/299011/12748
13. *Radioekologicheskii otklik Chernogo morya na chernobyl'skuyu avariyu* / G. G. Polikarpov, V. N. Egorov (Eds). Sevastopol : EKOSI-Gidrofizika, 2008, 667 p. (in Russ.). https://repository.marine-research.ru/handle/299011/9280
14. *Rukovodstvo po khimicheskomu analizu morskikh vod* : rukovodyashchii dokument RD 52.10.243-92. Saint Petersburg : Gidrometeoizdat, 1993, 264 p. (in Russ.). URL: https://meganorm.ru/Data2/1/4293815/4293815261.pdf [accessed: 04.05.2023].
15. *Rukovodstvo po metodam khimicheskogo analiza morskikh vod.* Leningrad : Gidrometeoizdat, 1977, 208 p. (in Russ.)
16. Hutchinson D. *Limnologiya: geograficheskie, fizicheskie i khimicheskie kharakteristiki ozer* : transl. from Engl. Moscow : Progress, 1969, 591 p. (in Russ.)
17. Chuzhikova-Proskurnina O. D., Proskurnin V. Yu., Tereshchenko N. N., Kobechinskaya V. G. Heavy metals in the coastal waters of Russian sector of the Black Sea and the Sea of Azov. *Ekosistemy*, 2022, no. 31, pp. 111–122. (in Russ.)
18. Artemov Yu. G. Software support for investigation of natural methane seeps by hydroacoustic method. *Morskoj ekologicheskij zhurnal*, 2006, vol. 5, no. 1, pp. 57–71. https://repository.marine-research.ru/handle/299011/850
19. Egorov V. N. *Theory of Radioisotopic and Chemical Homeostasis of Marine Ecosystems.* Cham, Switzerland : Springer, 2021, 320 p. https://doi.org/10.1007/978-3-030-80579-1
20. Gulin S. B., Aarkrog A., Polikarpov G. G., Nielsen S. P., Egorov V. N. Chronological study of ^{137}Cs input to the Black Sea deep and shelf sediments. In: *Radionuclides*

in the Oceans : RADOS 96–97 : [intern. symp., Octeville – Cherbourg, France, 7–11 Oct., 1996] : proceedings / Eds: P. Germain [et al.]. Les Ulis : Éd. de Physique, 1997, pt 1: Inventories, behaviour and processes, pp. 257–262. (Radioprotection ; vol. 32, spec. iss. C2).

21. Harvey B. K., Ibbett R. D., Lovett M. B., Williams K. J. *Analytical Procedures for the Determination of Strontium Radionuclides in Environmental Materials.* Lowestoft : [s. n.], 1989, 33 p. (Aquatic Environment Protection: Analytical Methods / MAFF, Direct. Fish. Res. ; no. 5).
22. Mirzoeva N., Polyakova T., Samyshev E., Churilova T., Mukhanov V., Melnik A., Proskurnin V., Sakhon E., Skorokhod E., Chuzhikova-Proskurnina O., Chudinovskih E., Minkina N., Moiseeva N., Melnikov V., Paraskiv A., Melnik L., Efimova T. Current assessment of water quality and biota characteristics of the pelagic ecosystem of the Atlantic sector of Antarctica: The multidisciplinary studies by the Institute of Biology of the Southern Seas. *Water*, 2022, vol. 14, iss. 24, art. no. 4103 (20 p.). https://doi.org/10.3390/w14244103
23. Papucci C. Sampling marine sediments for radionuclide monitoring. In: *Strategies and Methodologies for Applied Marine Radioactivity Studies*. Vienna : IAEA, 1997, chap. 13, pp. 279–297. (Training Course Series ; no. 7).
24. *PlasmaQuant MS and PlasmaQuant MS Elite Mass-spectrometers With Inductively Coupled Plasma (ICP-MS).* User's Manual. Analytik Jena AG, 2014, 143 p.
25. Redfield A. C. The biological control of chemical factors in the environment. *American Scientist*, 1958, vol. 46, no. 3, pp. 205–221.
26. Schafer C. T., Smith J. N., Loring D. H. Recent sedimentation events at the head of Saguenay Fjord, Canada. *Environmental Geology*, 1980, vol. 3, iss. 3, pp. 139–150. https://doi.org/10.1007/BF02473489
27. Warmer H., van Dokkum R. *Water Pollution Control in the Netherlands: Policy and Practice 2021* / [Institute for Inland Water Management and Waste Water Treatment. RIZA]. The Netherlands : RIZA, 2002, 76 p. (RIZA report 2002.009).

ВОЗМОЖНОСТЬ РЕАЛИЗАЦИИ КОНЦЕПЦИИ УСТОЙЧИВОГО РАЗВИТИЯ РЕКРЕАЦИОННОГО ПРИБРЕЖЬЯ ГОРОДА ЯЛТА В ОТНОШЕНИИ БИОГЕННЫХ ЭЛЕМЕНТОВ, РАДИОНУКЛИДОВ, ТЯЖЁЛЫХ МЕТАЛЛОВ И ХЛОРОРГАНИЧЕСКИХ СОЕДИНЕНИЙ (КРЫМ, ЧЁРНОЕ МОРЕ)

В. Н. Егоров, Н. Ю. Мирзоева, Ю. Г. Артёмов, В. Ю. Проскурнин, А. П. Стецюк, Ю. Г. Марченко, Д. Б. Евтушенко, И. Н. Мосейченко, О. Д. Чужикова-Проскурнина

ФГБУН ФИЦ «Институт биологии южных морей имени А. О. Ковалевского РАН»,
Севастополь, Российская Федерация
E-mail: *egorov.ibss@yandex.ru*

Проведено гидроакустическое зондирование, определены площадь и объём вод приустьевой зоны реки Водопадная до глубины 40 м в акватории города Ялта (Крым, Чёрное море). Концентрации биогенных элементов (NO_2, NO_3, NH_4 и PO_4) и тяжёлых металлов (Cu, Zn, Fe, Co, Ni, Mo, Cd, Pb и Hg) в пресной воде устья реки превышают их концентрации в прибрежной морской воде

в 3–64 раза. Выявлено влияние стока реки на эвтрофикацию вод изучаемой морской акватории. С использованием постчернобыльских радиоизотопов ^{90}Sr и ^{137}Cs выполнена датировка донных осадков и определена скорость седиментации с исследованной площади акватории региона. Рассчитаны потоки поступления загрязняющих веществ со стоком реки и периоды их оборота в рекреационном прибрежье города Ялта. Полученные результаты использованы для обоснования концепции устойчивого развития рекреационной зоны города Ялта по факторам загрязнения морской среды.

Ключевые слова: Чёрное море, Крым, вода, биогенные элементы, стронций-90, цезий-137, тяжёлые металлы, хлорорганические соединения, датировка донных отложений

1871
ИнБЮМ – IBSS

Морской биологический журнал
Marine Biological Journal
2023, vol. 8, no. 3, pp. 33–46
https://marine-biology.ru

UDC 597.556.253-169[470.116:28]

METAZOAN PARASITES OF TWO STICKLEBACK SPECIES AT THE SOLOVETSKY ARCHIPELAGO (WHITE SEA)

© 2023 **D. I. Lebedeva[1], D. O. Zaitsev[2], Ja. I. Alekseeva[3], and A. A. Makhrov[4,5]**

[1]Karelian Research Centre of RAS, Petrozavodsk, Russian Federation
[2]Petrozavodsk State University, Petrozavodsk, Russian Federation
[3]State Biological Museum named after K. A. Timiryazev, Moscow, Russian Federation
[4]Severtsov Institute of Ecology and Evolution of RAS, Moscow, Russian Federation
[5]Saint Petersburg State University, Saint Petersburg, Russian Federation
E-mail: *daryal78@gmail.com*

Received by the Editor 26.12.2022; after reviewing 20.01.2023;
accepted for publication 04.08.2023; published online 21.09.2023.

The Solovetsky Archipelago, situated in the White Sea, comprises six large islands. Out of them, the two largest ones, Bolshoy Solovetsky and Anzersky islands, possess an extensive system of lakes, streams, and canals, which are connected with each other and with the sea. The study of hydrobionts, including fish, from freshwater bodies of the Solovetsky Archipelago is of great importance for understanding historical processes of fauna formation. The freshwater ichthyofauna of the Solovetsky Islands has been monitored for almost 30 years. As a result of these long-term observations, two sticklebacks were recognized as the most abundant native fish species of the Solovetsky Archipelago: the three-spined stickleback *Gasterosteus aculeatus* and the nine-spined stickleback *Pungitius pungitius*. These fish play an important role in inshore and offshore communities of the White Sea, being a common prey of predatory fish species and marine mammals. There have been few parasitological studies of the White Sea sticklebacks. Most parasitological data available on sticklebacks from the White Sea concern its marine forms from various areas and sticklebacks from the river mouth areas at the White Sea coast. So far, there is no information on parasites of sticklebacks of the Solovetsky Archipelago. In this paper, we present data on parasites of two stickleback species, *P. pungitius* (freshwater and marine forms) and *G. aculeatus* (marine form), caught in the Solovetsky Archipelago waters (the White Sea). Standard parasitological investigation methods were implemented. *Diplostomum spathaceum* metacercariae were additionally identified with the use of mitochondrial marker *cox*1. The parasitic fauna of both stickleback species from two study sites at the Solovetsky Archipelago was poor. Ten parasite species belonging to Copepoda, Monogenea, Nematoda, Cestoda, and Trematoda were found. The marine three-spined stickleback caught off the coast of the archipelago was infected with 6 helminth species. The parasitic fauna of the nine-spined stickleback from a freshwater stream on Bolshoy Solovetsky Island comprised 4 helminth species, while the marine form harbored 5 species. *Cryptocotyle* sp. metacercariae were the most abundant and widespread parasites recorded during our study. Most of the parasite species were acquired by sticklebacks through various invertebrate food items. Zoonotic species (nematodes *Eustrongylides excisus*, cestodes *Diphyllobothrium* spp., and trematodes *Cryptocotyle* spp.) were revealed in fish analyzed. Further research is needed on the parasites of various fish species of the Solovetsky Archipelago, *inter alia* applying molecular methods.

Keywords: Bolshoy Solovetsky Island, Anzersky Island, *Gasterosteus aculeatus*, *Pungitius pungitius*, parasites, *Diplostomum*, *cox*1

The Solovetsky Archipelago, situated in the White Sea, comprises 6 large islands with a total area of 295.23 km^2 and more than 110 small islands. The largest 2 islands, Bolshoy Solovetsky and Anzersky, possess an extensive system of lakes connected by streams and canals with each other and with the sea [Prirodnaya sreda Solovetskogo arkhipelaga, 2007].

The study of hydrobionts, including fish, from freshwater bodies of the Solovetsky Archipelago is of certain interest for understanding historical processes of fauna formation [Bolotov, 2014]. Firstly, the freshwater ichthyofauna of the Solovetsky Islands was investigated by A. Zakhvatkin [1927a]. Then, it was monitored in 1989–2016, and 40 lakes located on these islands were examined. As a result of this long-term monitoring, 15 fish species have been classified into two groups: aboriginal and introduced ones (see the review of Ja. Alekseeva *et al.*, 2014). The changes in the condition of lake ichthyofauna have been identified and shown to be associated mainly with natural factors [Alekseeva, Makhrov, 2018; Alekseeva et al., 2014].

The most numerous aboriginal fish species on the Solovetsky Archipelago are the perch (*Perca fluviatilis* Linnaeus, 1758) and two sticklebacks: the three-spined stickleback *Gasterosteus aculeatus* (Linnaeus, 1758) and the nine-spined stickleback *Pungitius pungitius* (Linnaeus, 1758) [Alekseeva et al., 2014]. The three-spined stickleback is also the most abundant fish species in the White Sea in general, playing a significant role in inshore and offshore communities and being a common prey of predatory fish species [Lajus et al., 2020]. Moreover, both sticklebacks are a common component of the diet of marine mammals in the White Sea [Svetochev, Svetocheva, 2010; Svetocheva, Svetochev, 2015].

Recent genetic data indicate that the three-spined stickleback arrived in the White Sea basin from both Europe and North America after glacial recession [Artamonova et al., 2022]. Therefore, one may expect it to harbor a diverse parasitic fauna. However, there have been few parasitological studies of sticklebacks in the White Sea. Most parasitological information available on stickleback from the White Sea concerns its marine forms from various areas [Isakov, 1970, 1974; Rybkina et al., 2016; Shulman, Shulman-Albova, 1953]. There are also some parasitological data on sticklebacks from the river mouth areas at the White Sea coast [Lumme et al., 2016; Mitenev, Shulman, 2005]. So far, there is no information on the parasites of sticklebacks of the Solovetsky Archipelago.

In this study, we present the first data on the parasites of freshwater and marine forms of *Pungitius pungitius* and marine form of *Gasterosteus aculeatus* from the Solovetsky Archipelago.

MATERIAL AND METHODS

The material for the study was sampled in July 2016 and 2022 in two sampling sites situated on the watershed of Bolshoy Solovetsky Island of the Solovetsky Archipelago (Fig. 1).

The first sampling site was the so-called Filippovskie cages (N65.03°, E35.68°), a narrow bay separated from the sea by an artificial dam. It is thought to have served as enclosure for keeping marine fish in cages. Three-spined sticklebacks (14 specimens on 3 July, 2016, and 6 specimens on 3 July, 2022) and nine-spined sticklebacks (5 specimens on 3 July, 2022) were caught in the bay with a dip net. Three-spined sticklebacks were 60–70 mm long, while nine-spined sticklebacks were 40–60 mm.

The second sampling site was a small freshwater stream near the Solovetsky Settlement (N65.03°, E35.71°) flowing into the White Sea. Nine-spined sticklebacks were caught in the stream with a dip net on 2 July, 2016 (14 specimens), and on 3 July, 2022 (11 specimens). Their length ranged from 25 to 65 mm.

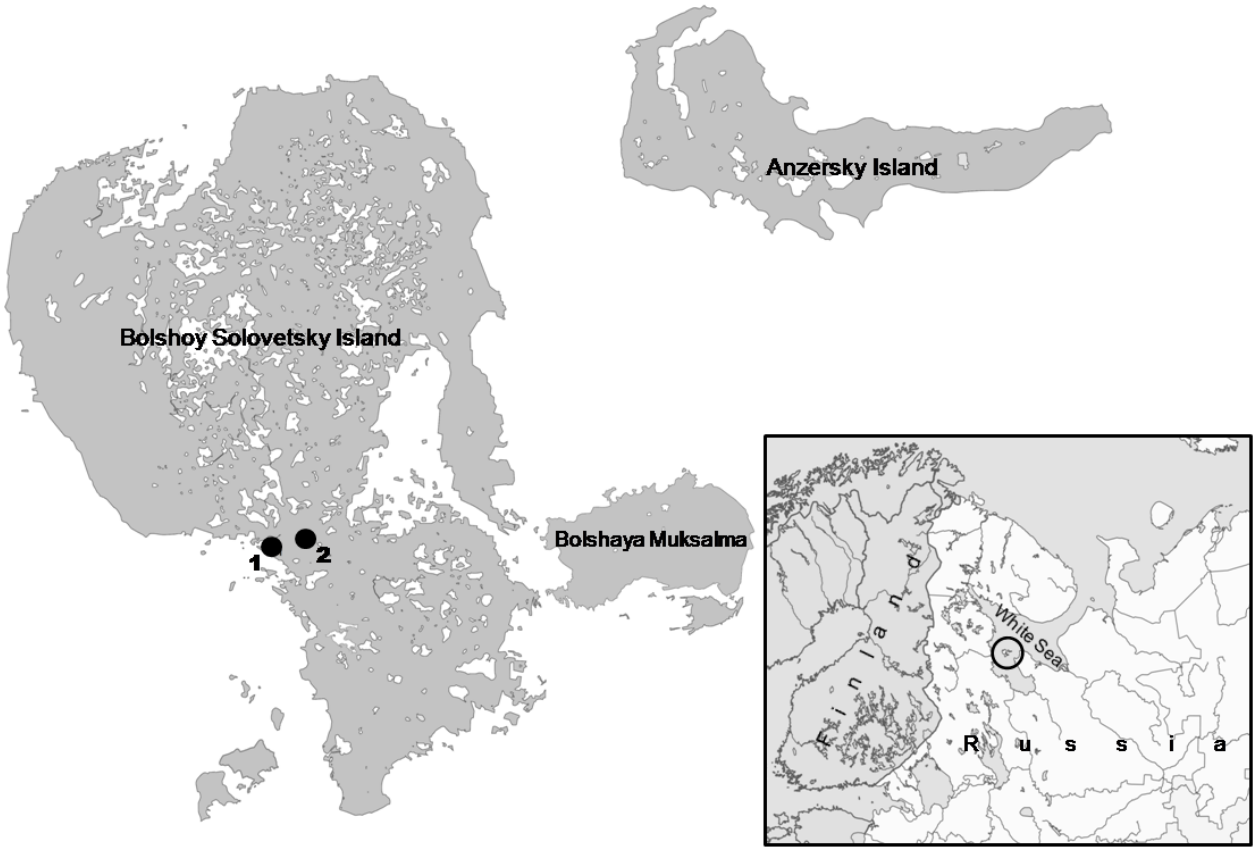

Fig. 1. Sampling sites: 1, Filippovskie cages; 2, a stream near the Solovetsky Settlement

All specimens were examined macroscopically for the presence of ectoparasites immediately after capture and then dissected and studied for endoparasitic helminths and other metazoan parasites using a standard parasitological method [Bykhovskaya-Pavlovskaya, 1985]. All parasites were preserved in 70% and 96% ethanol. Nematodes were cleared in 80% lactic acid, and temporary glycerol preparations were made. Parasitic copepods were fixed in 70% alcohol and mounted on slides with Faure–Berlese mounting medium. Monogeneans were cut into two parts. The opisthaptors were prepared for morphological examination, and then partially digested by proteinase K in a final concentration of 60 $\mu g \cdot mL^{-1}$ *prior* to their preservation in ammonium picrate-glycerin [Zietara, 2004]. Cestodes were stained with iron acetocarmine, dehydrated through a graded ethanol series, clarified in clove oil, and finally mounted in Canada balsam [Georgiev et al., 1986].

Trematodes were stained with acetocarmine, dehydrated, contrasted (cleared) with dimethyl phthalate, and finally mounted in Canada balsam. Trematodes of the genus *Diplostomum* von Nordmann, 1832 were sampled for an integrative study with the use of both molecular and morphological approach. Several metacercariae were stained with acetocarmine and mounted in Canada balsam. Measurements and morphological identification of parasites were made under an Olympus CX41 microscope according to the keys of S. Delyamure *et al.* [1985]; A. Shigin [1986]; A. Gusev [1987]; R. Bray and R. Campbell [1996]; F. Moravec [1994]; T. Scholz *et al.* [2007]; and O. Pugachev *et al.* [2010].

Ecological parameters characterizing fish infection, prevalence, and mean abundance were calculated according to A. Bush *et al.* [1997].

Diplostomum metacercariae were investigated applying molecular method. Genomic DNA was isolated from an ethanol-fixed specimen (in total, two metacercaria from two different fish species were studied this way) using DNA-Extran kits (Syntol, Russia). The fragment of the mtDNA *cox*1 gene was amplified using the primers Cox1_schist_5' (5'-TCTTTRGATCATAAGCG-3') and Cox1_schist_3' (5'-TAATGCATMGGAAAAAAACA-3') of A. Lockyer *et al.* [2003]. PCR assay was carried out in 25 μL of reaction mixture containing 10 ng of total DNA, 75 mM of Tris-HCl (pH 8.8), 20 mM of $(NH_4)_2SO_4$, 0.01% Tween 20, 5 mM of $MgCl_2$, 0.25 mM of each dNTP, 1.5 pmol of each primer, and 0.6–0.7 U of Taq DNA polymerase. Cycling parameters of PCR amplification followed those of [Lockyer et al., 2003].

PCR products were purified using ColGen Extraction Kit (Syntol) following the manufacturer's instructions and then sequenced directly using the same primers of PCR reactions with MegaBACE 1000 DNA Analysis System (Beagle, Saint Petersburg, Russia) (https://biobeagle.com/). Consensus sequences (404 bp) were assembled in MEGA v. 10 [Kumar et al., 2018]. The sequences were deposited in GenBank with accession numbers ON995624 and ON995625.

Identity of newly-generated sequences was checked with the Basic Local Alignment Search Tool (BLAST, https://blast.ncbi.nlm.nih.gov/Blast.cgi). The novel sequences were aligned with the representative sequences of *Diplostomum* spp. previously reported from different places with MUSCLE algorithms implemented in MEGA v. 10 [Kumar et al., 2018] and edited manually. The *cox*1 alignment (353 nt) comprised 2 novel and 44 sequences of *Diplostomum* spp. from GenBank. *Tylodelphys clavata* (JX986908) were used as an outgroup.

Bayesian Inference analysis was conducted using MrBayes software (v. 3.2.3) [Ronquist et al., 2012] with TN93 + I + G model assigned in jModelTest 2.1.2 [Darriba et al., 2012]. Markov chain Monte Carlo (MCMC) simulations were run for 3,000,000 generations, log-likelihood scores were plotted, and only the final 75% of trees were used to produce the consensus trees by setting the "burn in" parameter at 7,500. FigTree v. 1.4 software [Rambaut, 2018] was used to visualize the trees.

RESULTS

The parasitic fauna of the two stickleback species examined in our study was represented by 10 species (Tables 1, 2) from 5 systematic groups: Copepoda, Monogenea, Nematoda, Cestoda, and Trematoda. Six of these species were found in sticklebacks caught in the sea: *Thersitina gasterostei* (Pagenstecher, 1861); *Bothriocephalus scorpii* (Müller, 1776) Cooper, 1917; *Diphyllobothrium* sp.; *Hysterothylacium aduncum* (Rudolphi, 1802) Deardorff & Overstreet, 1981; *Podocotyle reflexa* (Creplin, 1825) Odhner, 1905; and *Cryptocotyle* sp. The monogenean *Gyrodactylus arcuatus* Bychowsky, 1933 was registered in both marine and freshwater sticklebacks. Three species were recorded in sticklebacks caught in the freshwater stream: *Eustrongylides excisus* Jägerskiöld, 1909; *Proteocephalus ambiguus* (Dujardin, 1845) Weinland, 1858; and *Diplostomum spathaceum* (Rudolphi, 1819) Olsson, 1876.

The morphological taxonomy of the genus *Diplostomum* is rather complex; so, we barcoded the metacercariae with the mitochondrial marker *cox*1 (Fig. 2). The sequences formed a well-supported clade with representatives of *D. spathaceum* from different host species and geographical locations, with the *p*-distance values ranging from −0.2 to 1.1%. The *p*-distance value for metacercariae sequences from *P. pungitius* and *G. aculeatus* was 0.2%.

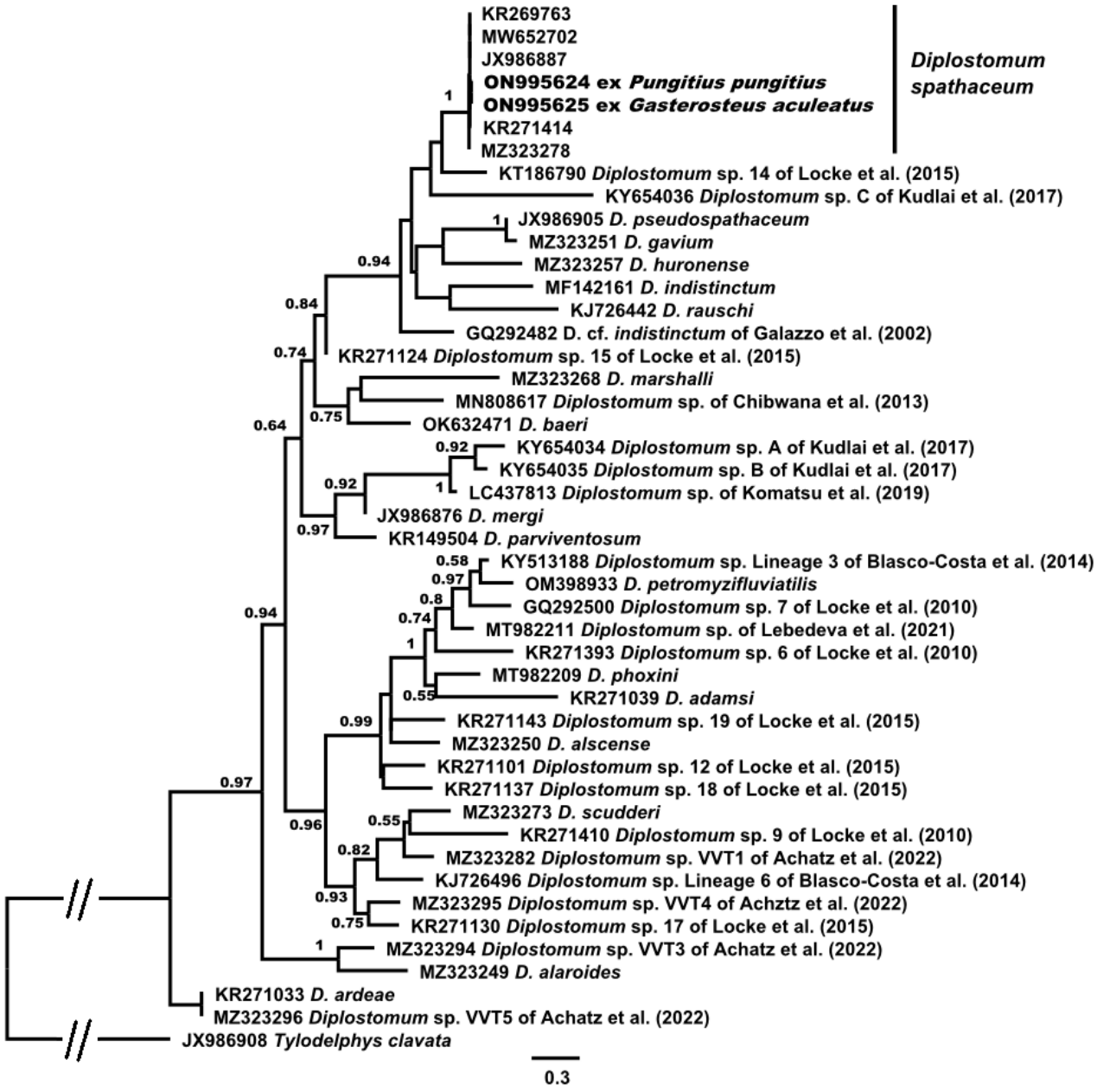

Fig. 2. Phylogenetic tree of *Diplostomum* spp. based on the partial *cox*1 mtDNA sequences (353 bp) inferred using Bayesian Inference analysis. Values lower than 0.5 are not shown. New sequences are in bold

The nine-spined stickleback harbored representatives of all 5 systematic groups recorded in our study (Table 1). Ectoparasites were represented by the crustacean *T. gasterostei* and the monogenean *G. arcuatus*. The latter parasite was the most common, although not numerous. The most species-rich group of endoparasites were cestodes: 3 species, each represented by 1 individual, were found (see Table 1). The cestode *P. ambiguus* was observed in the intestines of *P. pungitius* freshwater form, while *B. scorpii* was noted in the intestines of the marine form. Several plerocercoids of *Diphyllobothrium* sp. were registered on the intestinal wall of two marine nine-spined sticklebacks. The larvae of nematodes *E. excisus* were found on the intestinal wall in almost half of the fish specimens from the stream, though only 1 larva *per* fish was recorded in all the cases. Speaking about trematodes,

Cryptocotyle spp. metacercariae infected all individuals of the marine stickleback, and the infection was high. In contrast, *D. spathaceum* larvae were found only in several individuals of the freshwater fish (Table 1).

Table 1. Parasites of the nine-spined stickleback *Pungitius pungitius* of Bolshoy Solovetsky Island

Parasite species	Freshwater locality				Marine locality	
	2016		2022		2022	
	P, %	M (min–max)	P, %	M (min–max)	P, %	M (min–max)
Copepoda						
Thersitina gasterostei (Pagenstecher, 1861)	–	–	–	–	4 / 5*	1.4 (1–3)
Monogenea						
Gyrodactylus arcuatus Bychowskiy, 1933	14	1.3 (8–10)	82	4.7 (1–18)	4 / 5	1.5 (1–3)
Nematoda						
Eustrongylides excisus Jägerskiöld, 1909, l.	43	0.5 (1–2)	–	–	–	–
Cestoda						
Bothriocephalus scorpii (Müller, 1776) Cooper, 1917	–	–	–	–	1 / 5	0.4 (2)
Proteocephalus ambiguus (Dujardin, 1845) Weinland, 1858	–	–	27	0.45 (1–3)	–	–
Diphyllobothrium sp., pl.	–	–	–	–	2 / 5	1.0 (1–4)
Trematoda						
Diplostomum spathaceum (Rudolphi, 1819) Olsson, 1876, mtc	29	0.5 (1–3)	–	–	–	–
Cryptocotyle sp., l.	–	–	–	–	5 / 5	4.6 (1–9)
Number of fish examined	14		11		5	
Number of parasite species	4		2		5	

Note: P, prevalence; M, mean abundance; min–max, minimum and maximum number of parasite individuals *per* fish; l., larva; pl., plerocercoid; mtc, metacercaria; *, number of invaded hosts / number of investigated hosts.

The parasitic fauna of three-spined sticklebacks, all of which were caught in the sea, was represented by 6 species belonging to 4 systematic groups: Copepoda, Monogenea, Nematoda, and Trematoda. In contrast with the nine-spined stickleback, no Cestoda species were found in the three-spined stickleback (Table 2).

Metacercariae of *Cryptocotyle* sp., the most numerous and widespread parasites of marine *G. aculeatus*, were found on the skin, fins, and gills. Ectoparasites *T. gasterostei* from the gills and operculum were less numerous. Single specimens of *G. arcuatus* were observed on the gills of several fish. Larvae of nematodes *H. aduncum* were detected on the intestinal wall in 4 out of 6 fish examined. A metacercaria recorded in the lens of one stickleback belonged to *D. spathaceum*, which was also confirmed by molecular methods (Fig. 2). One specimen of the trematode *P. reflexa* was registered in the intestine. In our study, all the parasite species found in the three-spined stickleback were parasites of marine fish, except for *D. spathaceum*.

Table 2. Parasites of *Gasterosteus aculeatus* of Bolshoy Solovetsky Island

Parasite species	Marine locality			
	2016		2022	
	P, %	M (min–max)	P, %	M (min–max)
Copepoda				
Thersitina gasterostei (Pagenstecher, 1861)	93	5.9 (1–31)	5 / 6*	4.2 (1–9)
Monogenea				
Gyrodactylus arcuatus Bychowskiy, 1933	14	1.3 (8–10)	6 / 6	3.8 (1–8)
Nematoda				
Hysterothylacium aduncum (Rudolphi, 1802) Deardorff & Overstreet, 1981, l.	–	–	4 / 6	2.5 (2–6)
Trematoda				
Diplostomum spathaceum (Rudolphi, 1819) Olsson, 1876, mtc	7	0.1 (1)	–	–
Podocotyle reflexa (Creplin, 1825) Odhner, 1905	–	–	1 / 6	0.2 (1)
Cryptocotyle spp., mtc	100	3.1 (1–5)	6 / 6	5.4 (3–12)
Number of fish examined	14		6	
Number of parasite species	4		5	

Note: P, prevalence; M, mean abundance; min–max, minimum and maximum number of parasite individuals *per* fish; l., larva; mtc, metacercaria; *, number of invaded hosts / number of investigated hosts.

DISCUSSION

The parasitic fauna of *G. aculeatus* (marine form) and *P. pungitius* (marine and freshwater forms) obtained from two study sites at the Solovetsky Archipelago comprised 10 species. Marine forms of these two sticklebacks had only 3 parasite species in common: *T. gasterostei*, *G. arcuatus*, and *Cryptocotyle* sp. (see Tables 1, 2). Their other helminths were different, which reflected the differences in their life styles.

Two parasites, *G. arcuatus* and *D. spathaceum*, were recorded both in marine and freshwater sticklebacks. This finding agrees with the literature data. According to L. Isakov [1970] and J. Lumme *et al.* [2016], *G. arcuatus* can parasitize both marine and freshwater fish. *D. spathaceum* metacercariae have been found in fish from brackish waters [Karvonen, Marcogliese, 2020].

The finding of the trematode *P. reflexa* in *G. aculeatus* intestines is very interesting, even though only 1 specimen was recorded. This species has never been registered in the sticklebacks of the White Sea before, while a close species, *Podocotyle atomon* (Rudolphi, 1802) Odhner, 1905, has been observed [Rybkina et al., 2016; Shulman, Shulman-Albova, 1953].

Sticklebacks become infected with various parasites found in our study in several ways. Only 2 species, *G. arcuatus* and *T. gasterostei*, have direct life cycles. Those are transmitted from one host to another or reproduce on the same host. This infection mode suggests that there is a constant source of infection in both marine and freshwater fish populations.

Other parasite species were acquired by the sticklebacks through various invertebrate food objects. We found chitinous odds of insects and crustaceans, small gastropod, and bivalves in the intestines of freshwater nine-spined stickleback. The gut of marine nine-spined sticklebacks contained only amorphous contents. In the intestines of marine three-spined stickleback, odds of insect larvae, crustaceans, small bivalves, and algae were recorded.

The presence of large number of helminths registered in our study indicates that sticklebacks feed on benthos. We found the larvae of nematodes *E. excises*, whose development is associated with benthic oligochaetes *Lumbriculus* Grube, 1844, *Tubifex* Lamarck, 1816, and *Limnodrilus* Claparède, 1862 [Baruš et al., 1978]. Species of these 3 genera have been recorded in the Solovetsky Islands waters [Popchenko, 1972].

The same fish was infected with *D. spathaceum* metacercariae, whose larvae leave their first intermediate host and actively penetrate the second intermediate host through the skin [Shigin, 1986]. In all probability, while feeding on benthos, the sticklebacks were infected with diplostomes from *Lymnaea* spp. These molluscs were noted in water bodies of the Solovetsky Archipelago, in particular, in the small lake, through which the stream where we caught sticklebacks flows [Bespalaya et al., 2021; Zakhvatkin, 1927b]. The nematode *H. aduncum* infects fish feeding on marine invertebrates, such as polychaetes, amphipods, copepods, and chaetognaths. The trematode *P. reflexa* infects fish through various crustaceans [Køie, 1981; Moravec, 1994].

Marine forms of both stickleback species were infected by *Cryptocotyle* spp. metacercariae that actively penetrated the host after they left their intermediate host, the mudsnail *Peringia ulvae* (Pennant, 1777) [Golovin et al., 2021; Gonchar, 2020]. This finding indicates that the fish keep close to the littoral shallows.

The nine-spined sticklebacks from the stream examined in 2022 mostly fed on plankton. It is evidenced by the infection with the cestode *P. ambiguus*, which occurs through eating planktonic crustaceans *Eudiaptomus gracilis* (Sars G. O., 1863) and *Cyclops strenuus* Fischer, 1851 [Scholz, 1999], common on Bolshoy Solovetsky Island [Zakhvatkin, 1927a]. Moreover, these fish were not infested with diplostomids (see Table 1).

In the sea, the nine-spined stickleback is also more likely to feed on plankton, as evidenced by infection with the cestodes *B. scorpii* and *Diphyllobothrium* sp. The fish become infected with the former parasite by eating planktonic crustaceans *Acartia* (*Acartiura*) *longiremis* (Lilljeborg, 1853), which was described for the White Sea as an intermediate host of *B. scorpii* [Grozdilova, Makrushin, 1985].

The parasitic fauna of both stickleback species from two study sites at the Solovetsky Archipelago included parasites common for these fish in nearby northern ecosystems of the White and Barents seas [Isakov, 1974; Mitenev, Shulman, 2005; Rybkina et al., 2016; Shulman, Shulman-Albova, 1953] but was poorer in general. It was also poorer than the parasitic fauna of sticklebacks from Onega and Ladoga, large lakes situated further to the south [Rumyantsev, 2007]. Some of the helminths found in all the above-mentioned water bodies, such as *Schistocephalus solidus* (Müller, 1776) Steenstrup, 1857 and *Diplostomum pungitii* Shigin, 1965, are absent in the sticklebacks from the Solovetsky Archipelago. Apparently, this is due to the absence of the first intermediate hosts necessary for the helminth development or due to a local habitat separation from definitive hosts, fish-eating birds, though the latter ones are numerous and diverse at the Solovetsky Archipelago [Cherenkov et al., 2014]. To the north, V. Mitenev and B. Shulman [2005] recorded only *Schistocephalus pungitii* Dubinina, 1959 in *P. pungitius*, and the closest locality of *S. solidus* in *G. aculeatus* is Mashinnoe Lake, Karelian coast of the White Sea [Borvinskaya et al., 2021]. Besides, the parasitic fauna of freshwater sticklebacks of the Solovetsky Archipelago does not include numerous nonspecific species, especially larval forms of trematodes

Ichthyocotylurus Odening, 1969, *Apatemon* Szidat, 1928, *Tylodelphys* Diesing, 1850, and *Diplostomum*, noted in many northern water bodies [Kuhn et al., 2015; Mitenev, Shulman, 2005; Rumyantsev, 2007; Soldánová et al., 2017].

Zoonotic species found in our material deserve special mention. Those were represented by larvae of the nematode *E. excisus* in freshwater *P. pungitius*, plerocercoids of *Diphyllobothrium* spp. in marine *P. pungitius*, and metacercariae of *Cryptocotyle* spp. in all marine fish. These parasites may cause diseases of birds and mammals, possibly including humans [Duflot et al., 2021; Guardone et al., 2021; Waeschenbach et al., 2017]. Their presence in our material is a consequence of the fact that both stickleback species are an integral part of the diet of ringed seal [Svetochev, Svetocheva, 2010; Svetocheva, Svetochev, 2015], which probably promotes the abundance and dispersal of these parasites.

Nematodes *Eustrongylides* spp. are cosmopolitan parasites using several freshwater fish species as intermediate or paratenic hosts. These nematodes have not been found in either of the two stickleback species before [Moravec, 1994]. In all likelihood, their invasion is related to their ubiquitous distribution and temporary contact with the final host, the cormorant *Phalacrocorax carbo* (Linnaeus, 1758), which forms large colonies on the Solovetsky Archipelago [Cherenkov et al., 2014]. Similarly, *E. excisus* was shown to infect the large-scale sand smelt (*Atherina boyeri* A. Risso, 1810) in the lake Massaciuccoli (Italy) [Guardone et al., 2021].

Another exciting finding is the discovery on the intestinal wall of the marine nine-spined stickleback of plerocercoids of the genus *Diphyllobothrium* Cobbold, 1921. According to A. Waeschenbach et al. [2017], this genus now includes only the worms whose development ends in marine mammals and, probably, in humans. Those are a threat to human health, and their investigation is very important. The larvae found in our study presumably belong to 1 of 4 *Diphyllobothrium* spp. previously noted in marine mammals in the White Sea: *Diphyllobothrium cordatum* (Leuckart, 1863) Gedoelst, 1911; *D. lanceolatum* (Krabbe, 1865) Cooper, 1921; *D. roemeri* (Zschokke, 1903) Meggitt, 1924; and *D. tetrapterum* (von Siebold, 1848) [Delyamure et al., 1985]. However, taking into account the species composition and migratory pathways of marine mammals from the White Sea to the Barents Sea and back [Lukin, Ognetov, 2009; Stenson et al., 2020; Svetochev et al., 2017], it cannot be ruled out that we found *Diphyllobothrium schistochilos* (Germanos, 1895) Cooper, 1858, which has been identified in the Barents Sea, but has never been recorded in the White Sea before [Schaeffner et al., 2018].

High infection levels of sticklebacks by *Cryptocotyle* spp. metacercariae, which were noted during our study and in different spots of the White Sea [Golovin et al., 2021; Rybkina et al., 2016], are associated with favorable conditions for the implementation of the life cycle of this trematode. Its first intermediate hosts are mudsnails *P. ulvae*, and its final hosts are fish-eating birds or marine mammals [Duflot et al., 2021]. *P. ulvae* are numerous in the White Sea [Golovin et al., 2021; Gonchar, 2020]; moreover, fish-eating birds (for example, the cormorant) and marine mammals (including the ringed seal) are widespread in the White Sea and around the Solovetsky Islands [Cherenkov et al., 2014; Chernetsky et al., 2011; Lukin et al., 2006; Surkov, 1957].

Future research of the fish parasites from the Solovetsky Archipelago, *inter alia* molecular studies, will be expanded for several reasons. Firstly, the data on parasites of various freshwater fish species of the Solovetsky Islands, which are now lacking, would be useful to explore the historical processes of formation of the islands' fauna. Secondly, the systematics of many parasite groups (e. g., *Diphyllobothrium* and *Diplostomum*) is currently being revised with the use of the integrative method, and any information on these helminths is in demand. Finally, fish play a significant role in maintaining populations of epizootically important species (*Eustrongylides excisus*, *Cryptocotyle* spp., and *Diphyllobothrium* sp.).

This work was carried out within the framework of the state research assignment No. 122032100130-3 and the Russian Science Foundation grant No. 19-14-00066-P (https://rscf.ru/project/19-14-00066/).

Acknowledgement. The authors are grateful to D. Sc. Anna Suschuk for her help with the identification of free-living benthic nematodes from fish food.

REFERENCES

1. Alekseeva Ja. A., Andreeva A. P., Gruzdeva M. A., Dvoryankin G. A., Kuzishchin K. V., Makhrov A. A., Novoselov A. P., Popov I. Yu. Freshwater ichthyofauna of Solovetsky Islands (White Sea): Natural colonization and recent introductions. *Russian Journal of Biological Invasions*, 2014, vol. 5, iss. 3, pp. 125–133. https://doi.org/10.1134/S2075111714030023
2. Alekseeva Ya. A., Makhrov A. A. Monitoringovye issledovaniya ikhtiofauny ozer Solovetskogo arkhipelaga (1995–2016 gg.). *Solovetskii sbornik*, 2018, vol. 14, pp. 137–149. (in Russ.)
3. Artamonova V. S., Bardukov N. V., Aksenova O. V., Ivanova T. S., Ivanov M. V., Kirillova E. A., Koulish A. V., Lajus D. L., Malyutina A. M., Pashkov A. N., Reshetnikov S. I., Makhrov A. A. Round-the-world voyage of the threespine stickleback (*Gasterosteus aculeatus*): Phylogeographic data covering the entire species range. *Water*, 2022, vol. 14, iss. 16, art. no. 2484 (23 p.). https://doi.org/10.3390/w14162484
4. Bespalaya Y. V., Aksenova O. V., Bolotov I. N., Aksenov A. S. Freshwater mollusks in lakes of the Solovetsky Islands (the White Sea). In: *Lake Water: Properties and Uses (Case Studies of Hydrochemistry and Hydrobiology of Lakes in Northwest Russia)* / O. S. Pokrovsky, Y. Bespalaya, T. Y. Vorobyeva, L. S. Shirokova (Eds). New York, USA : Nova Science Publishers, 2021, pp. 249–265.
5. Baruš V., Sergeeva T. P., Sonin M. D., Ryzhikov K. M. *Helminths of Fish-Eating Birds of the Palaearctic Region 1. Nematoda.* Prague : Academia, 1978, 318 p. https://doi.org/10.1007/978-94-009-9972-5
6. Bolotov I. N. Pathways of formation of the fauna of the Solovetsky Archipelago, the White Sea, Northwest Russia. *Entomological Review*, 2014, vol. 94, iss. 4, pp. 562–578. https://doi.org/10.1134/S0013873814040095
7. Borvinskaya E. V., Kochneva A. A., Drozdova P. B., Balan O. V., Zgoda V. G. Temperature-induced reorganisation of *Schistocephalus solidus* (Cestoda) proteome during the transition to the warm-blooded host. *Biology Open*, 2021, vol. 10, iss. 11, art. no. bio058719 (11 p.). https://doi.org/10.1242/bio.058719
8. Bray R. A., Campbell R. A. New plagioporines (Digenea: Opecoelidae) from deep-sea fishes of the North Atlantic Ocean. *Systematic Parasitology*, 1996, vol. 33, iss. 2, pp. 101–113. https://doi.org/10.1007/BF00009426
9. Bush A. O., Lafferty K. D., Lotz J. M., Shostak A. W. Parasitology meets ecology on its own terms: Margolis et al. revisited. *Journal of Parasitology*, 1997, vol. 83, no. 4, pp. 575–583. https://doi.org/10.2307/3284227
10. Bykhovskaya-Pavlovskaya I. E. *Parazity ryb. Rukovodstvo po izucheniyu.* Leningrad : Nauka, 1985, 121 p. (in Russ.). https://repository.marine-research.ru/handle/299011/9748
11. Cherenkov A. E., Semashko V. Yu., Tertitsky G. M. *Ptitsy Solovetskikh ostrovov i Onezhskogo zaliva Belogo morya : materialy issledovaniya (1983–2013 gg.).* Arkhangelsk : [s. n.], 2014, 383 p. (in Russ.)
12. Chernetsky A. D., Krasnova V. V., Bel'kovich V. M. Studies of the structure of the Solovetsky reproductive gathering of beluga whales (*Delphinapterus leucas*) in the White Sea using the photo identification method. *Oceanology*, 2011, vol. 51, no. 2, pp. 275–280. https://doi.org/10.1134/S0001437011020044

13. Darriba D., Taboada G. L., Doallo R., Posada D. jModelTest 2: More models, new heuristics and parallel computing. *Nature Method*, 2012, vol. 9, no. 8, pp. 772. https://doi.org/10.1038/nmeth.2109
14. Delyamure S. L., Skryabin A. S., Serdiukov A. M. Difillobotriidy – lentochnye gel'minty cheloveka, mlekopitayushchikh i ptits. In: *Osnovy tsestodologii.* Moscow : Nauka, 1985, vol. 11, 200 p. (in Russ.)
15. Duflot M., Gay M., Midelet G., Kania P. W., Buchmann K. Morphological and molecular identification of *Cryptocotyle lingua* metacercariae isolated from Atlantic cod (*Gadus morhua*) from Danish seas and whiting (*Merlangius merlangus*) from the English Channel. *Parasitology Research*, 2021, vol. 120, iss. 10, pp. 3417–3427. https://doi.org/10.1007/s00436-021-07278-6
16. Georgiev B. B., Biserkov V., Genov T. *In toto* staining method for cestodes with iron acetocarmine. *Helminthologia*, 1986, vol. 23, pp. 279–281.
17. Golovin P. V., Ivanov M. V., Ivanova T. S., Rybkina E. V., Lajus D. L. Characteristics of threespine stickleback (*Gasterosteus aculeatus* L.) infection with metacercariae of *Cryptocotyle* spp. trematodes during the spawning season in the White Sea. *Trudy Karel'skogo nauchnogo tsentra Rossiiskoi akademii nauk. Ekologicheskie issledovaniya*, 2021, no. 5, pp. 93–108. (in Russ.). https://doi.org/10.17076/eco1299
18. Gonchar A. Genetic diversity in monoxenous and trixenous digeneans sharing one molluscan host species. *Parazitologiya*, 2020, vol. 54, iss. 6, pp. 491–503. https://doi.org/10.31857/S1234567806060036
19. Guardone L., Ricci E., Susini F., Polsinelli E., Guglielmone G., Armani A. First detection of *Eustrongylides excisus* (Nematoda: Dioctophymatidae) in big-scale sand smelt (*Atherina boyeri*) from the lake Massaciuccoli (Northwest Tuscany, Italy): Implications for public health and seafood quality. *Food Control*, 2021, vol. 120, art. no. 107517 (8 p.). https://doi.org/10.1016/j.foodcont.2020.107517
20. Gusev A. V. Podklass Veslonogie rakoobraznye. Copepoda. In: *Opredelitel' parazitov presnovodnykh ryb fauny SSSR.* Vol. 3: *Paraziticheskie mnogokletochnye*. (Chast' vtoraya) / O. N. Bauer (Ed.). Leningrad : Nauka, 1987, pp. 382–515. (Opredeliteli po faune SSSR, izdavaenye Zoologicheskim institutom AN SSSR : iss. 149). (in Russ.)
21. Grozdilova T. A., Makrushin A. V. *Acartia* (Copepoda, Crustacea) – promezhutochnyi khozyain *Brachyphallus crenatus* (Trematoda). In: *Ekologicheskie issledovaniya perspektivnykh ob"ektov marikul'tury v Belom more* : sbornik / V. G. Kulachkova (Ed.). Leningrad : Zoologicheskii institut, 1985, pp. 84–86. (in Russ.)
22. Isakov L. S. On resistance of some specific ectoparasites of *Gasterosteus* to changes in the regime of salinity. *Parazitologiya*, 1970, vol. 4, iss. 1, pp. 18–24. (in Russ.)
23. Isakov L. S. Analysis of parasitofauna of sticklebacks of genus *Gasterosteus* and *Pungitius*. In: *VI Vsesoyuznoe soveshchanie po boleznyam i parazitam ryb* : tezisy dokladov. Moscow : [s. n.], 1974, pp. 97–100.
24. Karvonen A., Marcogliese D. J. Diplostomiasis (*Diplostomum spathaceum* and related species). In: *Climate Change and Infectious Fish Diseases* / P. T. K. Woo, J.-A. Leong, K. Buchmann (Eds). Wallingford : CABI, 2020, pp. 434–456. https://doi.org/10.1079/9781789243277.0434
25. Kuhn J. A., Kristoffersen R., Knudsen R., Jakobsen J., Marcogliese D. J., Locke S. A., Primicerio R., Amundsen P.-A. Parasite communities of two three-spined stickleback populations in subarctic Norway–effects of a small spatial-scale host introduction. *Parasitology Research*, 2015, vol. 114, iss. 4, pp. 1327–1339. https://doi.org/10.1007/s00436-015-4309-2
26. Kumar S., Stecher G., Li M., Knyaz Ch., Tamura K. MEGA X: Molecular Evolutionary Genetics Analysis across computing platforms. *Molecular Biology and Evolution*, 2018, vol. 35, iss. 6, pp. 1547–1549. https://doi.org/10.1093/molbev/msy096

27. Køie M. On the morphology and life-history of *Podocotyle reflexa* (Creplin, 1825) Odhner, 1905, and a comparison of its developmental stages with those of *P. atomon* (Rudolphi, 1802) Odhner, 1905 (Trematoda, Opecoelidae). *Ophelia*, 1981, vol. 20, iss. 1, pp. 17–43. https://doi.org/10.1080/00785236.1981.10426560
28. Lajus D. L., Golovin P. V., Zelenskaia A. E., Demchuk A. S., Dorgham A. S., Ivanov M. V., Ivanova T. S., Murzina S. A., Polyakova N. V., Rybkina E. V., Yurtseva A. O. Threespine stickleback of the White Sea: Population characteristics and role in the ecosystem. *Contemporary Problems of Ecology*, 2020, vol. 13, iss. 2, pp. 132–145. https://doi.org/10.1134/S1995425520020079
29. Lockyer A. E., Olson P. D., Østergaard P., Rollinson D., Johnston D. A., Attwood S. W., Southgate V. R., Horak P., Snyder S. D., Le T. H., Agatsuma T., McManus D. P., Carmichael A. C., Naem S., Littlewood D. T. J. The phylogeny of the Schistosomatidae based on three genes with emphasis on the interrelationships of *Schistosoma* Weinland, 1858. *Parasitology*, 2003, vol. 126, iss. 3, pp. 203–224. http://doi.org/10.1017/S0031182002002792
30. Lukin L. R., Ognetov G. N., Boyko N. S. *Ekologiya kol'chatoi nerpy v Belom more* / Rossiiskaya akademiya nauk, Ural'skoe otdelenie. Ekaterinburg : [s. n.], 2006, 166 p. (in Russ.)
31. Lukin L. R., Ognetov G. N. *Morskie mlekopitayushchie Rossiiskoi Arktiki: ekologo-faunisticheskii analiz* / Rossiiskaya akademiya nauk, Ural'skoe otdelenie. Ekaterinburg : Nauka, Ural'skoe otdelenie, 2009, 201 p. (in Russ.)
32. Lumme J., Mäkinen H., Ermolenko A. V., Gregg J. L., Ziętara M. S. Displaced phylogeographic signals from *Gyrodactylus arcuatus*, a parasite of the three-spined stickleback *Gasterosteus aculeatus*, suggest freshwater glacial refugia in Europe. *International Journal for Parasitology*, 2016, vol. 46, iss. 9, pp. 545–554. https://doi.org/10.1016/j.ijpara.2016.03.008
33. Mitenev V. K., Shulman B. S. Parasite fauna in sticklebacks (Gasterosteidae) from water bodies of the Kola Region. *Parazitologiya*, 2005, vol. 39, iss. 1, pp. 16–24. (in Russ.)
34. Moravec F. *Parasitic Nematodes of Freshwater Fishes of Europe.* Dordrecht : Springer, 1994, 470 p.
35. Popchenko V. I. Maloshchetinkovye chervi ozer Solovetskogo arkhipelaga. In: *Vodnyye maloshchetinkovye chervi (sistematika, ekologiya, issledovaniya fauny SSSR)*. Moscow : Nauka, 1972, pp. 42–50. (Trudy Vsesoyuznogo gidrobiologicheskogo obshchestva ; vol. 17). (in Russ.)
36. *Prirodnaya sreda Solovetskogo arkhipelaga v usloviyakh menyayushchegosya klimata* / Yu. G. Shvartsman, I. N. Bolotov (Eds.) ; Rossiiskaya akademiya nauk, Ural'skoe otdelenie. Ekaterinburg : [s. n.], 2007, 184 p. (in Russ.)
37. Pugachev O. N., Gerasev P. I., Gussev A. V. Ergens R., Khotenowsky I. *Guide to Monogenoidea of Freshwater Fish of Palaeacrtic and Amur Regions.* Milano : LediPublishing, 2010, 567 p.
38. Rambaut A. *FigTree v1.4. Molecular Evolution, Phylogenetics and Epidemiology* : [site]. 2018. URL: https://github.com/rambaut/figtree/releases [accessed: 15.10.2022].
39. Ronquist F., Teslenko M., van Der Mark P., Ayres D. L., Darling A., Höhna S., Huelsenbeck J. P. MrBayes 3.2: Efficient Bayesian phylogenetic inference and model choice across a large model space. *Systematic Biology*, 2012, vol. 61, iss. 3, pp. 539–542. https://doi.org/10.1093/sysbio/sys029
40. Rumyantsev E. A. *Parazity ryb v ozerakh Evropeiskogo Severa (fauna, ekologiya, evolyutsiya).* Petrozavodsk : Petrozavodskii gos. un-t, 2007, 249 p. (in Russ.)
41. Rybkina E. V., Demchuk A. S., Lajus D. L., Ivanova T. S., Ivanov M. V., Galaktionov K. V. Dynamics of parasite community during early ontogenesis of marine threespine stickleback, *Gasterosteus aculeatus*. *Evolutionary Ecology Research*, 2016, vol. 17, pp. 335–354.
42. Schaeffner B. C., Ditrich O., Kuchta R. A century of taxonomic uncertainty: Re-description

of two species of tapeworms (Diphyllobothriidea) from Arctic seals. *Polar Biology*, 2018, vol. 41, iss. 12, pp. 2543–2559. https://doi.org/10.1007/s00300-018-2396-0

43. Scholz T. Life cycles of species of *Proteocephalus*, parasites of fishes in the Palearctic Region: A review. *Journal of Helminthology*, 1999, vol. 73, iss. 1, pp. 1–19. https://doi.org/10.1017/S0022149X99000013
44. Scholz T., Hanzelová V., Škeříková A., Shimazu T., Rolbiecki L. An annotated list of species of the *Proteocephalus* Weinland, 1858 aggregate *sensu* de Chambrier et al. (2004) (Cestoda: Proteocephalidea), parasites of fishes in the Palaearctic Region, their phylogenetic relationships and a key to their identification. *Systematic Parasitology*, 2007, vol. 67, iss. 2, pp. 139–156. https://doi.org/10.1007/s11230-006-9089-8
45. Shigin A. A. *Trematody fauny SSSR. Rod Diplostomum. Metatserkarii.* Moscow : Nauka, 1986, 255 p. (in Russ.)
46. Shulman S. S., Shulman-Albova P. E. *Parasity ryb Belogo morya.* Moscow : Izd-vo Akademii nauk SSSR, 1953, 199 p. (in Russ.)
47. Soldánová M., Georgieva S., Roháčová Ja., Knudsen R., Kuhn J. A., Henriksen E. H., Siwertsson A., Shaw J. C., Kuris A. M., Amundsen P.-A., Scholz T., Lafferty K. D., Kostadinova A. Molecular analyses reveal high species diversity of trematodes in a sub-Arctic lake. *International Journal of Parasitology*, 2017, vol. 47, iss. 6, pp. 327–345. https://doi.org/10.1016/j.ijpara.2016.12.008
48. Stenson G. B., Haug T., Hammill M. O. Harp seals: Monitors of change in differing ecosystems. *Frontiers in Marine Science*, 2020, vol. 7, art. no. 569258 (20 p.). https://doi.org/10.3389/fmars.2020.569258
49. Surkov S. S. *Raspredeleniye i zapasy lysuna v Belom more.* Murmansk : PINRO, 1957, 60 p. (in Russ.)
50. Svetochev V. N., Svetocheva O. N. Winter feeding of the ringed seal (*Pusa hispida*) in the White Sea. In: *Marine Mammals of the Holarctic* : collection of scientific papers after the Sixth International Conference (Kaliningrad, Russia, October 11–15, 2010). Kaliningrad : Kapros, 2010, pp. 507–511.
51. Svetochev V. N., Svetocheva O. N., Kavtsevich N. N. Raspredelenie i migratsii nerpy (*Pusa hispida*) v Belom more po dannym sputnikovoi telemetrii. *Evraziiskoe nauchnoe ob"edinenie*, 2017, vol. 2, no. 11 (33), pp. 90–93. (in Russ.)
52. Svetocheva O. N., Svetochev V. N. Analysis of seasonality in trophic relationships of true seals (Phocideae) in the White Sea. *Czech Polar Reports*, 2015, vol. 5, no. 2, pp. 230–240. https://doi.org/10.5817/CPR2015-2-20
53. Waeschenbach A., Brabec J., Scholz T., Littlewood D. T. J., Kuchta R. The catholic taste of broad tapeworms – multiple routes to human infection. *International Journal of Parasitology*, 2017, vol. 47, iss. 13, pp. 831–843. https://doi.org/10.1016/j.ijpara.2017.06.004
54. Zakhvatkin A. A. *Solovetskie ozera : kratkii gidrobiologicheskii ocherk* / Solovetskoe obshchestvo kraevedeniya ; Biologicheskaya stantsiya. Solovki : Izdanie Byuro pechati USLON, 1927a, 142 p. (Materialy / Solovetskoe obshchestvo kraevedeniya ; iss. 9). (in Russ.)
55. Zakhvatkin A. A. Izmenchivost' *Limnea stagnalis* L. v Solovetskikh ozerakh. In: Zakhvatkin A. A., Yurkanskii V. N., Shershevskaya E. G. *K poznaniyu fauny Solovetskikh ostrovov* / Solovetskoe obshchestvo kraevedeniya ; Biologicheskaya stantsiya. Solovki : Izdanie Byuro pechati USLON, 1927b, pp. 7–16. (Materialy / Solovetskoe obshchestvo kraevedeniya ; iss. 7). (in Russ.)
56. Zietara M. S., Lumme J. Comparison of molecular phylogeny and morphological systematics in fish parasite genus *Gyrodactylus* Nordmann, 1832 (Monogenea, Gyrodactylidae). *Zoologica Poloniae*, 2004, vol. 49, no. 1–4, pp. 5–28.

МНОГОКЛЕТОЧНЫЕ ПАРАЗИТЫ ДВУХ ВИДОВ КОЛЮШЕК СОЛОВЕЦКОГО АРХИПЕЛАГА (БЕЛОЕ МОРЕ)

Д. И. Лебедева[1], Д. О. Зайцев[2], Я. И. Алексеева[3], А. А. Махров[4,5]

[1]Карельский научный центр РАН, Петрозаводск, Российская Федерация

[2]Петрозаводский государственный университет, Петрозаводск, Российская Федерация

[3]Государственный биологический музей имени К. А. Тимирязева, Москва, Российская Федерация

[4]Институт проблем экологии и эволюции имени А. Н. Северцова РАН, Москва, Российская Федерация

[5]Санкт-Петербургский государственный университет, Санкт-Петербург, Российская Федерация

E-mail: *daryal78@gmail.com*

Соловецкий архипелаг, расположенный в Белом море, состоит из шести крупных островов. Среди них два самых больших острова, Большой Соловецкий и Анзерский, характеризуются наличием обширной системы озёр, ручьёв и каналов, которые связаны между собой и с морем. Изучение гидробионтов, в том числе рыб, из пресноводных водоёмов Соловецкого архипелага необходимо для понимания исторических процессов формирования фауны. Мониторинг пресноводной ихтиофауны Соловецких островов ведётся более 30 лет. В результате этих наблюдений наиболее многочисленными аборигенными видами рыб на Соловецком архипелаге были признаны два вида колюшек — трёхиглая *Gasterosteus aculeatus* и девятииглая *Pungitius pungitius*. Эти рыбы играют важную роль в прибрежных и морских сообществах Белого моря, являясь обычной добычей хищных видов рыб и морских млекопитающих. Паразитологических исследований колюшек в Белом море проведено немного. Большинство имеющихся паразитологических сведений по колюшке из Белого моря касаются её морских форм из разных районов и колюшки из устьев рек на побережье Белого моря. До настоящего времени не было данных о паразитах колюшки Соловецкого архипелага. Нами получены первые сведения по паразитам двух видов колюшек, *P. pungitius* (пресноводная и морская форма) и *G. aculeatus* (морская форма), выловленных в водах Соловецкого архипелага (Белое море). Были применены стандартные методы паразитологического исследования. Метацеркарии *Diplostomum spathaceum* были дополнительно молекулярно идентифицированы с использованием митохондриального маркера *cox*1. Паразитофауна обоих видов колюшек из двух мест исследования на Соловецком архипелаге была бедной. Обнаружено 10 видов паразитов, относящихся к группам Copepoda, Monogenea, Nematoda, Cestoda и Trematoda. Морская трёхиглая колюшка, выловленная у береговой зоны архипелага, была заражена 6 видами гельминтов. Паразитофауна пресноводной девятииглой колюшки из ручья на Большом Соловецком острове включала 4 вида гельминтов; морская форма была инвазирована 5 видами. Метацеркарии *Cryptocotyle* sp. были самыми многочисленными и широко распространёнными паразитами, зарегистрированными в нашем исследовании. Большинство видов паразитов приобретаются колюшками через различных беспозвоночных как объектов питания. У проанализированных рыб выявлены имеющие важное значение зоонозные виды паразитов (нематоды *Eustrongylides excisus*, цестоды *Diphyllobothrium* spp. и трематоды *Cryptocotyle* spp.). Необходимы дальнейшие исследования паразитов различных видов рыб Соловецкого архипелага, в том числе с использованием молекулярных методов.

Ключевые слова: остров Большой Соловецкий, остров Анзерский, *Gasterosteus aculeatus*, *Pungitius pungitius*, паразиты, *Diplostomum*, *cox*1

1871
ИнБЮМ – IBSS

Морской биологический журнал
Marine Biological Journal
2023, vol. 8, no. 3, pp. 47–61
https://marine-biology.ru

UDC 582.261.1-152.4

INTERACTIONS OF THE DIATOM ALGAE *PSEUDO-NITZSCHIA HASLEANA* AND *THALASSIOSIRA PSEUDONANA* IN THE MIXED CULTURE

© 2023 **Zh. V. Markina[1] and A. Yu. Popik[2]**

[1]A. V. Zhirmunsky National Scientific Center of Marine Biology, FEB RAS, Vladivostok, Russian Federation
[2]Institute of Automation and Control Processes, FEB RAS, Vladivostok, Russian Federation
E-mail: *zhannav@mail.ru*

Received by the Editor 16.05.2022; after reviewing 08.06.2022;
accepted for publication 04.08.2023; published online 21.09.2023.

Representatives of the genus *Pseudo-nitzschia* (Bacillariophyta) cause blooms in different areas of the World Ocean. Therefore, it is necessary to know their ecological features, including the way those interact with other species of unicellular algae. Moreover, for rapid identification of these algae in the environment, a certain technique is needed. Thus, we assessed the dynamics of cell abundance for *Pseudo-nitzschia hasleana* and *Thalassiosira pseudonana* in mono- and mixed cultures by their direct counting in a Nageotte chamber. Temperature curves of chlorophyll *a* fluorescence obtained by laser-induced fluorescence in a temperature chamber were also analyzed. The experiments lasted for 14 days. As shown, *P. hasleana* had different effect on *T. pseudonana* depending on initial abundance of *T. pseudonana*. At initial concentration of 0.8×10^4 cells·mL^{-1}, a pronounced stimulation of the growth of this diatom occurred. At initial concentrations of 1.6×10^4 and 3.2×10^4 cells·mL^{-1}, *T. pseudonana* growth was inhibited. In the mixed culture, *T. pseudonana* remained at the stationary growth phase, while in a monoculture, the population entered the dying phase by the 14th day of the experiment. *T. pseudonana* had an inhibitory effect on *P. hasleana* growth. The experiment with *P. hasleana* and *T. pseudonana* co-cultivation showed as follows: chlorophyll *a* fluorescence of the mixture is more affected by the microalga with much higher concentration. The fluorescent signal of two separately cultivated monocultures can potentially be used to search for these cultures in a mixture.

Keywords: *Pseudo-nitzschia hasleana*, *Thalassiosira pseudonana*, allelopathy, chlorophyll *a* fluorescence, microalgae identification

Natural phytoplankton communities are affected by many environmental factors. Those can cause blooms or, conversely, prevent them [Lima-Mendez et al., 2015]. As shown, the dominance of *Pseudo-nitzschia* spp. toxic complex is associated with a decrease in N : Si ratio in the presence of sewage effluents. *Pseudo-nitzschia australis* Frenguelli, 1939 is capable of urea osmotrophy and active growth on it, which is the reason for blooms of this species [Burkholder et al., 2008]. The effect of biotic factors, in particular, microalgae interaction with each other, remains a less studied problem [Long et al., 2018]. Evaluation of the growth of mixed microalgae cultures in a laboratory experiment is one of the ways to analyze biotic interactions. Specifically, population–population relationships are investigated; boundaries of the stability of coexisting species are determined; and the conditions for their dominance and elimination are assesses [Mikheev et al., 2018]. However, there is still no standardized methodology for studying the effects of algal populations on each other, as in toxicological research [Long et al., 2018].

Pseudo-nitzschia representatives are ubiquitous in the waters of the World Ocean [Huang et al., 2009; Sobrinho et al., 2017; Trainer et al., 2012; Yasakova, 2013]. Those are of interest to researchers not only because of their periodic blooms, but also because of the presence of domoic acid which is toxic to warm-blooded animals [Trainer et al., 2012]. *Pseudo-nitzschia* abundance in a monospecific bloom can reach 1×10^6 cells·mL^{-1} [Louw et al., 2017], and the bloom can last for two months [Bates et al., 1989]. At the same time, *Pseudo-nitzschia* spp. can account for 99% of the total phytoplankton [Lundholm et al., 2005].

In the phytoplankton community, together with *Pseudo-nitzschia* spp., representatives of another genus of diatoms, *Thalassiosira*, are regularly recorded [Balzano et al., 2017; Orlova et al., 2009]. These genera were shown to have the same iron requirement [Cohen et al., 2017]. *Thalassiosira pseudonana* is involved in the phytoplankton succession cycle and is of great ecological importance as a species affecting the formation of phytoplankton blooms [Ianora et al., 2011]. The interest in this microalga is, among other things, due to cases of salmon death during its mass reproduction [Mardones, 2020]. Species of this genus are often found in the waters of temperate and polar seas [Harris et al., 1995].

As a rule, the mutual effect of cultures is assessed on allelopathically aggressive species, and to a lesser extent, on coexisting ones [Phatarpekar et al., 2000]. We have shown earlier that fluorescent characteristics of *Pseudo-nitzschia* can be used to identify it in water [Popik et al., 2022]. However, due to the mutual effect of algae during co-cultivation, the question arises whether the joint growth of different species can also affect chlorophyll *a* fluorescence in microalgae, making it difficult to identify them in the natural environment. Therefore, the aim of this work is to study growth and temperature curves of chlorophyll *a* fluorescence in diatoms *Pseudo-nitzschia hasleana* and *Thalassiosira pseudonana* in the mixed culture.

MATERIAL AND METHODS

The objects of study were strains of unicellular algae cultures, *Pseudo-nitzschia hasleana* Lundholm, 2012 MBRU_PH18 and *Thalassiosira pseudonana* Hasle & Heimdal, 1970 MBRU_TSP-02 (Bacillariophyta). The algae were grown on medium f [Guillard, Ryther, 1962] prepared on the basis of filtered and sterilized seawater with a salinity of 32‰, in 250-mL Erlenmeyer flasks with 100 mL of a culture medium, at a temperature of +18 °C, an illumination intensity of 70 μmol·m^{-2}·s^{-1}, and a light–dark period of 14 h : 10 h (light : dark). Cultures at the exponential growth stage were used as inoculum. Initial cell concentrations were 0.1×10^4 cells·mL^{-1} for *P. hasleana* and 0.8×10^4, 1.6×10^4, and 3.2×10^4 cells·mL^{-1} for *T. pseudonana*. Biovolume ratios for *P. hasleana* : *T. pseudonana* cells were 1 : 1, 1 : 2, and 1 : 4. The biovolume of *P. hasleana* was 210 μm^3, and that of *T. pseudonana* was 26.5 μm^3. Algae biovolumes were calculated by the formulas from [Hillebrand et al., 1999].

The experiments were conducted in two stages. At the first one, the dynamics of the microalgae abundance in monocultures at various initial concentrations was studied, while at the second one, the microalgae growth in the mixed culture of *P. hasleana* and *T. pseudonana* was investigated. The experiments lasted for 14 days. Sampling for cell counting was carried out on the 3rd, 7th, 10th, and 14th day. Cell abundance was established in a Nageotte chamber. Fluorescence spectra of microalgae, as well as temperature curves of chlorophyll *a* fluorescence intensity and chlorophyll *a* fluorescence wavelength, were determined according to the methods described earlier [Popik et al., 2022; Voznesenskiy et al., 2019]. The experiments were carried out in triplicate. The data were statistically processed in MS Excel. The graphs show the mean values and standard deviations.

RESULTS

***Pseudo-nitzschia hasleana* and *Thalassiosira pseudonana* growth in monocultures.** For 3 days, the concentration of *P. hasleana* cells remained low, and by the 7th day, it increased to 1×10^4 cells·mL^{-1} (Fig. 1). From the 10th to 14th day, cell abundance rose from 3.8×10^4 to 32.4×10^4 cells·mL^{-1}.

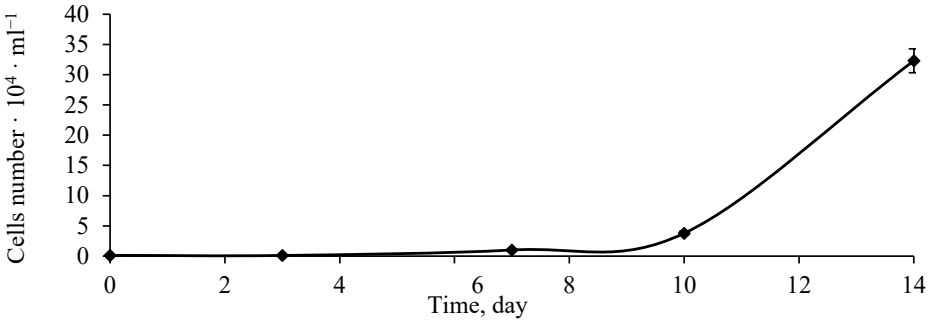

Fig. 1. Growth curve of *Pseudo-nitzschia hasleana* in the monoculture

By the 3rd day of the experiment, the abundance of *T. pseudonana* cells did not differ significantly at all initial cell concentrations (Fig. 2). On the 10th day, the maximum value was registered. On the last days, cell abundance in cultures decreased.

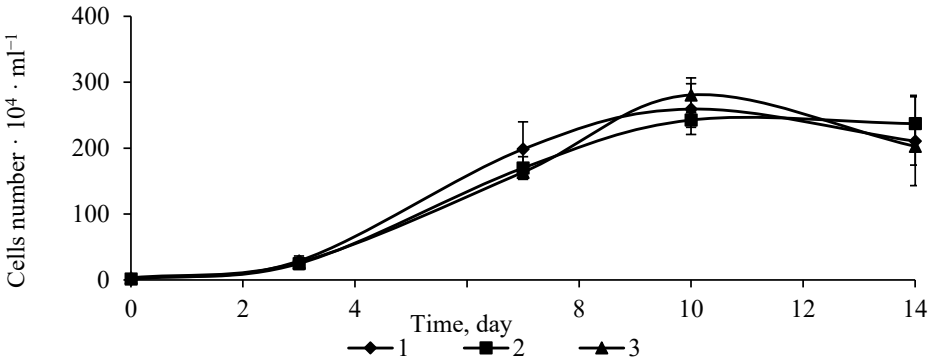

Fig. 2. Growth curve of *Thalassiosira pseudonana* in the monoculture. Initial concentration of cells, cells·mL^{-1}: 1, 0.8×10^4; 2, 1.6×10^4; 3, 3.2×10^4

***Pseudo-nitzschia hasleana* and *Thalassiosira pseudonana* growth in mixed cultures.** The abundance of *P. hasleana* cells increased after the 3rd day of the experiment (Fig. 3). At initial concentration of *T. pseudonana* cells of 0.8×10^4 cells·mL^{-1}, *P. hasleana* entered the stationary growth phase on the 7th day; at higher initial *T. pseudonana* concentrations, the abundance of *P. hasleana* cells rose even on the last day.

The abundance of *T. pseudonana* cells in the mixture increased from the beginning of the experiment at all its initial concentrations (Fig. 4). At 3.2×10^4 cells·mL^{-1}, the alga growth was inhibited after the 7th day: cell abundance was 137×10^4 cells·mL^{-1}, while in the monoculture, the value was 203×10^4 cells·mL^{-1}.

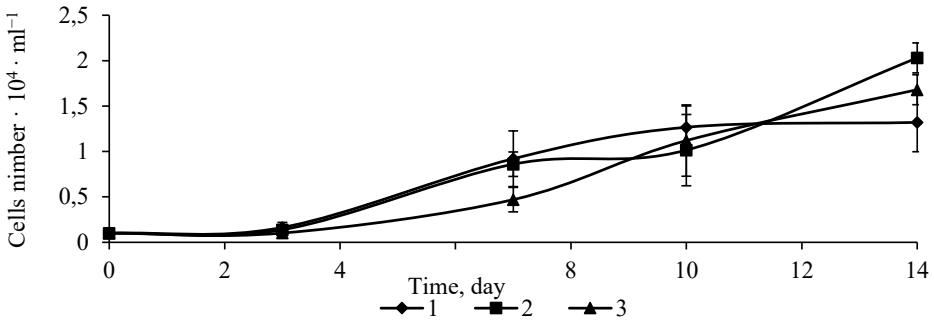

Fig. 3. Growth curve of *Pseudo-nitzschia hasleana* in the mixed culture with *Thalassiosira pseudonana*. Initial concentration of *T. pseudonana* cells, cells·mL^{-1}: 1, 0.8×10^4; 2, 1.6×10^4; 3, 3.2×10^4

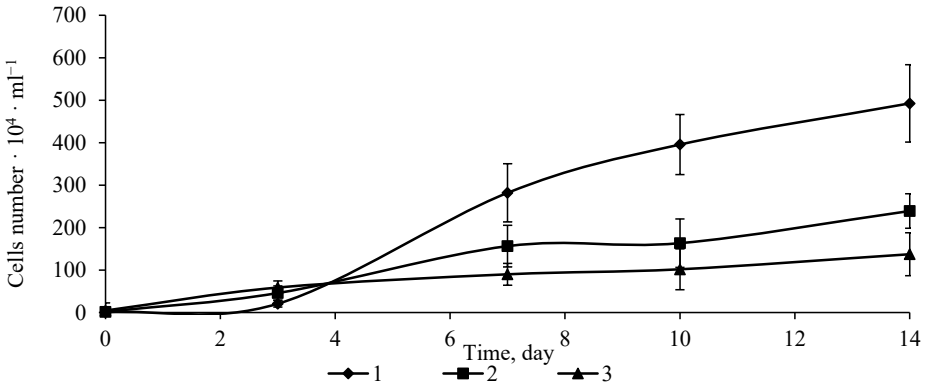

Fig. 4. Growth curve of *Thalassiosira pseudonana* in the mixed culture with *Pseudo-nitzschia hasleana*. Initial concentration of *T. pseudonana* cells, cells·mL^{-1}: 1, 0.8×10^4; 2, 1.6×10^4; 3, 3.2×10^4

Fluorescence of *P. hasleana* cells during the first week correlates with their concentration. As *Pseudo-nitzschia* sp. cultures grow, cell size decreases [Lelong et al., 2012; Trainer et al., 2012]. Therefore, the amount of chlorophyll *per* cell drops, which results in decreased fluorescence. This effect should be observed with longer cultivation, but even in our experiment, a drop in the intensity of chlorophyll *a* fluorescence was recorded on the 14th day compared to that on the 7th day (Figs 5, 6).

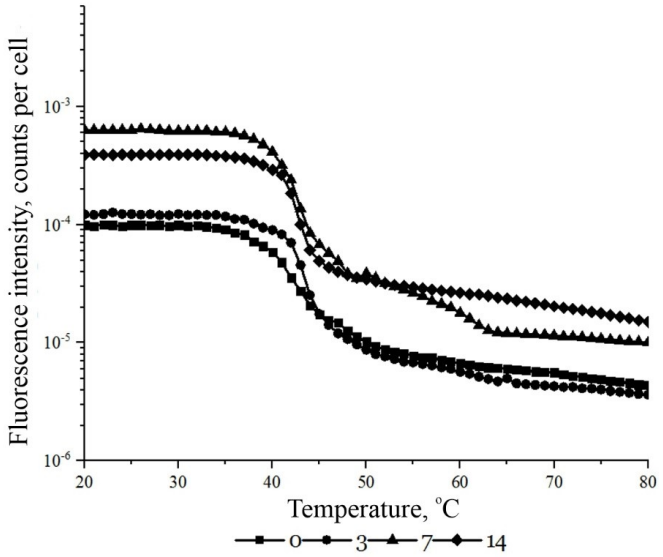

Fig. 5. Fluorescence temperature curves of *Pseudo-nitzschia hasleana* cells during cultivation for two weeks: 0, the beginning of the experiment; 3, the 3rd day; 7, the 7th day; 14, the last day

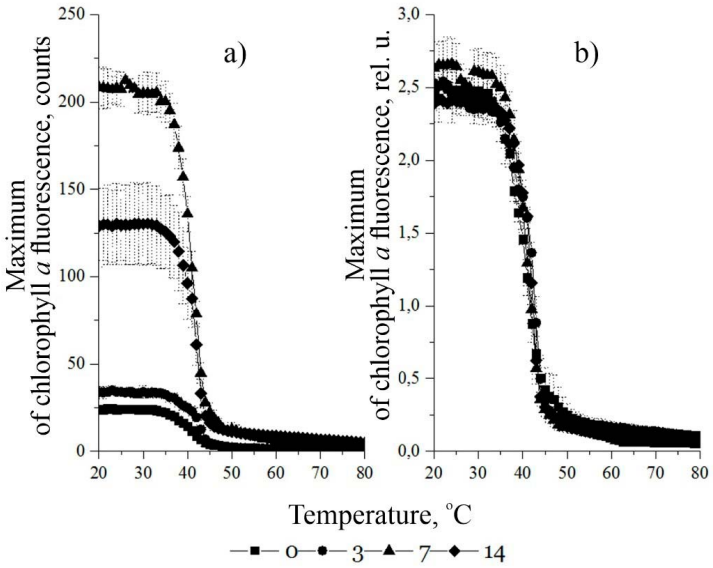

Fig. 6. Temperature curves of *Pseudo-nitzschia hasleana* chlorophyll *a* fluorescence: a, absolute values; b, normalized to mean intensity. The time of the experiment: 0, the beginning; 3, the 3rd day; 7, the 7th day; 14, the last day

The shape of temperature curves of chlorophyll *a* fluorescence for the microalga *P. hasleana* (Fig. 6) was analyzed by us earlier [Popik et al., 2022]. Temperature curves of chlorophyll *a* fluorescence wavelength for *P. hasleana* monoculture, which were obtained during the experiment, showed as follows. Within the range of +20…+40 °C, the maximum intensity of chlorophyll *a* fluorescence occurred at a wavelength of 682.5 nm (Fig. 7).

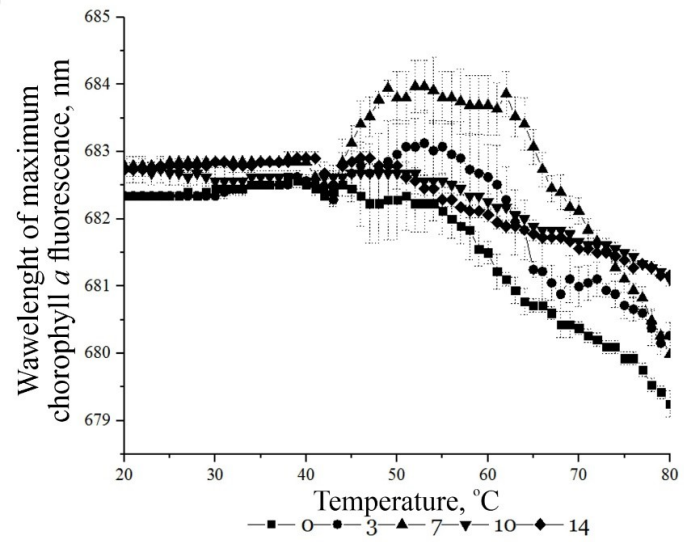

Fig. 7. Changes in the wavelength of chlorophyll *a* fluorescence maximum for *Pseudo-nitzschia hasleana* monocultures. The time of the experiment: 0, the beginning; 3, the 3rd day; 7, the 7th day; 10, the 10th day; 14, the last day

T. pseudonana monoculture, sown at a concentration of 0.8×10^4 cells·mL^{-1}, reaches growth limits (the stationary phase) within 10 days. Then, the culture begins to die off, which may manifest itself in a decrease in the intensity of fluorescence of individual cells (Fig. 8).

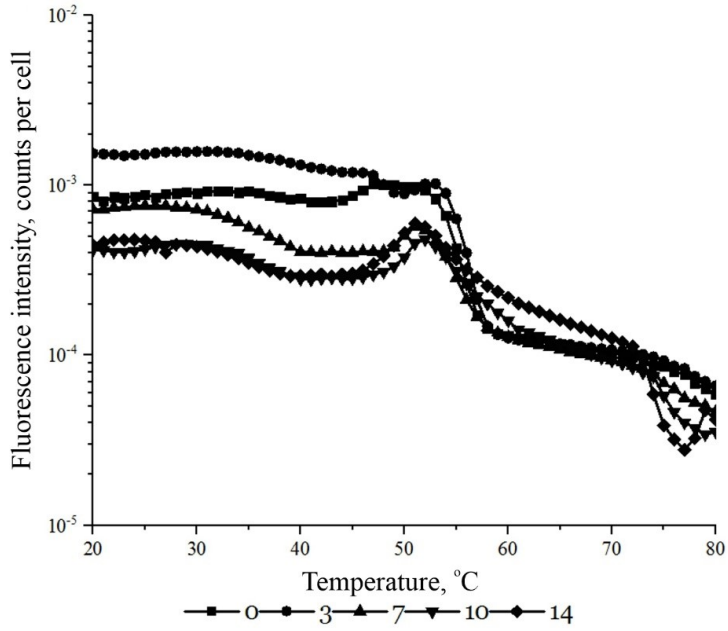

Fig. 8. Fluorescence temperature curves of *Thalassiosira pseudonana* cells during cultivation for two weeks. The time of the experiment: 0, the beginning; 3, the 3rd day; 7, the 7th day; 10, the 10th day; 14, the last day

It can be concluded that the microalga in laboratory culture is in approximately the same state as microalgae during real bloom. In this case, the normalized fluorescence temperature curve (hereinafter NFTC) of the culture changes (Fig. 9), and the differences in its form correspond to three stages: NFTC at low concentrations (the 0th day), NFTC of a growing culture (the 3rd day), and NFTC of a "stagnating" culture (the 7th–14th days) with high concentration (Fig. 10). If we do not take into account a rise in chlorophyll *a* fluorescence observed for *T. pseudonana* on the 3rd day of the experiment, we can conclude that there is an inverse correlation between an increase in the culture concentration and chlorophyll *a* fluorescence. A rise in chlorophyll *a* fluorescence after reseeding may be caused by the corresponding stress of the culture.

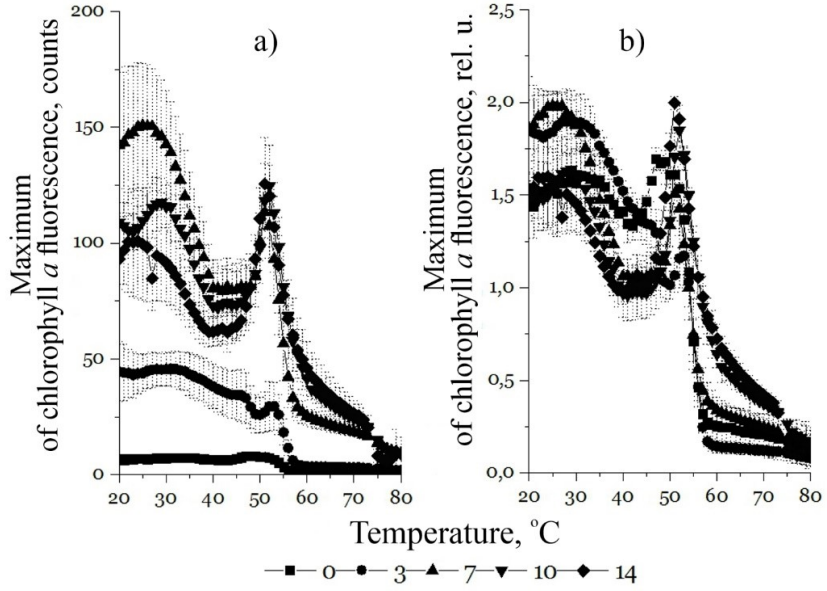

Fig. 9. Fluorescence temperature curves of chlorophyll *a* for the culture of the microalga *Thalassiosira pseudonana*: a, absolute values; b, normalized to mean intensity. The time of the experiment: 0, the beginning; 3, the 3rd day; 7, the 7th day; 14, the last day

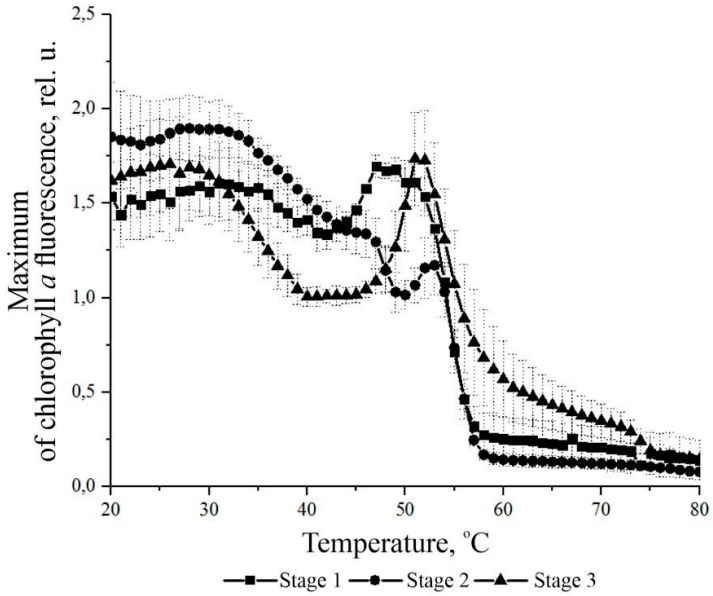

Fig. 10. Fluorescence temperature curves of chlorophyll *a* for the culture of the microalga *Thalassiosira pseudonana* corresponding to different stages of development. Stage 1 is the initial one, during which there is no significant growth; stage 2 corresponds to rapid, exponential growth; stage 3 is the stage of "stagnation"

For *T. pseudonana*, temperature curves of fluorescence for all three stages have certain similarities. These are stable high chlorophyll *a* fluorescence in the range of +20…+32 °C, the presence of a local maximum of its fluorescence at +50…+53 °C, and stabilization of chlorophyll *a* fluorescence at a low level at temperatures above +60 °C. At the same time, the initial stage is characterized by higher value of chlorophyll *a* fluorescence at a local maximum, than that for normal temperatures. For the growth stage, the local maximum of chlorophyll *a* fluorescence is significantly lower in terms of its intensity than fluorescence at initial stages. The local maximum of the intensity of chlorophyll *a* fluorescence at the "stagnation" stage is comparable to the intensity at +20 °C.

At all stages of cultivation, temperature curves of chlorophyll *a* fluorescence for the monoculture remain relatively stable (Fig. 11); at +20…+45 °C, the wavelength of the maximum for chlorophyll *a* fluorescence is 685.5 nm. The difference in the wavelength of the maximum on the 1st day from that on other days may be due to the adaptation of the monoculture during its reseeding. Also, temperature curves of chlorophyll *a* fluorescence wavelength are stable for all days of cultivation within the range of +45…+52 °C. In this range, there is a sharp drop in the wavelength of the maximum for chlorophyll *a* fluorescence from 685.5 to 680.5 nm. Then, a slight increase in the wavelength is observed for 2–3 min (dT = 2…3 °C), which is followed by its slow monotonic decrease. At the same time, within the range of +55…+80 °C, temperature curves of chlorophyll *a* fluorescence wavelength for the culture at various stages of cultivation begin to differ from each other. This may be due to the different composition of pigment–protein complexes for a culture going through all stages of its growth.

Since *Pseudo-nitzschia* are capable of forming red tides [Trainer et al., 2012] and often co-evolve with other diatoms, studying fluorescent characteristics of mixtures of *Pseudo-nitzschia* and other microalgae is of particular interest for their further use in environmental monitoring. Due to different growth rates, on the 7th day of the experiment, microalgae in *P. hasleana* : *T. pseudonana* mixture had the concentrations of 1 : 30. With such a ratio, the effect of *P. hasleana* culture fluorescence in the mixture becomes insignificant: the main contributor to the fluorescent signal is *T. pseudonana*. Since fluorescent characteristics are planned to be used for environmental monitoring, there are no prospects in the investigation of mixtures, in which the fluorescent signal of chlorophyll *a* for *P. hasleana* cannot be measured.

Therefore, it was decided not to determine chlorophyll *a* fluorescence for mixtures during further cultivation. For the mixtures studied, in temperature curves of chlorophyll *a* fluorescence wavelength, the microalga *T. pseudonana* predominated (Fig. 12). The form of NFTC of the mixtures is highly correlated with the form of NFTC of *T. pseudonana*, as can be seen when comparing NFTC of a mixture and NFTC obtained as the sum of NFTC of the monocultures.

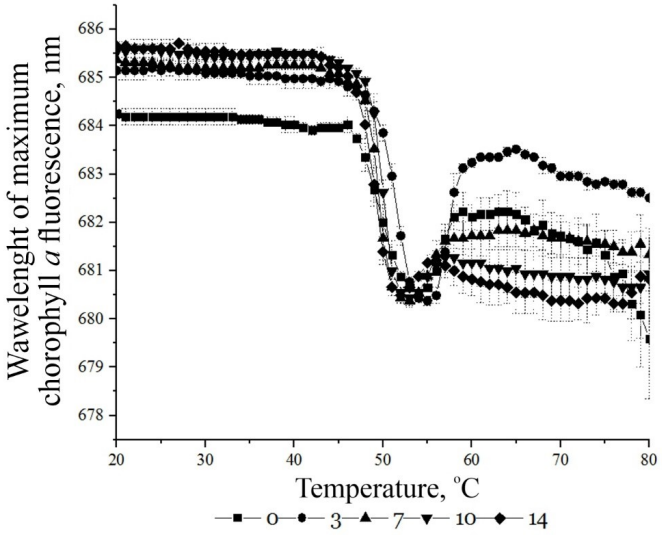

Fig. 11. Changes in chlorophyll *a* fluorescence maximum for monocultures of the microalga *Thalassiosira pseudonana*. The time of the experiment: 0, the beginning; 3, the 3rd day; 7, the 7th day; 10, the 10th day; 14, the last day

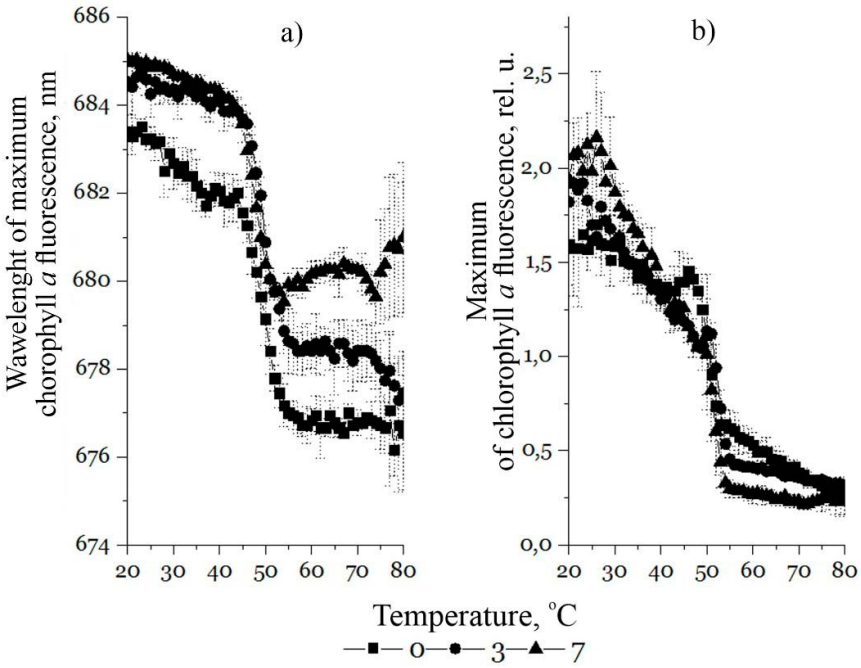

Fig. 12. Fluorescent characteristics of the mixed culture of *Pseudo-nitzschia hasleana* and *Thalassiosira pseudonana*: a, temperature curves of chlorophyll *a* fluorescence wavelength of the mixture; b, normalized fluorescence temperature curves of the mixture. The time of the experiment: 0, the beginning; 3, the 3rd day; 7, the 7th day

Fig. 13 provides a comparison of NFTC of mixtures and summed monocultures. The summation of NFTC was carried out based on the proportional ratio of cells in the culture mixture. When summing NFTC for the 0th day, we used NFTC of *T. pseudonana* at the initial stage. When summing NFTC for the 3rd and 7th days, we used NFTC of *T. pseudonana* at the exponential growth stage.

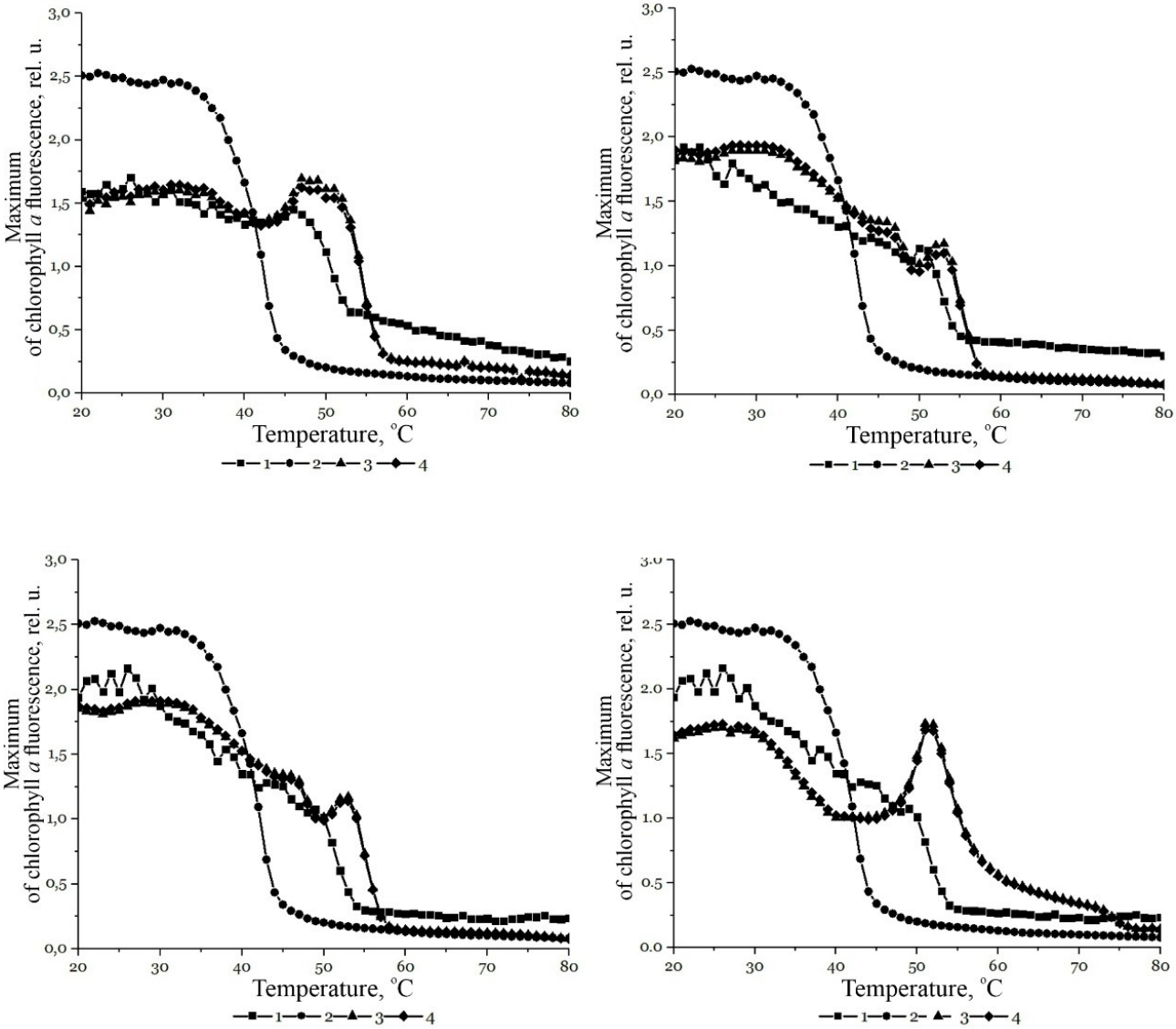

Fig. 13. Fluorescence temperature curves of the mixed culture of *Pseudo-nitzschia hasleana* and *Thalassiosira pseudonana* compared to fluorescence temperature curves of the corresponding monocultures and their mathematical sum: a, normalized fluorescence temperature curves (NFTC) of *Thalassiosira pseudonana* at the initial stage; b, *Thalassiosira pseudonana* NFTC at the beginning of the growth stage; c, *Thalassiosira pseudonana* NFTC at the end of the growth stage; d, *Thalassiosira pseudonana* NFTC at the "stagnation" stage; 1, measured characteristic of the mixture; 2, characteristics of *Pseudo-nitzschia hasleana* monoculture; 3, characteristics of *Thalassiosira pseudonana* monoculture; 4, characteristics of monoculture mixture

DISCUSSION

Exploitative competition (competition for a limiting resource) is one of the biotic factors that determine the structure of the phytoplankton community. Under such conditions, an organism with less consumption may be more successful than other ones in a given community and become a new dominant. Another strategy is interference competition. Specifically, an organism inhibits the growth of other ones directly or indirectly *via* the secretion of chemicals, cell–cell interactions, and so on. In eutrophic water areas, interference competition comes to the fore [Zhao et al., 2018]. Artificial media for microalgae cultivation are nutrient-rich; apparently, when *P. hasleana* and *T. pseudonana* are co-cultivated, interference competition occurs rather than exploitative one.

When algae were co-cultivated, no alterations in cell size and morphology were noted in any of the species. Interestingly, in the study of the effect of the macrophyte *Pyropia haitanensis* (T. J. Chang & B. F. Zheng) N. Kikuchi & M. Miyata, 2011 on *Pseudo-nitzschia multiseries* (Hasle) Hasle, 1995 and *Pseudo-nitzschia pungens* (Grunow ex Cleve) G. R. Hasle, 1993, valve curvature and chloroplast condensation were registered [Patil et al., 2020]. Also, in experiments on dinoflagellates of the genus *Alexandrium* Halim, 1960, when co-cultivated with other microalgae, *inter alia* diatoms, dinoflagellates negatively affected cell abundance and morphology of target species. Moreover, their physiological state changed under the effect of metabolites released by dinoflagellates: there were inhibition of photosystem II, an increase in the content of reactive oxygen species in cells, changes in lipid composition, membrane damage, and cell immobilization and sedimentation [Long et al., 2018; Tan et al., 2019; Zheng et al., 2016].

The growth of *T. pseudonana* with initial concentrations of 1.6×10^4 and 3.2×10^4 cells·mL^{-1} was suppressed when *P. hasleana* began to grow more intensively. At the same time, the stimulation of growth was recorded for *T. pseudonana* at the lowest initial concentration, 0.8×10^4 cells·mL^{-1}. As shown earlier, the initial concentration of monoculture cells in the mixture affects the response of the microalga to metabolites of another species. Specifically, when *Skeletonema costatum* (Greville) Cleve, 1873 was cultivated on *Heterosigma akashiwo* (Y. Hada) Y. Hada ex Y. Hara & M. Chihara, 1987 filtrates, *S. costatum* growth was inhibited at low cell concentration and was not affected at high one [Yamasaki et al., 2009]. The same was observed when cultivating *Phaeodactylum tricornutum* Bohlin, 1898 with *Prorocentrum donghaiense* D. Lu, 2001 [Cai et al., 2014]. Small algal species are thought to be more susceptible to allelopathic substances than large ones [Felpeto et al., 2019; Prasetiya et al., 2016]. At the same time, small species gain a competitive advantage due to their rapid growth [Mikheev et al., 2018]. In general, whether a toxic or toxin-sensitive species has an advantage depends on which species becomes a dominant in the environment [Hulot, Huisman, 2004]. In the experiment with *P. hasleana* and *T. pseudonana*, both species in mixed cultures had a mainly inhibitory effect on each other – with the exception of *T. pseudonana* at the lowest initial cell concentration in the medium. Apparently, interactions between algae depend on their species; so, it is now difficult to see a universal pattern of microalgae interaction. To date, the most studied toxic algae in terms of their effects on other species are *Alexandrium* dinoflagellates [Long et al., 2018; Zheng et al., 2016].

As shown in the experiments aimed at *Pseudo-nitzschia multiseries* and *Bacillaria* sp. co-cultivation, in *Bacillaria* sp., the abundance decreased by 50–70% [Sobrinho et al., 2017]. Inhibition of *T. pseudonana* growth in a mixed culture with *P. hasleana* was observed on the 3rd day of the experiment. Cell abundance of *Rhodomonas salina* (Wislouch) D. R. A. Hill & R. Wetherbee, 1989, *Chattonella marina* (Subrahmanyan) Hara & Chihara, 1982, and *Akashiwo sanguinea* (K. Hirasaka) Gert Hansen

& Moestrup, 2000, both due to lysis and growth inhibition, decreased when co-cultivated with *P. pungens*. At the same time, in *Prorocentrum minimum* (Pavillard) J. Schiller, 1933 and *Phaeocystis globosa* Scherffel, 1899, cell abundance in a mixed culture with *P. pungens* remained the same as in a monoculture [Xu et al., 2015].

Domoic acid has no toxic effect on microalgae [Lundholm et al., 2005; Poulin et al., 2018]. In this regard, it can be assumed that the inhibition of *T. pseudonana* growth results from the release of other substances. Diatoms are known to produce large amounts of polyunsaturated aldehydes [Pichierri et al., 2017], which trigger a cascade of reactions causing microalgal cell death *via* apoptosis [Ianora et al., 2011].

According to the theory of the paradox of the plankton, the great diversity of planktonic species in an ecosystem with limited resources is possible only if their cell concentrations are balanced with the availability of light and nutrients [Hutchinson, 1961]. To date, allelopathy is considered a key component in competition between microalgae [Ternon et al., 2018]. It can be assumed as follows: in natural communities, the interaction of *Thalassiosira* and *Pseudo-nitzschia* species is one of the limiters of their reproduction at a high nutrient content. Previously, on the example of *S. costatum* and *H. akashiwo*, it was shown that the interaction between these species is one of the factors of the monospecific bloom formation [Yamasaki et al., 2007]. An increase in the abundance of some species in the phytoplankton community can reduce the pressure of grazers on other species of this community. Thus, in the South China Sea, if *S. costatum* abundance increases, zooplankton pressure on *P. pungens* decreases; importantly, it is the second key factor, after temperature, for this species [Huang et al., 2009].

Conclusion. *Pseudo-nitzschia hasleana* and *Thalassiosira pseudonana* affected each other in a mixed culture. The effect of *P. hasleana* on *T. pseudonana* depended on the initial concentration of *T. pseudonana* cells. Specifically, at 0.8×10^4 cells·mL^{-1}, a pronounced stimulation of its growth occurred. At initial concentrations of 1.6×10^4 and 3.2×10^4 cells·mL^{-1}, inhibition of *T. pseudonana* growth was registered, and the effect increased with a rise in its initial concentration. However, in the mixed culture, *T. pseudonana* was at the stationary growth phase, while in the monoculture, the population began to die off. *T. pseudonana* had an inhibitory effect on *P. hasleana* growth, and *P. hasleana* abundance in the mixed culture was 16 times lower by the end of the experiment, than that in the monoculture. The experiment with co-cultivation of *P. hasleana* and *T. pseudonana* showed that chlorophyll *a* fluorescence in the mixture is more affected by the microalga with significantly higher concentration. There was no change in the curves of individual cultures in the mixtures.

The work was carried out with the financial support of the Russian Science Foundation grant No. 21-74-30004.

Acknowledgement. Cultures of the microalgae *Pseudo-nitzschia hasleana* MBRU_PH18 and *Thalassiosira pseudonana* MBRU_TSP-02 (Bacillariophyta) were provided by the Marine Biobank resource collection of the National Scientific Center of Marine Biology, FEB RAS (http://marbank.dvo.ru).

REFERENCES

1. Balzano S., Percopo I., Siano R., Gourvil P., Chanoine M., Marie D., Vaulot D., Sarno D. Morphological and genetic diversity of Beaufort Sea diatoms with high contributions from the *Chaetoceros neogracilis* species complex. *Journal of Phycology*, 2017, vol. 53, iss. 1, pp. 161–187. https://doi.org/10.1111/jpy.12489
2. Bates S. S., Bird C. J., de Freitas A. S. W., Foxall R., Gilgan M., Hanic L. A., Johnson G. R., McCulloch A. W., Odense P., Pocklington R.,

Quilliam M. A., Sim P. G., Smith J. C., Subba Rao D. V., Todd E. C. D., Walter J. A., Wrigh J. L. C. Pennate diatom *Nitzschia pungens* as the primary source of domoic acid, a toxin in shellfish from eastern Prince Edward Island, Canada. *Canadian Journal of Fisheries and Aquatic Sciences*, 1989, vol. 46, no. 7, pp. 1203–1215. https://doi.org/10.1139/f89-156

3. Burkholder J. A. M., Glibert P. M., Skelton H. M. Mixotrophy, a major mode of nutrition for harmful algal species in eutrophic waters. *Harmful Algae*, 2008, vol. 8, iss. 1, pp. 77–93. https://doi.org/10.1016/j.hal.2008.08.010
4. Cai Z., Zhu H., Duan S. Allelopathic interactions between the red-tide causative dinoflagellate *Prorocentrum donghaiense* and the diatom *Phaeodactylum tricornutum*. *Oceanologia*, 2014, vol. 56, iss. 3, pp. 639–650. https://doi.org/10.5697/oc.56-3.639
5. Cohen N. R., Ellis K. A., Lampe R. H., McNair H., Twining B. S., Maldonado M. T., Brzezinski M. A., Kuzminov F. I., Thamatrakoln K., Till C. P., Bruland K. W., Sunda W. G., Bargu S., Marchetti A. Diatom transcriptional and physiological responses to changes in iron bioavailability across ocean provinces. *Frontiers in Marine Science*, 2017, vol. 4, art. no. 360 (20 p.). https://doi.org/10.3389/fmars.2017.00360
6. Guillard R. R. L., Ryther J. H. Studies of marine planktonic diatoms: I. *Cyclotella nana* Hustedt, and *Detonula confervacea* (Cleve) Gran. *Canadian Journal of Microbiology*, 1962, vol. 8, no. 2, pp. 229–239. https://doi.org/10.1139/m62-029
7. Harris A. S. D., Medlin L. K., Lewis J., Jones K. J. *Thalassiosira* species (Bacillariophyceae) from a Scottish sea-loch. *European Journal of Phycology*, 1995, vol. 30, iss. 2, pp. 117–131. https://doi.org/10.1080/09670269500650881
8. Hillebrand H., Dürselen C. D., Kirschtel D., Pollingher U., Zohary T. Biovolume calculation for pelagic and benthic microalgae. *Journal of Phycology*, 1999, vol. 35, iss. 2, pp. 403–424. https://doi.org/10.1046/j.1529-8817.1999.3520403.x
9. Huang C., Lin X., Lin J., Du H., Dong Q. Population dynamics of *Pseudo-nitzschia* pungens in Zhelin Bay, China. *Journal of the Marine Biological Association of the United Kingdom*, 2009, vol. 89, iss. 4, pp. 663–668. https://doi.org/10.1017/S0025315408002919
10. Hulot F., Huisman J. Allelopathic interactions between phytoplankton species: The roles of heterotrophic bacteria and mixing intensity. *Limnology and Oceanography*, 2004, vol. 49, iss. 4, pt 2, pp. 1424–1434. https://doi.org/10.4319/lo.2004.49.4_part_2.1424
11. Hutchinson G. E. The paradox of the plankton. *The American Naturalist*, 1961, vol. 95, no. 882, pp. 137–145. https://doi.org/10.1086/282171
12. Felpeto A. B., Śliwińska-Wilczewska S., Klin M., Konarzewska Z., Vasconcelos V. Temperature-dependent impacts of allelopathy on growth, pigment, and lipid content between a subpolar strain of S*ynechocystis* sp. CCBA MA-01 and coexisting microalgae. *Hydrobiologia*, 2019, vol. 835, iss. 1, pp. 117–128. https://doi.org/10.1007/s10750-019-3933-8
13. Ianora A., Bentley M. G., Caldwell G. S., Casotti R., Cembella A. D., Engström-Öst J., Halsband C., Sonnenschein E., Legrand C., Llewellyn C. A., Paldavičienė A., Pilkaityte R., Pohnert G., Razinkovas A., Romano G., Tillmann U., Vaiciute D. The relevance of marine chemical ecology to plankton and ecosystem function: An emerging field. *Marine Drugs*, 2011, vol. 9, iss. 9, pp. 1625–1648. https://doi.org/10.3390/md9091625
14. Lelong A., Hégaret H., Soudant P., Bates S. S. *Pseudo-nitzschia* (Bacillariophyceae) species, domoic acid and amnesic shellfish poisoning: Revisiting previous paradigms. *Phycologia*, 2012, vol. 51, iss. 2, pp. 168–216. https://doi.org/10.2216/11-37.1
15. Lima-Mendez G., Faust K., Henry N., Decelle J., Colin S., Carcillo F., Chaffron S., Ignacio-Espinosa J. C., Roux S., Vincent F., Bittner L., Darzi Y., Wang J., Audic S., Berline L., Bontempi G., Cabello A. M., Coppola L., Cornejo-Castillo F. M., D'Ovidio F., de Meester L., Ferrera I., Garet-Delmas M.-J., Guidi L., Lara E., Pesant S., Royo-Llonch M., Alazar G., Sánchez P., Sebastian M., Souffreau C., Dimier C., Picheral M., Searson S., Kandels-Lewis S., Tara

Oceans Coordinators, Gorsky G., Not F., Ogata H., Speich S., Stemmann L., Weissenbach J., Wincker P., Acinas S. G., Sunagawa S., Bork P., Sullivan M. B., Karsenti E., Bowler C., de Vargas C., Raes J. Determinants of community structure in the global plankton interactome. *Science*, 2015, vol. 348, no. 6237, art. no. 1262073 (10 p.). https://doi.org/10.1126/science.1262073

16. Long M., Tallec K., Soudant P., Le Grand F., Donval A., Lambert C., Sarthou G., Jolley D. F., Hégaret H. Allelochemicals from *Alexandrium minutum* induce rapid inhibition of metabolism and modify the membranes from *Chaetoceros muelleri*. *Algal Research*, 2018, vol. 35, pp. 508–518. https://doi.org/10.1016/j.algal.2018.09.023
17. Louw D. C., Doucette G. J., Voges E. Annual patterns, distribution and long-term trends of *Pseudo-nitzschia* species in the northern Benguela upwelling system. *Journal of Plankton Research*, 2017, vol. 39, iss. 1, pp. 35–47. https://doi.org/10.1093/plankt/fbw079
18. Lundholm N., Hansen P. J., Kotaki Y. Lack of allelopathic effects of the domoic acid-producing marine diatom *Pseudo-nitzschia multiseries*. *Marine Ecology Progress Series*, 2005, vol. 288, pp. 21–33. https://doi.org/10.3354/meps288021
19. Mardones J. I. Screening of Chilean fish-killing microalgae using a gill cell-based assay. *Latin American Journal of Aquatic Research*, 2020, vol. 48, iss. 2, pp. 329–335. https://dx.doi.org/10.3856/vol48-issue2-fulltext-2400
20. Mikheev M. A., Ipatova V. I., Spirkina N. E. Biotic interactions between two species of microalgae in mixed culture. *Moscow University Biological Sciences Bulletin*, 2018, vol. 73, iss. 2, pp. 63–68. https://doi.org/10.3103/S0096392518020062
21. Orlova T. Yu., Stonik I. V., Shevchenko O. G. Flora of planktonic microalgae of Amursky Bay, Sea of Japan. *Russian Journal of Marine Biology*, 2009, vol. 35, iss. 1, pp. 60–78. https://doi.org/10.1134/S106307400901009X
22. Patil V., Abate R., Wu W., Zhang J., Lin H., Chen C., Liang J., Sun L., Li X., Li Y., Gao Y. Allelopathic inhibitory effect of the macroalga *Pyropia haitanensis* (Rhodophyta) on harmful bloom-forming *Pseudo-nitzschia* species. *Marine Pollution Bulletin*, 2020, vol. 161, pt A, art. no. 111752 (12 p.). https://doi.org/10.1016/j.marpolbul.2020.111752
23. Phatarpekar P. V., Sreepada R. A., Pednekar C., Achuthankutty C. T. A comparative study on growth performance and biochemical composition of mixed culture of *Isochrysis galbana* and *Chaetoceros calcitrans* with monocultures. *Aquaculture*, 2000, vol. 181, iss. 1–2, pp. 141–155. https://doi.org/10.1016/S0044-8486(99)00227-6
24. Pichierri S., Accoroni S., Pezzolesi L., Guerrini F., Romagnoli T., Pistocchi R., Totti C. Allelopathic effects of diatom filtrates on the toxic benthic dinoflagellate *Ostreopsis* cf. *ovata*. *Marine Environmental Research*, 2017, vol. 131, pp. 116–122. https://doi.org/10.1016/j.marenvres.2017.09.016
25. Popik A., Gamayunov E., Voznesenskiy S., Markina Zh., Orlova T. The study of fluorescence features of microalgae from the genus *Pseudo-nitzschia* and the possibility of their detection in water. *Algal Research*, 2022, vol. 64, art. no. 102662 (10 p.). https://doi.org/10.1016/j.algal.2022.102662
26. Poulin R. X., Poulson-Ellestad K. L., Roy J. S., Kubanek J. Variable allelopathy among phytoplankton reflected in red tide metabolome. *Harmful Algae*, 2018, vol. 71, pp. 50–56. https://doi.org/10.1016/j.hal.2017.12.002
27. Prasetiya F. S., Safitri I., Widowati I., Cognie B., Decottignies P., Gastineau R., Morançais M., Windarto E., Tremblay R., Mouget J. L. Does allelopathy affect co-culturing *Haslea ostrearia* with other microalgae relevant to aquaculture? *Journal of Applied Phycology*, 2016, vol. 28, iss. 4, pp. 2241–2254. https://doi.org/10.1007/s10811-015-0779-y
28. Sobrinho B. F., De Camargo L. M., Sandrini-Neto L., Kleemann C. R., da Costa Machado E., Mafra L. L. Growth, toxin production and allelopathic effects of *Pseudo-nitzschia multiseries* under iron-enriched conditions. *Marine Drugs*, 2017, vol. 15, iss. 10, art. no. 331 (16 p.). https://doi.org/10.3390/md15100331
29. Tan K., Huang Z., Ji R., Qiu Y., Wang Z., Liu J. A review of allelopathy on microalgae.

Microbiology, 2019, vol. 165, iss. 6, pp. 587–592. https://doi.org/10.1099/mic.0.000776

30. Ternon E., Pavaux A. S., Marro S., Thomas O. P., Lemée R. Allelopathic interactions between the benthic toxic dinoflagellate *Ostreopsis* cf. *ovata* and a co-occurring diatom. *Harmful Algae*, 2018, vol. 75, pp. 35–44. https://doi.org/10.1016/j.hal.2018.04.003
31. Trainer V. L., Bates S. S., Lundholm N., Thessen A. E., Cochlan W. P., Adams N. G., Trick C. G. *Pseudo-nitzschia* physiological ecology, phylogeny, toxicity, monitoring and impacts on ecosystem health. *Harmful Algae*, 2012, vol. 14, pp. 271–300. https://doi.org/10.1016/j.hal.2011.10.025
32. Voznesenskiy S. S., Gamayunov E. L., Popik A. Yu., Markina Zh. V., Orlova T. Yu. Temperature dependence of the parameters of laser-induced fluorescence and species composition of phytoplankton: The theory and the experiments. *Algal Research*, 2019, vol. 44, art. no. 101719 (11 p.). https://doi.org/10.1016/j.algal.2019.101719
33. Yamasaki Y., Shikata T., Nukata A., Ichiki S., Nagasoe S., Matsubara T., Shimasaki Y., Nakao M., Yamaguchi K., Oshima Y., Oda T., Ito T., Jenkinson I. R., Asakawa M., Honjo T. Extracellular polysaccharide-protein complexes of a harmful alga mediate the allelopathic control it exerts within the phytoplankton community. *The ISME Journal*, 2009, vol. 3, iss. 7, pp. 808–817. https://doi.org/10.1038/ismej.2009.24
34. Yamasaki Y., Nagasoe S., Matsubara T., Shikata T., Shimasaki Y., Oshima Y., Honjo T. Allelopathic interactions between the bacillariophyte *Skeletonema costatum* and the raphidophyte *Heterosigma akashiwo*. *Marine Ecology Progress Series*, 2007, vol. 339, pp. 83–92. https://doi.org/10.3354/meps339083
35. Yasakova O. N. The seasonal dynamics of potentially toxic and harmful phytoplankton species in Novorossiysk Bay (Black Sea). *Russian Journal of Marine Biology*, 2013, vol. 39, iss. 2, pp. 107–115. https://doi.org/10.1134/S1063074013020090
36. Xu N., Tang Y. Z., Qin J., Duan S., Gobler C. J. Ability of the marine diatoms *Pseudo-nitzschia multiseries* and *P. pungens* to inhibit the growth of co-occurring phytoplankton *via* allelopathy. *Aquatic Microbial Ecology*, 2015, vol. 74, no. 1, pp. 29–41. https://doi.org/10.3354/ame01724
37. Zhao M., Chen X., Ma N., Zhang Q., Qu D., Li M. Overvalued allelopathy and overlooked effects of humic acid-like substances on *Microcystis aeruginosa* and *Scenedesmus obliquus* competition. *Harmful Algae*, 2018, vol. 78, pp. 18–26. https://doi.org/10.1016/j.hal.2018.07.003
38. Zheng J.-W., Li D.-W., Lu Y., Chen J., Liang J.-J., Zhang L., Yang W.-D., Liu J.-S., Lu S.-H., Li H.-Y. Molecular exploration of algal interaction between the diatom *Phaeodactylum tricornutum* and the dinoflagellate *Alexandrium tamarense*. *Algal Research*, 2016, vol. 17, pp. 132–141. https://doi.org/10.1016/j.algal.2016.04.019

ВЗАИМОДЕЙСТВИЕ ДИАТОМОВЫХ ВОДОРОСЛЕЙ *PSEUDO-NITZSCHIA HASLEANA* И *THALASSIOSIRA PSEUDONANA* В СМЕШАННОЙ КУЛЬТУРЕ

Ж. В. Маркина[1], А. Ю. Попик[2]

[1]Национальный научный центр морской биологии имени А. В. Жирмунского ДВО РАН, Владивосток, Российская Федерация

[2]Институт автоматики и процессов управления ДВО РАН, Владивосток, Российская Федерация

E-mail: *zhannav@mail.ru*

Представители рода *Pseudo-nitzschia* (Bacillariophyta) вызывают цветения в разных районах Мирового океана, поэтому важно знать экологические особенности этих видов, в том числе то, как они взаимодействуют с другими видами одноклеточных водорослей. Кроме того,

необходима методика быстрой идентификации данных водорослей в среде. В связи с этим нами оценена динамика численности клеток *Pseudo-nitzschia hasleana* и *Thalassiosira pseudonana* в моно- и смешанных культурах путём их прямого подсчёта в камере Нажотта. Также проанализированы температурные кривые флуоресценции хлорофилла *a*, полученные методом лазерно-индуцированной флуоресценции в температурной камере. Опыты проводили в течение 14 суток. Показано, что *P. hasleana* оказывала различное действие на *T. pseudonana* в зависимости от начальной численности *T. pseudonana*. При начальной концентрации $0{,}8 \times 10^4$ кл.·мл$^{-1}$ происходила выраженная стимуляция роста этой диатомовой водоросли. При начальных концентрациях $1{,}6 \times 10^4$ и $3{,}2 \times 10^4$ кл.·мл$^{-1}$ отмечено ингибирование её роста. В смешанной культуре *T. pseudonana* оставалась в стационарной фазе роста, тогда как в монокультуре популяция входила в фазу отмирания к 14-м суткам опыта. *T. pseudonana* ингибировала рост *P. hasleana*. Эксперимент с совместным культивированием *P. hasleana* и *T. pseudonana* показал, что на флуоресценцию хлорофилла *a* смеси оказывает большее воздействие та микроводоросль, концентрация которой значительно выше. Флуоресцентный сигнал двух культивируемых отдельно монокультур потенциально может быть использован для их поиска в смеси.

Ключевые слова: *Pseudo-nitzschia hasleana*, *Thalassiosira pseudonana*, аллелопатия, флуоресценция хлорофилла *a*, идентификация микроводорослей

1871
ИнБЮМ – IBSS

Морской биологический журнал
Marine Biological Journal
2023, vol. 8, no. 3, pp. 62–86
https://marine-biology.ru

UDC 582.263-152.6(292.471:285.2)

CLADOPHORA (CHLOROPHYTA) AS AN ECOLOGICAL ENGINEER IN HYPERSALINE LAKE CHERSONESSKOYE: DISTRIBUTION OF DIATOM ALGAE IN THE STRUCTURED SPACE OF PLANT MATS

© 2023 **A. V. Prazukin, R. I. Lee, D. S. Balycheva, Yu. K. Firsov, and V. V. Kholodov**
A. O. Kovalevsky Institute of Biology of the Southern Seas of RAS, Sevastopol, Russian Federation
E-mail: *prazukin@mail.ru*

Received by the Editor 05.05.2021; after reviewing 09.09.2021;
accepted for publication 04.08.2023; published online 21.09.2023.

The genus *Cladophora* is one of the largest genera of green algae, representatives of which are found in all water bodies throughout the world. *Cladophora* creates habitats for different groups of organisms, including epiphytic unicellular algae. The aim of the article is to examine the vertical distribution of diatoms in the structured space of *Cladophora* mats and in benthic sediments of a hypersaline lake in Crimea. In the vertical structure of the *Cladophora* mat, the floating and benthic mats were distinguished, each having a characteristic structure. The total of 20 diatom species of 12 genera were observed throughout this study. The total abundance of diatoms and their biomass on *Cladophora* (*per* unit of dry biomass) and in benthic sediments (*per* unit of dry mass) varied over a wide range. On *Cladophora*, the abundance varied from 1.85×10^6 to 69.52×10^6 cells·g^{-1}, and the biomass, from 7.77 to 157.43 mg·g^{-1}. In the bottom sediment, the abundance varied from 6.05×10^6 to 16.87×10^6 cells·g^{-1}, and the biomass, from 7.76 to 36.39 mg·g^{-1}. The share of the diatom biomass in the wet mass of the entire *Cladophora* mat averaged 1.06%.

Keywords: diatoms, epibionts, filamentous green algae, floating mats, hypersaline lake

The genus *Cladophora* Kützing, 1843 is one of the largest genera of green algae, representatives of which are found in all water bodies worldwide: freshwater, marine, and hypersaline ones [Dodds, Gudder, 1992; Higgins et al., 2008; Prazukin et al., 2020; Zulkifly et al., 2013]. Due to morphological features of *Cladophora* thallus and the ability of these algae to form extensive benthic and floating mats [Bootsma et al., 2004; Higgins et al., 2008; Gubelit, Berezina, 2010; Messyasz et al., 2015; Prazukin et al., 2008, 2018, 2019], *Cladophora* can be characterized as an ecological engineer [Zulkifly et al., 2012, 2013]. This organism creates, changes, and maintains the habitat [Jones et al., 1994]. *Cladophora* creates habitats for various groups of organisms, *inter alia* epiphytic unicellular algae. On its surface, communities of unicellular algae are formed, with a great variety of taxonomic groups [Hardwick et al., 1992; Malkin et al., 2009; Mpawenayo, Mathooko, 2005; Zulkifly et al., 2012, 2013]; those create high density and biomass of cells [Bergey et al., 1995; Malkin et al., 2009; Marks, Power, 2001; Stevenson, Stoermer, 1982; Young et al., 2010].

In Crimea, there are many saline lakes [Anufriieva, 2018; Shadrin et al., 2017] where floating and benthic *Cladophora* mats are formed constantly or with a certain periodicity, covering large parts of lake water areas [Ivanova et al., 1994; Prazukin et al., 2008, 2018, 2019].

Unicellular algae of Crimean saline lakes and, in particular, epiphytic unicellular algae on *Cladophora* remain poorly studied [Nevrova, Petrov, 2008; Senicheva et al., 2008]. There is the question: how are microepiphytes distributed along the vertical component of *Cladophora* mats? To answer, we chose a small hypersaline lake, Lake Chersonesskoye, where a biogeochemical cycle of substances with *Cladophora* participation occurs annually. We hypothesized that *Cladophora* mats are ecological engineers in Lake Chersonesskoye during the spring–autumn period. To test this hypothesis, we considered the vertical distribution of diatom algae in the structured space of *Cladophora* mats formed in different parts of the lake shoreline.

MATERIAL AND METHODS

Study area. For 20 years (2000–2020), investigations were carried out on Lake Chersonesskoye (44°35′09″N, 33°23′39″E), located at Cape Khersones, Crimean Peninsula [Gubanov, Bobko, 2012; Mukhanov et al., 2004; Pavlovskaya et al., 2009; Prazukin, 2015; Prazukin et al., 2008, 2018, 2019, 2021a, b; Senicheva et al., 2008; Shadrin et al., 2008, 2017]. The above-mentioned works portrayed a detailed description of the water body and its inhabitants, which allows us to restrict ourselves to a brief representation. It is a small lake with a surface area of 0.05 km^2, a catchment area of 0.92 km^2, an average depth of 0.38 m, and a maximum depth of 1.5 m. The lake is separated from the sea by a narrow boulder–pebble isthmus; it is fed mainly due to the filtration of seawater and its inflow during severe storms (Fig. 1A–C). In some years, the maximum values of water temperature (+43 °C) were registered in July and August in the lake upper layer; the minimum temperatures were down to –0.5 and –0.7 °C (December 2004). The maximum salinity value for the observation period was 340 g·L^{-1} (August 2009), and the minimum was 27 g·L^{-1} (May 2018). Throughout the entire study period, 61 algal species were found in the lake phytoplankton [Senicheva et al., 2008]. Macrophytes were represented by 6 species, 5 of them belonging to green filamentous algae of the phylum Chlorophyta (*Cladophora vadorum* (Areschoug) Kützing, 1849; *C. siwachensis* C. J. Meyer, 1922; *C. echinus* (Biasoletto) Kützing, 1849; *Ulothrix implexa* (Kützing) Kützing, 1849; and *Rhizoclonium tortuosum* (Dillwyn) Kützing, 1845) and 1 belonging to the seagrass phylum Angiospermae (*Ruppia cirrhosa* (Petagna) Grande, 1918) [Prazukin et al., 2008]. Macrophytic vegetation of the lake is characterized by seasonal dynamics of biomass [Prazukin et al., 2008]. In winter months, macrophytic vegetation can be preserved in small, narrow, and intermittent strands of filamentous algae along the entire lake shoreline and in small thickets of *R. cirrhosa* in the southwestern part of the lake. However, three times during the observation period (2000–2020), a complete absence of *Cladophora* in the lake was recorded in winter. In mid-March, *Cladophora* mats begin their formation along the shoreline; by mid-August, those can occupy up to 60–90% of the lake area. In autumn months, floating mats are destroyed; they lose their ability to stay afloat and sink to the lake bottom; and active destruction processes occur.

Our previous studies showed that *Cladophora* mats have a well-defined vertical structure, which changes during the vegetative cycle [Prazukin et al., 2008, 2018]. In late summer and autumn, a great variety of mat conditions is observed in different parts of the lake. Moreover, in a small lake area, one can find mats with clear signs of destruction and mats that retain their juvenile and mature structure.

In May and June 2017, practically every day, daytime air temperature in the lake area exceeded +20 °C; early to mid-July, the values varied from +26 to +35 °C. There was no precipitation during these months. *Cladophora* mats were formed only in the shore area of the lake. Apparently, due to high temperatures, those began to deteriorate in late July, and a wide range of their states was observed.

We selected two sites: at the southeastern (*D*) and northeastern (*E*) shores of the lake (Fig. 1). At each site, two visually different biotopes were identified (*D1*, *D2* and *E3*, *E4*) (Fig. 2). There were no obvious signs of mat destruction at *D1*, and the same could be said about the mat at *E3*, while the mats at *D2* and *E4* were aging.

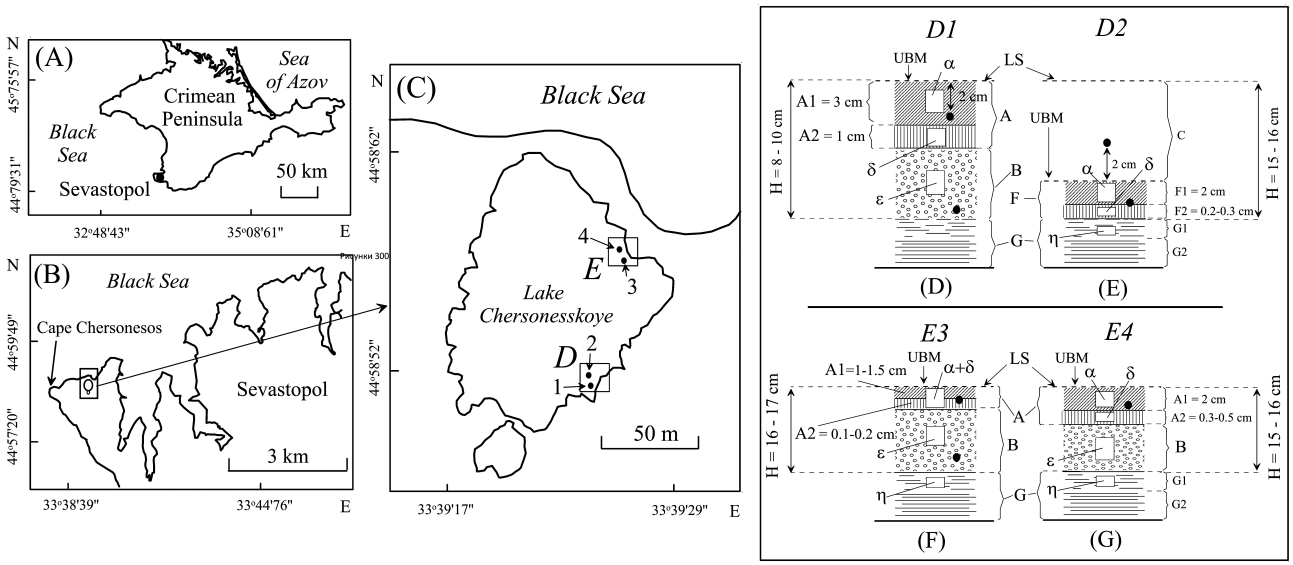

Fig. 1. Lake Chersonesskoye on Crimean Peninsula in various scales (A–C) with the layout of sampling stations (C) and algal mat layers (D–G); sampling stations near the southeastern (*D1*, *D2*) and northeastern (*E3*, *E4*) shores of the lake. On D–G: the upper (A1) and lower (A2) layers of the floating mat (A); the algal layer under the floating mat (B); the upper (F1) and lower (F2) layers of the benthic mat (F); the "liquid" (G1) and "solid" (G2) layers of the bottom sediments (G); H, depth; UBM, the upper boundary of the *Cladophora* mat; LS, the upper boundary of the lake; C, the water layer between the bottom mat and the upper boundary of the lake; α, δ, ε, η, sampling points within the boundaries of the mat and in the bottom sediments. Spots of water temperature measurements within the boundaries of the mat and beyond it are marked with black dots

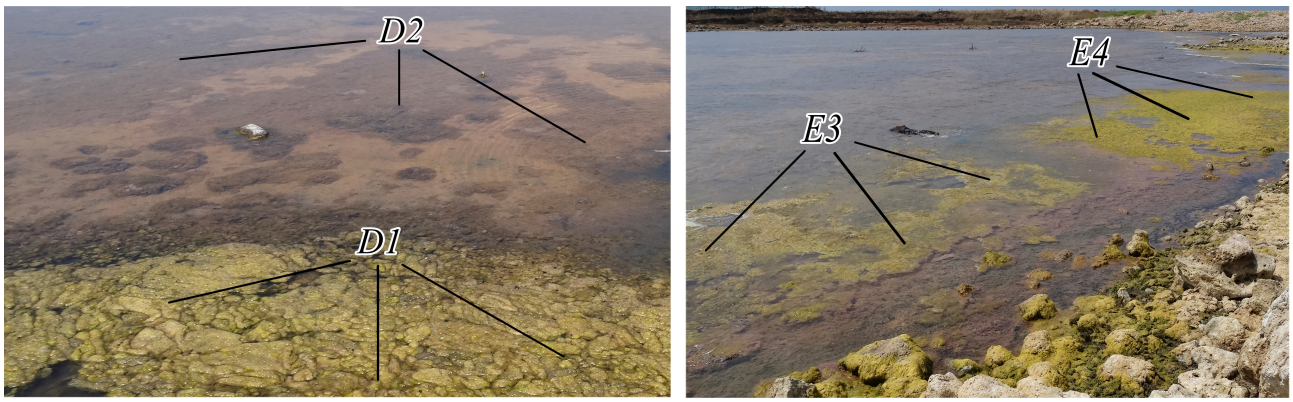

Fig. 2. Stations (*D1*, *D2*, *E3*, *E4*) and sampling points at the southeastern (a) and northeastern (b) shores of the lake. The sampling points are marked by lines

Sampling and sample processing. On 26 July, 2017, 30 samples of the *Cladophora* mat and 9 samples of benthic sediments were taken from the southeastern (sta. *D1* and *D2*) and northeastern (sta. *E3* and *E4*) shores of the lake (Figs 1C, 2) to analyze the species structure and biomass of diatoms. From each horizontal mat layer (α, δ, ε, see Fig 1D–G), 0.5–1 g (wet mass) of *Cladophora* were sampled with tweezers. Each algae sample was placed in a 10-mL glass container.

Benthic sediments were sampled in triplicate from the upper 1-cm layer using a cylindrical plastic sampler with a working section area of 7.1 cm^2. Soil was placed in a glass container and mixed with 3 mL of 40% formalin solution.

At all the stations, algae were sampled in triplicate to assess the vertical structure of *Cladophora* mats. A cylindrical sampler with a cross-sectional area S_0 = 0.0452 m^2 was used: this allowed algae sampling in layers throughout the entire water column, as described earlier [Kühl, Jørgensen, 1992]. When sampling, algae of each horizontal layer of the *Cladophora* mat were placed in separate plastic bags.

At sta. *D1*, *E3*, and *E4*, water temperature and salinity were measured directly in the floating mat (in the middle of the layer) and in the algal layer underneath (near the bottom) using a mercury thermometer with an accuracy of 0.1 °C and a Kelilong WZ212 refractometer; at sta. *D2*, measurements were carried out at a 2-cm distance above the benthic mat and in it. At sta. *D1* and *D2*, water temperature within the mat and beyond it was measured at short time intervals for 6.5 h, from 10:00 a.m. to 04:40 p.m.

Sample processing in the laboratory. Samples of the *Cladophora* mat taken to assess its vertical structure were washed in freshwater, dried on filter paper, and weighed on a WT-250 electronic balance (Techniprot, Poland) (sample wet mass, W_{wet}). To determine dry mass (W_{dry}), the samples were dried at a temperature of +105 °C to constant weight and weighed on the same balance.

Fragments of *Cladophora* thalli sampled from different horizons of the mat to determine microphytofouling were quickly delivered to the laboratory. There, the state of their fouling was assessed under a microscope, and diameters of *Cladophora* thalli were measured. Then, samples were fixed by adding 1.5 mL of 40% formalin solution and maintained for 1–3 weeks. After that, *Cladophora* thalli were placed in a Petri dish, and epiphytic algae were carefully removed with tweezers and a scalpel or a plastic spatula. Then, *Cladophora* was washed and squeezed into the dish. The process was monitored under a microscope; the washing of microalgae was continued until they were completely absent on a randomly taken fragment of macrophyte thalli (Fig. 3).

To determine the species composition of diatom algae, their shells were cleaned from organic matter by the "cold" method, and permanent preparations were made according to the technique described in [Diatoms of the USSR, 1992]. Species were identified in accordance with literature sources, including species guides [Diatomovyi analiz. Kniga 2, 1949; Diatomovyi analiz. Kniga 3, 1950; Guslyakov et al., 1992; Lange-Bertalot, 2001; Proshkina-Lavrenko, 1963; Witkowski et al., 2000] and numerous publications. Nomenclature names of microalgal taxa are given according to the Internet database https://www.algaebase.org/ [2020]. Microphotography and identification of diatoms were carried out under an Olympus BX53F light microscope using a ×100 immersion objective (Olympus immersion oil, n = 1.518), with a Jenoptik ProgRes Gryphax Arktur camera and Gryphax Arktur software. Moreover, to analyze fine structures of diatom shells, those were photographed under a Hitachi SU3500 scanning electron microscope (magnification factor 5–300,000; resolution up to 3 nm; and depth of field 0.5 mm).

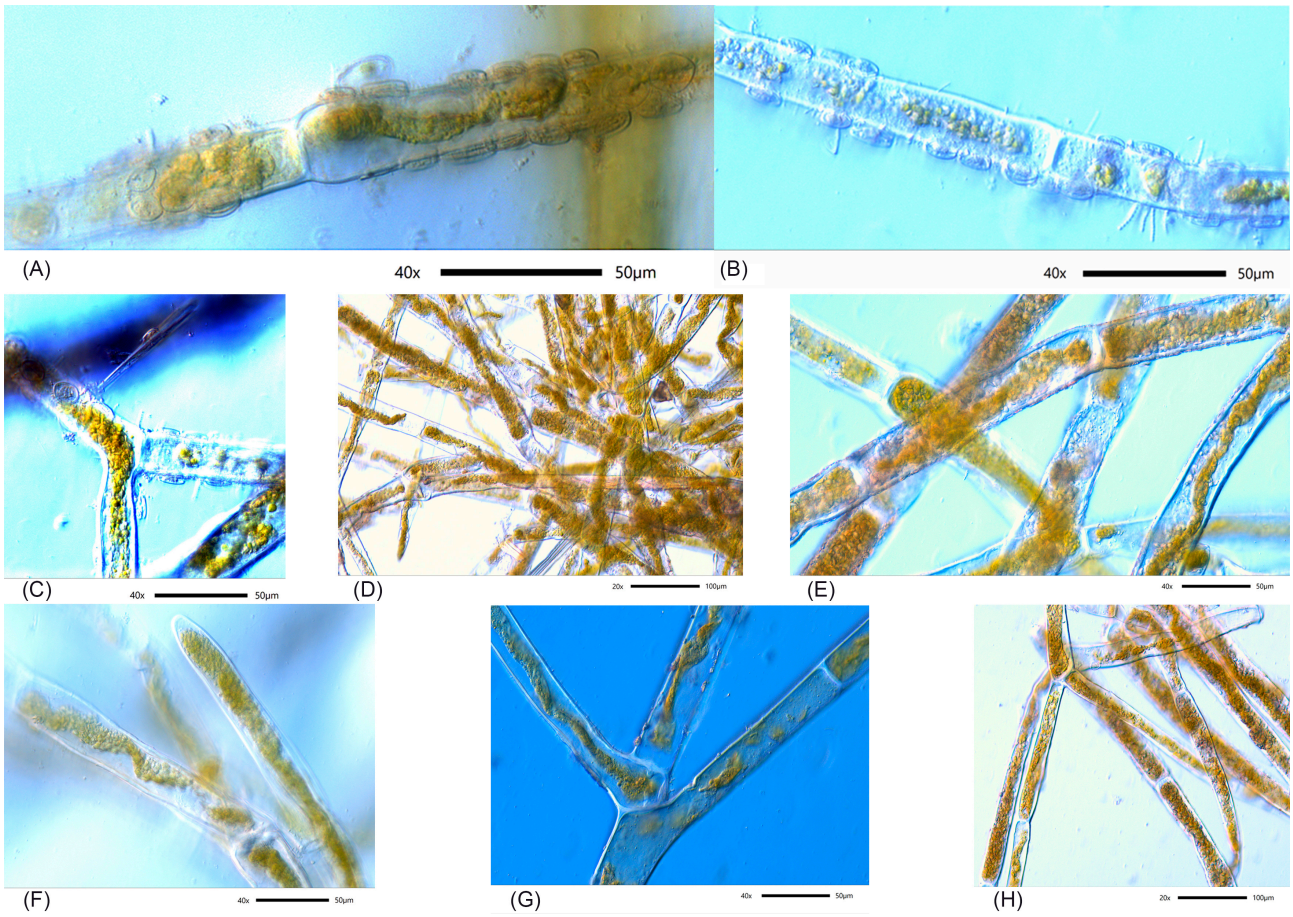

Fig. 3. Fragments of *Cladophora* thalli as seen under a light microscope (Olympus BX53F): A–C, before cleaning, overgrown with diatoms; D–H, after cleaning (processing)

The sample volume (V_{sus}), obtained as a result of the above manipulations, was measured with an accuracy of 0.1 mL; from it, a quota (V_{qu} = 0.02 mL) was taken to determine the quantitative characteristics of diatom algae. Removed *Cladophora* thalli of each sample were washed in freshwater, dried on filter paper, and weighed on a microanalytical balance with an accuracy of 10^{-4} g. Then, these samples were dried at +105 °C to constant weight (W_{Cl}) and weighed on the same balance.

In case when *Cladophora* thalli were subject to significant destruction, a sample was vigorously shaken. The contents were homogenized and diluted with water to required suspension density (sample volume, V_{sus}); from it, a quota (V_{qu} = 0.02 mL) was taken with a dispenser to determine the quantitative characteristics of diatoms.

To analyze the species structure of diatom algae in benthic sediments, a soil sample was diluted with water to obtain an arbitrary volume (V_{sus} was measured with an accuracy of 0.1 mL) and thoroughly mixed; from this suspension, a 0.02-mL quota (V_{qu}) was taken with a dispenser for subsequent measurements of diatom characteristics under a microscope. The remaining soil suspension was centrifuged for 3 min at 500 rpm. The precipitate was placed on a metal foil, dried at a temperature of +105 °C to constant weight (W_{sed}), and weighed on a microanalytical balance. The above operation was also carried out when working with suspension obtained from destroyed *Cladophora* thalli.

Diatom cells were counted under a LOMO Mikmed-2 light microscope (magnification from ×40 to ×1,500) on special lined counting glasses; on their surface, a few drops of suspension from a thoroughly mixed test sample were applied with a 0.02-mL dispensing pipette. To calculate the cell mass of diatoms, we used the true volume method (formulas for the geometric similarity of cells) proposed by I. Kiselev [1956]. The calculation of biomass and abundance was carried out according to standard techniques [Vodorosli, 1989].

Calculation of indicators and statistical processing of data. Based on the data obtained, certain indicators were calculated.

A. The volumetric concentration of *Cladophora* biomass at different sampling points was calculated using the equation:

$$C_W = W_{dry}/V_{mat}\,, \tag{1}$$

where C_W is the amount of dry mass of algae *per* unit volume of the mat, kg·m^{-3} (dry weight);

W_{dry} is dry weight of the *Cladophora* mat sample, kg;

V_{mat} is the mat volume, m^3.

The value of V_{mat} was calculated by the formula:

$$V_{mat} = S_0 \cdot h\,, \tag{2}$$

where V_{mat} is the volume of a floating or bottom mat, m^3;

S_0 is the cross-sectional area of a cylindrical sampler equal to 0.0452 m^2;

h is the thickness of a floating or bottom mat, m.

B. Dry and wet mass of the *Cladophora* mat algae *per* unit of the lake area at the sampling point were calculated applying the following formulas:

$$m_{dry} = W_{dry}/S_0\,, \tag{3}$$

$$m_{wet} = W_{wet}/S_0\,, \tag{4}$$

where m_{dry} is dry mass of the *Cladophora* mat algae *per* unit of the lake area at the sampling point, g·m^{-2} (dry mass);

m_{wet} is wet mass of the *Cladophora* mat algae *per* unit of the lake area at the sampling point, g·m^{-2} (wet mass);

W_{dry} is dry weight of the mat sample, g;

W_{wet} is wet weight of the mat sample, g;

S_0 is the surface area of the lake from which the sample was taken, m^2.

C. The abundance of the *i* species of diatom algae *per* unit of dry *Cladophora* mass or dry mass of benthic sediment was calculated by the formulas as follows:

$$N_i = (N_{i(qu)}/V_{qu}) \cdot (V_{sus}/W_{Cl})\,, \tag{5}$$

$$N_i = (N_{i(qu)}/V_{qu}) \cdot (V_{sus}/W_{sed})\,, \tag{6}$$

where N_i is the abundance of the *i* species of diatoms *per* unit of dry mass of benthic sediment, cells·g^{-1} (dry mass);

$N_{i(qu)}$ is the abundance of the *i* species of diatom algae in the volume of a sample quota (V_{qu} = 0.02 mL), cells;

V_{sus} is the sample volume, mL;

W_{Cl} is dry mass of *Cladophora* in the sample, g;

W_{sed} is dry mass of benthic sediment in the sample, g.

D. The amount of biomass of the *i* species of diatoms *per* unit of dry *Cladophora* mass or dry mass of benthic sediment was calculated according to the formula:

$$W_i = N_i \cdot B_{mid}\,, \tag{7}$$

where W_i is the amount of biomass of the *i* diatom species *per* unit of dry *Cladophora* mass, mg·g^{-1} (dry mass);

B_{mid} is mean cell mass of each diatom species, mg.

The individual cell mass for the *i* species (B_{mid}) was calculated as follows:

$$B_{mid} = v_i \cdot \rho\,, \tag{8}$$

where v_i is the mean cell volume of the *i* diatom species, μm^{-3} (it was calculated using the formulas for the geometric similarity of cells);

ρ is the specific weight of a diatom cell (ρ = 1.2×10^{-9} mg·μm^{-3} [Oxiyuk, Yurchenko, 1971]).

E. The total abundance of diatom cells in the *Cladophora* mat *per* unit of the lake area at the sampling point was calculated using the formula (the number of algal species in samples varied from 3 to 13):

$$N_D/S_0 = \sum_{n=3}^{13}(m_{dry} \cdot N_i)_n\,, \tag{9}$$

where N_D/S_0 is the total abundance of diatom cells in the *Cladophora* mat *per* unit of the lake area at the sampling point, cells·m^{-2};

m_{dry} is dry mass of the *Cladophora* mat algae *per* unit of the lake area at the sampling point, g·m^{-2} (dry mass);

N_i is the abundance of the *i* diatom species *per* unit of *Cladophora* dry mass, cells·g^{-1} (dry mass);

n is the number of algal species in samples.

F. The total biomass of diatom algae in the *Cladophora* mat *per* unit of the lake area at the sampling point was calculated applying the formula:

$$W_D/S_0 = \sum_{n=3}^{13}(m_{dry} \cdot W_i)_n\,, \tag{10}$$

where W_D/S_0 is the total biomass of diatom cells in the *Cladophora* mat *per* unit of the lake area at the sampling point, g·m^{-2};

W_i is the amount of the *i* diatom species *per* unit of dry *Cladophora* mass, mg·g^{-1} (dry mass);

n is the number of algal species in samples.

G. The calculation of mean values, their standard deviations (*SD*), correlation coefficients (*R*), and variability (*CV*), as well as the parameters of the regression equations, was carried out in MS Excel 2007. To compare the species composition of the communities of unicellular algae, the indices of similarity of Jaccard and Czekanowski–Sørensen–Dice were used [Semkin, 2009]:

$$K_J = c/(a + b - c)\,, \tag{11}$$

$$K_{CSD} = 2c/(a + b)\,, \tag{12}$$

where K_J and K_{CSD} are the indices of similarity of Jaccard and Czekanowski–Sørensen–Dice, respectively;

c is the number of species common for both sites or time periods;

a is the number of species found in the first case;

b is the number of species found in the second case.

The threshold values for making a conclusion about the similarity of the species composition are 0.42 (Jaccard) and 0.59 (Czekanowski–Sørensen–Dice) [Semkin, 2009].

RESULTS

Temperature and salinity inside and outside the mat. In the upper mat layer at sta. *D1*, salinity was 71 g·L^{-1}; at sta. *E3* and *E4*, the values were 67 and 67.3 g·L^{-1}, respectively.

Air temperature at 2:40 p.m. at a height of 1 m from the mat was +32.8 °C. Water temperature in the floating mat and in the algal layer underneath (sta. *D1*), as well as in the benthic mat and above it (sta. *D2*), changed regularly throughout the day (from 10 a.m. to 04:40 p.m.) (Fig. 4A, B). As a function of the time of day (t), at this time interval, it is described by the equations as follows.

Variation of water temperature (T) in the floating mat (sta. *D1*):

$$T = 28.984 + 0042t - 0.000086t^2$$

$$(\text{the standard error of approximation, } s = 0.51; R^2 = 0.95)\ .$$

Variation of water temperature (T) in the algal layer under the mat (sta. *D1*):

$$T = 27.107 + 0.038t - 0.000066t^2 (s = 0.29; R^2 = 0.99)\ .$$

Variation of water temperature (T) in the water layer above the benthic mat (sta. *D2*):

$$T = 28.157 + 0.042t - 0.000079t^2 (s = 0.38; R^2 = 0.98)\ .$$

Variation of water temperature (T) in the benthic mat (sta. *D2*):

$$T = 28.202 + 0.042t - 0.000076t^2 (s = 0.48; R^2 = 0.97)\ .$$

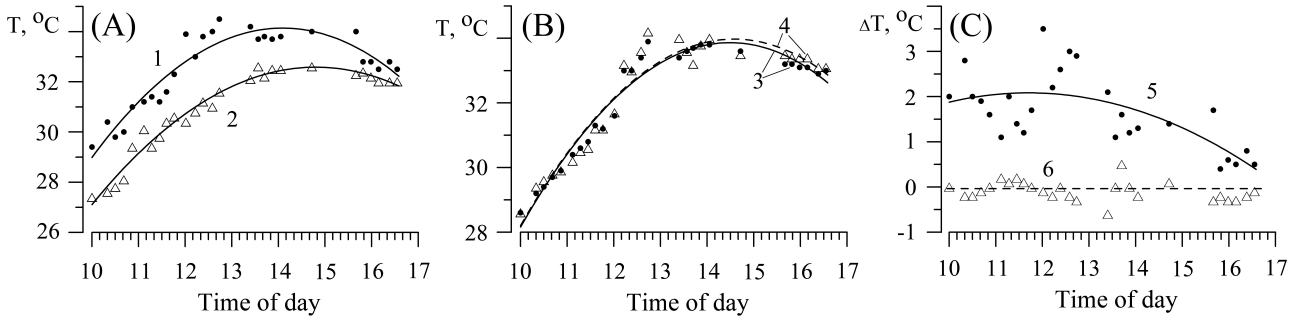

Fig. 4. A, water temperature variations in the floating mat (1) and in the algal layer underneath (2) at station *D1*; B, water temperature variations in the bottom mat (4) and above it (3) at station *D2*; C, difference (ΔT) between water temperature in the floating mat and in the algal layer underneath (5) and water temperature within the bottom mat and above it (6)

The values of water temperature in the floating mat (sta. *D1*) throughout the considered time period were higher than in the algal layer underneath. The temperature difference in the first half of the day averaged 2 °C; in the second half, it decreased to 0.5–1 °C (Fig. 4A, C). Water temperature values in the benthic mat and in 2 cm above it (sta. *D2*) almost did not differ (Fig. 4B, C); the temperature difference was 0.1–0.3 °C. For one hour, from 03:40 p.m. to 04:40 p.m., water temperature in the benthic mat was higher than above it.

Water temperature measured in the floating mat and in the algal layer underneath at sta. *E3* at 05 p.m. was +31.2 and +31.5 °C, respectively.

Structure of the *Cladophora* mat. At sta. *D1*, *E3*, and *E4*, in the vertical structure of the *Cladophora* mat, a floating mat (A) and the algal layer underneath (B) are distinguished (Fig. 1D, F, G). In all these cases, the floating mat was a dense accumulation of *Cladophora* near the water surface (3.6–15.2 kg·m^{-3} of dry mass, Table 1), where two horizontal layers were clearly distinguished: the upper (A1), relatively thick (1–3 cm), dirty green or yellow, and the lower (A2), thin (0.1–1 cm), green or dark green (Fig. 5). The algal layer under the floating mat, freely floating in water of *Cladophora* thalli, was characterized by a low bulk density (0.2–1.4 kg·m^{-3} of dry mass, see Table 1), and the algae forming it differed in color at various stations. Thus, at sta. *D1*, those were dark green; at sta. *E3*, dirty green; and at sta. *E4*, pink. In the latter case, the algae were in a state of decomposition; on their surface, purple bacteria *Chromatium* Perty, 1852 and *Ectothiorhodospira* Pelsh, 1936 developed, giving them the appropriate color. Within the entire algal mat, the floating mat accounted for 86.9% of *Cladophora* biomass at sta. *D1* and 62.2 and 66% at sta. *E3* and *E4*, respectively; the share of the upper layer in the floating mat ranged from 75 to 86.7% of its mass (Table 1, Fig. 6a–c).

At sta. *D2*, the benthic mat of algae, a mat lying on the bottom, was structurally similar to the floating mat; on the bottom surface, it occurred in separate “spots” of different sizes (Figs 1E, 2A). The upper mat layer was no more than 2 cm thick and was dirty orange, which indicated the presence of purple bacteria in high abundance. The bottom layer was thin, 0.2–0.3 cm, and dark green.

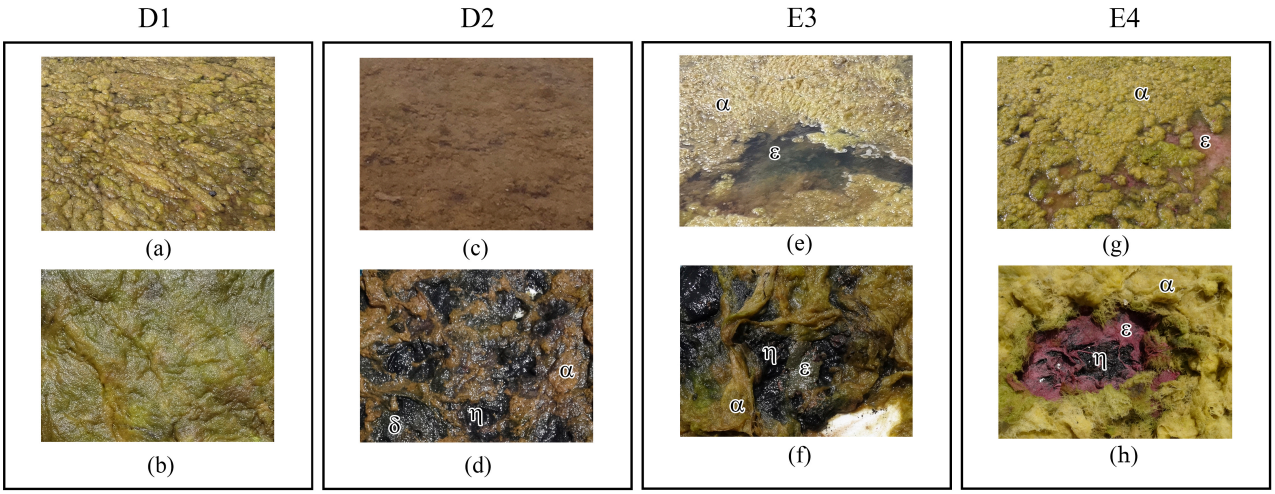

Fig. 5. View of *Cladophora* mats and their separate elements at sampling stations (*D1*, *D2*, *E3*, *E4*). Top (a) and bottom view (b) of the floating mat at station *D1*. Top view (c, d) of the bottom mat at station *D2*. On d: the bottom mat upper layer is partially removed (α), uncovering underlying layers (δ, η). Top view of the floating mat at stations *E3*, *E4* (e, g). On f, h: the floating mat upper layer is partially removed (α), uncovering underlying layers (ε, η)

Table 1. Quantitative characteristics of the *Cladophora* mat and epiphytic diatoms, Lake Chersonesskoye, 26.07.2017

Sta.	Vertical layer	*Cladophora*						Diatoms			
								per unit of *Cladophora* dry biomass		*per* unit of the lake area	
		m_{dry}, $g \cdot m^{-2}$ (dry mass)	*SD*	*CV*	C_w, $kg \cdot m^{-3}$ (dry weight)	*SD*	*CV*	N_D/W_{Cl}, $\times 10^6$ cells$\cdot g^{-1}$	W_D/W_{Cl}, $mg \cdot g^{-1}$ (wet mass)	N_D/S_0, $\times 10^8$ cells$\cdot m^{-2}$	W_D/S_0, $g \cdot m^{-2}$ (wet mass)
D1	The floating mat (A)	441.740	40.719	0.092	11.044	1.018	0.092	24.892	55.284	109.959	24.421
	Algae under the floating mat (B)	66.369	5.967	0.090	1.368	0.317	0.232	30.907	73.263	20.513	4.862
	A + B	508.109	42.673	0.084	–	–	–	–	–	130.472	29.284
E3	The floating mat (A)	54.646	12.978	0.237	3.643	0.865	0.237	20.559	45.802	11.234	2.503
	Algae under the floating mat (B)	33.181	9.113	0.275	0.222	0.052	0.233	10.124	21.746	3.359	0.722
	A + B	87.827	22.040	0.251	–	–	–	–	–	14.594	3.224
E4	The floating mat (A)	342.035	33.135	0.097	15.202	1.473	0.097	2.881	13.291	10.073	4.647
	Algae under the floating mat (B)	176.564	16.031	0.091	1.315	0.084	0.064	3.108	10.319	5.488	1.822
	A + B	518.600	49.149	0.095	–	–	–	–	–	15.560	6.469

Note: m_{dry}, dry *Cladophora* biomass *per* unit of the lake surface; *SD*, standard deviation; *CV*, coefficient of variation; C_w, concentration of dry mass of *Cladophora* in the mat volume; N_D/W_{Cl}, the abundance of diatom cells *per* unit of dry *Cladophora* biomass; W_D/W_{Cl}, wet mass of diatom cells *per* unit of dry *Cladophora* biomass; N_D/S_0, the abundance of diatom cells *per* unit of the lake surface area; W_D/S_0, wet biomass of diatom cells *per* unit of the lake surface area.

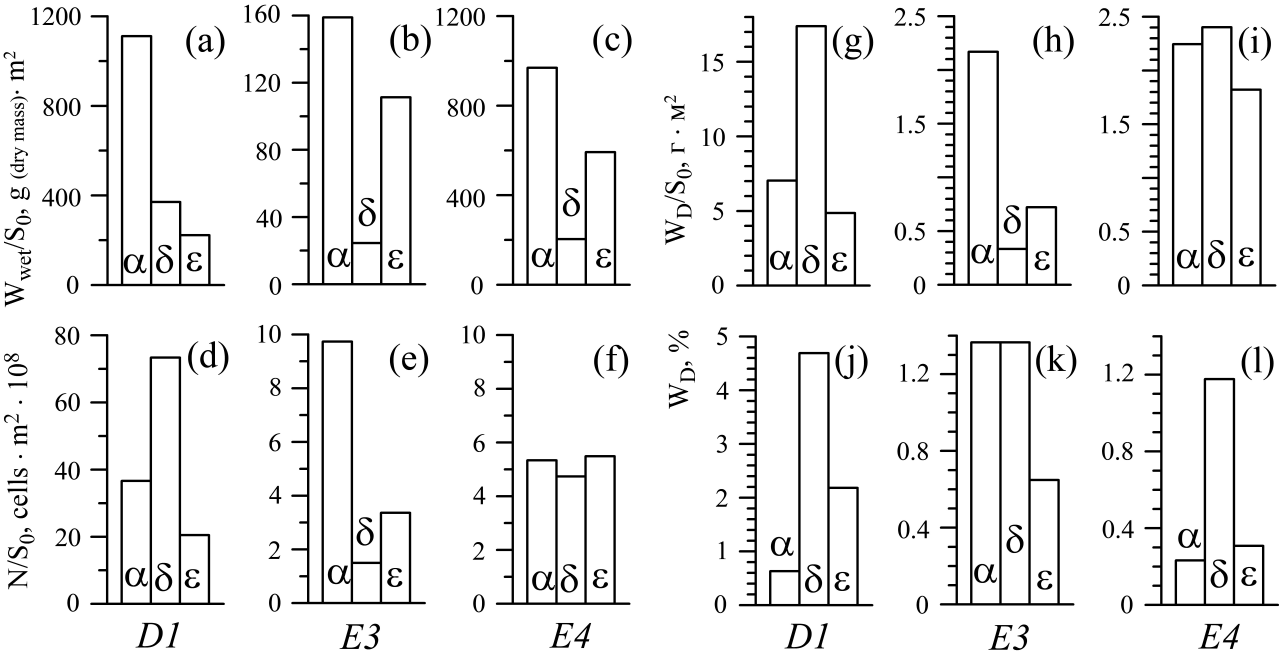

Fig. 6. *Cladophora* biomass *per* unit of the lake bottom surface at various horizons of the mat (a–c). The total abundance (d–f) and biomass (g–i) of diatoms *per* unit of the lake bottom surface at various horizons of the mat. The share of diatom mass in the total mass of the *Cladophora* mat (j–l). *D1*, *E3*, *E4*, sampling stations; α, δ, ε, sampling points

The species composition of diatom algae in *Cladophora* mats and benthic sediments. At the time of the study, 23 microalgal species were found on *Cladophora* and in bottom sediments in the area of the stations surveyed: Chromista (Ochrophyta, Bacillariophyceae), 20 species (Table 2, Fig. 7); Chromista (Myzozoa, Dinophyceae), 3 species (*Gymnodinium* sp.; *Kryptoperidinium foliaceum* (F. Stein) Lindemann, 1924; and *Protoceratium reticulatum* (Claparède & Lachmann) Bütschli, 1885). Within this article, we are going to limit ourselves to considering the species composition and quantitative characteristics of diatom algae of *Cladophora* mats and benthic sediments. Out of the diatoms identified, only one species (*Cocconeis kujalnitzkensis* Gusliakov et Gerasimiuk, 1992) was recorded in all the samples studied (see Supplement s1). Frequency of occurrence of *Nitzschia inconspicua* Grunow, 1862 in the samples was 92%, and the value for *Halamphora coffeiformis* (C. A. Agardh) Levkov, 2009 and *Mastogloia braunii* Grunow, 1863 was 85%. Four species (*Achnanthes brevipes* C. A. Agardh, 1824; *Mastogloia lanceolata* Thwaites ex W. Smith, 1856; *Navicula cancellata* Donkin, 1872; and *Nitzschia pusilla* Grunow, 1862), accounting for 20% of the species number, were identified only in 2 samples out of 13. Other four species (*Amphora* sp. 1; *Neosynedra provincialis* (Grunow) D. M. Williams & Round, 1986; *Nitzschia sigma* (Kützing) W. Smith, 1853; and *Thalassiosira eccentrica* (Ehrenberg) Cleve, 1904) were registered just in 1 sample. The maximum species diversity, 14 species, was observed in the benthic mat. In the floating mat, the value varied from 3 to 8, averaging 5.7 (*SD* = 2.517; *CV* = 0.444); in the algal layer under the floating mat, it varied from 4 to 10, averaging 6.3 (*SD* = 3.25; *CV* = 0.507). In terms of species richness, the samples of benthic sediments were less variable (*CV* = 0.143); the number of species in these samples ranged within 6–8, averaging 7 (*SD* = 1.000).

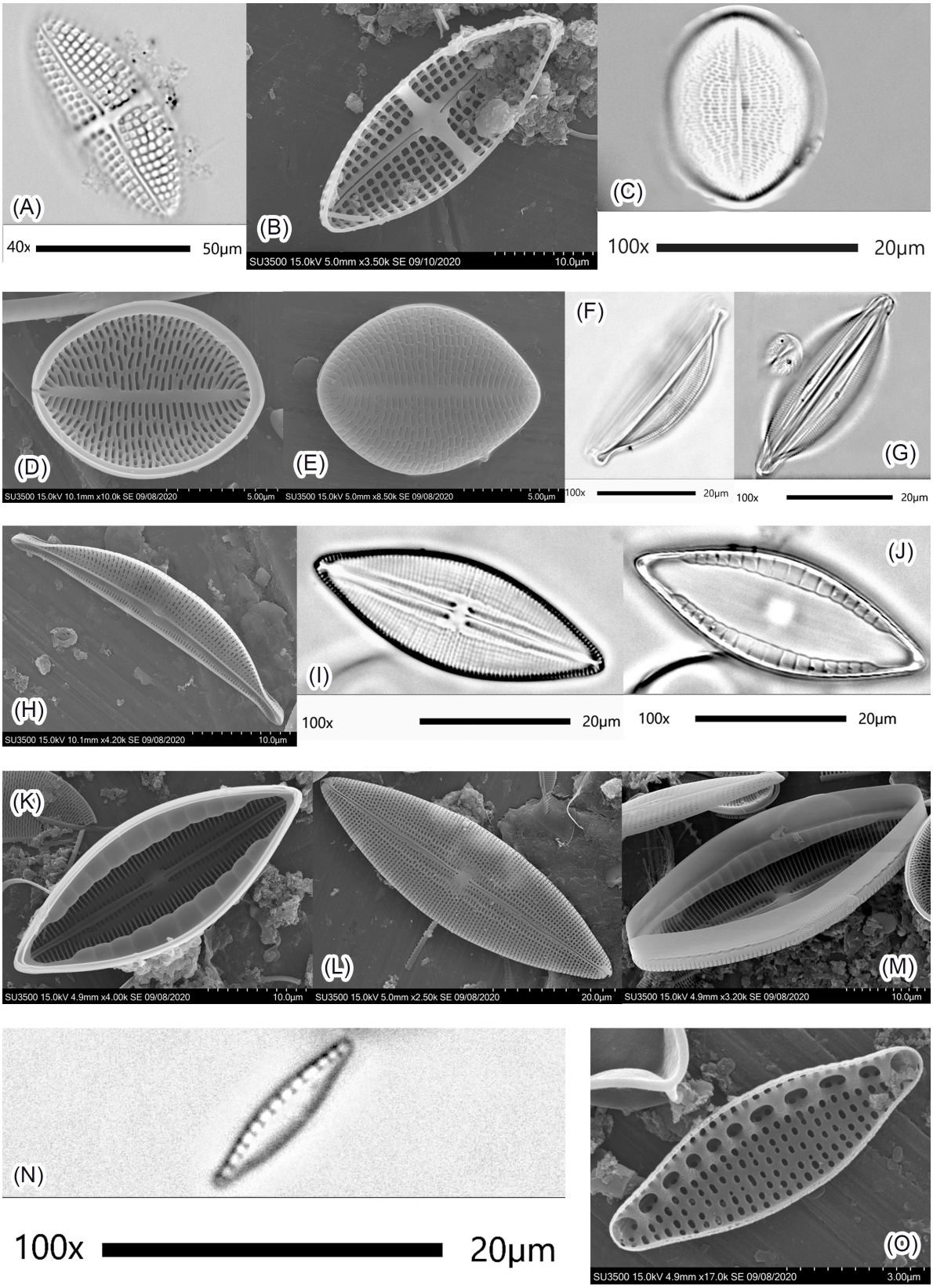

Fig. 7. Diatom species to be frequently found on *Cladophora* thalli in Lake Chersonesskoye as seen from different angles: A, B, *Achnanthes brevipes*; C–E, *Cocconeis kujalnitzkensis*; F–H, *Halamphora coffeiformis*; I–M, *Mastogloia braunii*; N–O, *Nitzschia inconspicua*. A, C, F, G, L, J, N, under a light microscope (Olympus BX53F); B, D, E, H, K–M, O, under a scanning electron microscope (Hitachi SU3500)

Table 2. Average, minimum, and maximum values of the individual cell mass for diatoms identified in the samples (Lake Chersonesskoye, 26.07.2017)

Species	Individual cell mass, $B_i \times 10^{-6}$, mg		
	average	minimum	maximum
Achnanthes brevipes C. A. Agardh, 1824	3.842	3.458	4.226
Achnanthes longipes C. A. Agardh, 1824	5.795	2.151	8.904
Amphora sp. 1	4.421	–	–
Cocconeis kujalnitzkensis Gusliakov et Gerasimiuk, 1992	2.082	1.345	2.954
Cyclotella caspia Grunow, 1878	0.467	0.111	0.926
Cylindrotheca closterium (Ehrenberg) Reimann et J. C. Lewin, 1964	0.128	0.095	0.178
Halamphora coffeiformis (C. A. Agardh) Levkov, 2009	2.239	0.342	4.746
Halamphora hyalina (Kützing) Rimet et R. Jahn in Rimet et al., 2018	3.824	3.455	4.521
Mastogloia braunii Grunow, 1863	6.802	5.469	9.260
Mastogloia lanceolata Thwaites ex W. Smith, 1856	8.619	7.988	9.250
Navicula cancellata Donkin, 1872	0.452	0.415	0.490
Navicula pennata var. *pontica* Mereschkowsky, 1902	1.061	0.381	2.355
Navicula ramosissima (C. Agardh) Cleve, 1895	0.231	0.117	0.283
Neosynedra provincialis (Grunow) D. M. Williams & Round, 1986	0.227	–	–
Nitzschia inconspicua Grunow, 1862	0.192	0.118	0.286
Nitzschia pusilla Grunow, 1862	0.116	0.100	0.132
Nitzschia sigma (Kützing) W. Smith, 1853	7.438	–	–
Nitzschia tenuirostris Mereschkowsky, 1902	0.186	0.132	0.235
Parlibellus delognei (Van Heurck) E. J. Cox, 1988	1.845	1.082	2.628
Thalassiosira eccentrica (Ehrenberg) Cleve, 1904	1.654	–	–

The values of the similarity coefficients of the species composition (K_J and K_{CSD}) between the samples are given in Table 3. K_J and K_{CSD} values, calculated when comparing the diatoms of plant mats at sta. *E3* and *E4* (the northeastern shore of the lake), were 0.67 and 0.80, respectively. This means a lack of clear dissimilarity in the species composition of the compared objects. Comparison of the species composition of diatoms at sta. *D1* and *D2* (the southeastern shore of the lake) showed their similarity as well; however, the values of the coefficients were close to the threshold ones (0.44 and 0.62, respectively), exceeding them only slightly. A pairwise comparison of diatoms in plant mats of the stations on the southeastern and northeastern shores revealed a noticeable dissimilarity between them (see Table 3). A more detailed comparison of diatoms, separately for the floating mat and for the algal layer underneath at different stations, also revealed a clear similarity between stations on the same shore and a dissimilarity between stations on the northeastern and southeastern shores (Table 3). Comparison of the species composition of the benthic mat, its upper and lower layers (sta. *D2*), with that of similar layers of the floating mat at sta. *D1* and *E4* did not reveal any similarity for diatom communities. A pairwise comparison of benthic sediment samples from different stations showed as follows: in benthic sediments at each station, the composition of diatoms peculiar to them alone is formed. Another type of comparison, comparison of the samples by the vertical component of the mat at all the stations studied, revealed that the upper and lower layers of the floating mat, the algal layer underneath, and benthic sediments do not differ in diatom species composition. There is an exception, a slight dissimilarity at sta. *D2* between the benthic mat and benthic sediments; K_J and K_{CSD} values are in the threshold zone, accounting for 0.40 and 0.57, respectively.

Table 3. The similarity coefficients of the diatom species composition in the considered objects under pairwise comparison (Lake Chersonesskoye, 26.07.2017)

Pairwise comparison objects	K_J	K_{CSD}
Comparison of the upper and lower layers of the mat at different stations		
1α – 1δ	0.44	0.62
2α – 2δ	0.71	0.83
4α – 4δ	0.67	0.80
Comparison of the upper layer of the floating mat and the algal layer underneath at different stations		
1α – 1ε	0.55	0.71
4α – 4ε	1.00	1.00
Comparison of the floating mat and the algal layer underneath at different stations		
1(α + δ) – 1ε	0.73	0.84
3(α + δ) – 3ε	0.75	0.86
4(α + δ) – 4ε	0.83	0.91
Comparison of the floating mat and the soil layer underneath at different stations		
2(α + δ) – 2η	0.40	0.57
3(α + δ) – 3η	0.50	0.67
4(α + δ) – 4η	0.56	0.71
Comparison of the algal layer under the floating mat and the soil layer underneath at different stations		
3ε – 3η	0.67	0.80
4ε – 4η	0.63	0.77
Comparison of the upper layer of the floating mat at sta. *D1* and *E4*		
1α – 4α	0.33	0.50
Comparison of the upper layer of the bottom mat at sta. *D2* with the upper layer of the floating mat at sta. *D1* and *D4*		
2α – 1α	0.38	0.56
2α – 4α	0.33	0.50
2α – (1 + 4)α	0.33	0.50
Comparison of the lower layer of the floating mat at sta. *D1* and *E4*		
1δ – 4δ	0.38	0.55
Comparison of the lower layer of the bottom mat at sta. *D2* with the lower layer of the floating mat at sta. *D1* and *D4*		
2δ – 1δ	0.36	0.53
2δ – 4δ	0.29	0.44
2δ – (1 + 4)δ	0.40	0.57
Comparison of the bottom mat under the floating mat at different stations with each other		
1ε – 3ε	0.40	0.57
1ε – 4ε	0.36	0.53
3ε – 4ε	0.80	0.89
Comparison of floating mats at different stations with each other		
1(α + δ) – 3(α + δ)	0.20	0.33
1(α + δ) – 4(α + δ)	0.25	0.40
3(α + δ) – 4(α + δ)	0.80	0.89
Comparison of the bottom mat at sta. *D2* with the floating mat at different stations		
2(α + δ) – 1(α + δ)	0.35	0.52
2(α + δ) – 3(α + δ)	0.21	0.35
2(α + δ) – 4(α + δ)	0.33	0.50
2(α + δ) – (1 + 3 + 4)(α + δ)	0.50	0.67

Continue on the next page…

Pairwise comparison objects	K_J	K_{CSD}
Comparison of soils under the mat at different stations with each other		
2η – 3η	0.18	0.31
2η – 4η	0.36	0.53
3η – 4η	0.40	0.57
Comparison of entire plant mats at different stations with each other		
D1 – D2	0.44	0.62
D1 – E3	0.33	0.50
D1 – E4	0.29	0.44
D2 – E3	0.29	0.44
D2 – E4	0.33	0.50
E3 – E4	0.67	0.80

Average, minimum, and maximum values of the individual cell mass for diatoms identified in the samples. These values are given in Table 2. The total row of cell biomass values fits into two orders of magnitude, with the minimum registered cell biomass in *Cylindrotheca closterium* (Ehrenberg) Reimann et J. C. Lewin, 1964 (0.095×10^{-6} mg) and the maximum recorded in *M. braunii* (9.26×10^{-6} mg). Each algal species occurred within its characteristic range of B_i values, and it was relatively narrow for most species (Fig. 8A). Four algae stood out (*Achnanthes longipes* C. A. Agardh, 1824; *Cyclotella caspia* Grunow, 1878; *H. coffeiformis*; and *N. pennata* var. *pontica* Mereschkowsky, 1902): their individual cell mass varied within a relatively wide range. Moreover, there were four species (*Amphora* sp. 1; *N. sigma*; *N. provincialis*; and *T. eccentrica*) represented by single specimens in the samples. The range of variation of the individual cell mass (ΔB_i) expands with an increase in the average cell size (B_{mid}), characteristic of each algal species (Fig. 8B), and this relationship is described by the equation:

$$\log \Delta B_i = -0.578 + 0.944 \log B_{mid} \ (s = 0.361; R^2 = 0.87) \ .$$

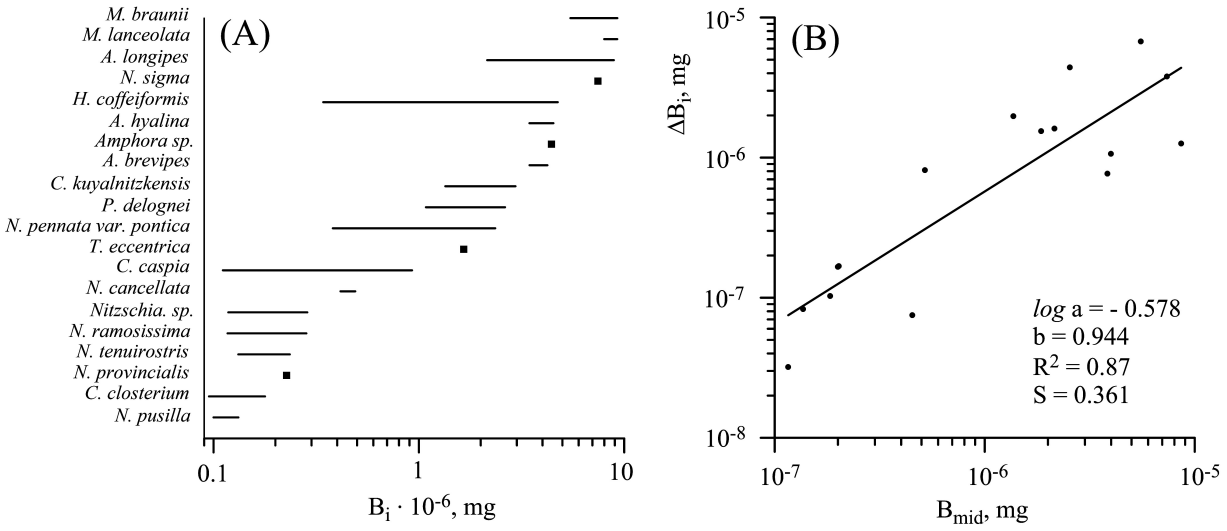

Fig. 8. A, the individual cell mass (B_i) variation ranges in different diatom species identified in the samples (Lake Chersonesskoye, 26.07.2017); B, dependence of the individual cell mass (ΔB_i) variation range on the average cell size (B_{mid}) characteristic of each algal species

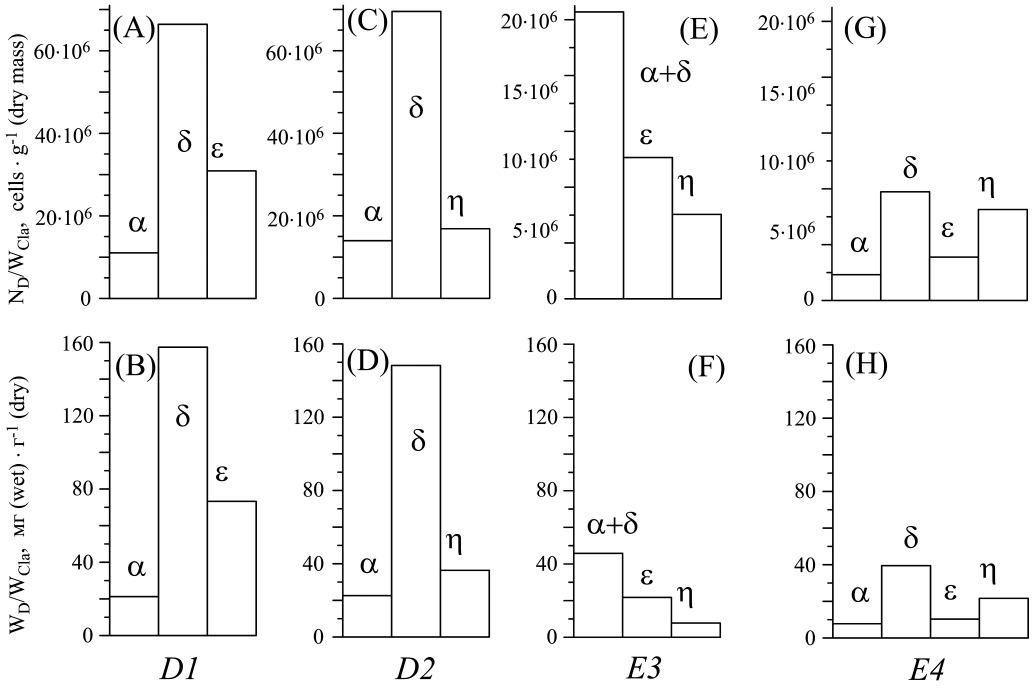

Fig. 9. Total abundance (A, C, E, G) and biomass (B, D, F, H) of diatom algae *per* unit of dry *Cladophora* mass and bottom sediments at stations *D1*, *D2*, *E3*, *E4*; α, δ, ε, η, sampling points

The total abundance and biomass of diatoms *per* unit of dry mass of *Cladophora* and benthic sediments. At the sampling points, the total abundance of diatoms and their biomass on *Cladophora* (*per* unit of dry biomass) and in benthic sediments (*per* unit of dry mass) varied over a wide range (see Supplements s1, s2, Fig. 9). On *Cladophora*, the abundance varied from 1.85×10^6 to 69.52×10^6 cells·g^{-1}; the biomass, from 7.77 to 157.43 mg·g^{-1}. In benthic sediments, the abundance varied from 6.05×10^6 to 16.87×10^6 cells·g^{-1}; the biomass, from 7.76 to 36.39 mg·g^{-1}. At all the stations, high values of the cell abundance and biomass *per* unit of *Cladophora* mass were recorded in the lower layer of the floating mat: 47.911×10^6 cells·g^{-1} (*SD* = 34.783; *CV* = 0.726) and 115.06 mg·g^{-1} (*SD* = 65.599; *CV* = 0.570), respectively. Low values were registered in its upper layer: 8.957×10^6 cells·g^{-1} (*SD* = 6.329; *CV* = 0.707) and 17.21 mg·g^{-1} (*SD* = 8.197; *CV* = 0.476), respectively. In the algal layer under the floating mat, mean values of the abundance and biomass were 14.713×10^6 cells·g^{-1} (*SD* = 14.457; *CV* = 0.983) and 35.11 mg·g^{-1} (*SD* = 33.532; *CV* = 0.955), respectively. The values of the characteristics studied at sta. *D1* and *D2* (the southeastern shore of the lake) were approximately the same and noticeably higher than those observed at sta. *E3* and *E4* (the northeastern shore of the lake), with the lowest values at sta. *E4*. In terms of the cell abundance *per* unit of dry mass of benthic sediment, sta. *E3* and *E4* did not differ much from one another, but the values were 3 times lower than those determined at sta. *D2*. At the same time, in terms of cell mass *per* unit of dry mass of benthic sediment, sta. *E3* and *E4* differed from one another by 3 times, while sta. *D2* exceeded them by 5 and 3 times, respectively.

At sta. *D1*, *D2*, and *E3*, one species, *C. kujalnitzkensis*, prevailed in the abundance in both the upper and lower mat layers. At sta. *D1* and *E3*, it averaged 96.1% (*SD* = 1.9; *CV* = 0.02); at sta. *D2*, 54.1%. At sta. *E4*, two species, *M. braunii* and *C. kujalnitzkensis*, contributed much to the total abundance of the floating mat diatoms. There, in the upper mat layer, *M. braunii* accounted for 67.5% of the total abundance, and *C. kujalnitzkensis*, for 20.2%. In the lower mat layer, their contribution was approximately the same: 44.8 and 54.1%, respectively.

At all the stations studied, *C. kujalnitzkensis* prevailed in the abundance in the algal layer under the floating mat, where its share averaged 72.2% (*SD* = 15.33; *CV* = 0.212). At sta. *D2* and *E4*, this species prevailed in the abundance in benthic sediments as well (70.3 and 66.8%, respectively); at sta. *E3*, the prevailing species was *N. inconspicua* (76.3%).

The distribution of various diatom species taking into account their contribution to the total mass at different stations is largely repeated in the samples with their distribution by the abundance. The main contributor to the total biomass of diatoms (from 63 to 99%) in the upper and lower mat layers at sta. *D1*, *D2*, and *E3* was *C. kujalnitzkensis*. This species also prevailed (79.2% of the diatom mass) in the algal layer under the mat at sta. *D1* and *E3*. At sta. *E4*, *M. braunii* prevailed in the floating mat and in the algal layer underneath (84.7 and 55.2% of the diatom mass, respectively). At the same station, in the algal layer under the floating mat, the contribution of *C. kujalnitzkensis* to the total diatom biomass was 38.5%. In the upper and lower layers of the floating mat, its contribution was even less, 6.47 and 18%, respectively.

In benthic sediments at sta. *D2*, *C. kujalnitzkensis* accounted for 66.4% of the total diatom biomass, while at sta. *E4* and *E3*, its value dropped to 38 and 4.97%, respectively. At sta. *E4*, 58.3% of the diatom biomass in benthic sediments was formed by *M. braunii*. At sta. *E3*, the main contributors to its formation were two algal species, *H. coffeiformis* and *M. braunii* (40.9 and 43.1%, respectively).

The total abundance and biomass of diatoms of the *Cladophora* mat *per* unit of the lake bottom surface. The total abundance of diatoms of the *Cladophora* mat *per* unit of the lake bottom surface varied from 14.59×10^8 cells·m^{-2} at sta. *E3* to 130.47×10^8 cells·m^{-2} at sta. *D1* and averaged 53.54×10^8 cells·m^{-2} (*SD* = 66.63×10^8; *CV* = 1.24). Their total biomass ranged from 3.22 to 29.28 g·m^{-2} (wet weight), with average value of 12.99 g·m^{-2} (*SD* = 14.20; *CV* = 1.09) (see Table 1, Fig. 6d–i). The share of the diatom biomass in the wet mass of the entire *Cladophora* mat averaged 1.06% (*SD* = 0.68; *CV* = 0.64), while in separate mat layers, it differed noticeably. For example, in the lower layer of the floating mat (δ) at sta. *D1*, it reached 4.69% with average values of 2.41% (*SD* = 1.98; *CV* = 0.82) calculated for three stations (Fig. 6j–l). In the upper layer of the floating mat (α), this indicator varied widely as well, but average value was low, 0.74% (*SD* = 0.57; *CV* = 0.77). The same was observed in the *Cladophora* layer under the floating mat (ε), 1.05% (*SD* = 0.99; *CV* = 0.95).

The absolute values of the abundance and biomass of diatoms calculated *per* unit of the lake bottom surface in relation to various mat layers at sta. *D1* were many times higher than those observed at sta. *E3* and *E4* (Fig. 6d–i). The nature of the distribution of diatoms over the layers of the *Cladophora* mat is peculiar to each station. In terms of diatom mass and abundance, the lower layer of the floating mat stands out at sta. *D1*, and the upper layer, at sta. *E3*. At sta. *E4*, the distribution of diatoms over the *Cladophora* mat layers was relatively uniform.

DISCUSSION

This investigation is one of the areas of our activity in studying Crimean hypersaline lakes and, in particular, Lake Chersonesskoye near the city of Sevastopol. The research is driven by the hypothesis that *Cladophora* mats in Lake Chersonesskoye are the main habitat-forming elements in spring–autumn and that they spatially structure communities of epiphytic unicellular algae.

In literature, different numbers of diatom species found as epiphytes on *Cladophora* are published. Specifically, in [Malkin et al., 2009], the number is 17; that is how many species were identified on 26 May on *Cladophora* (*Cladophora glomerata* (L.) Kützing, 1843), which begins its vegetative

growth in the Great Lakes. Interestingly, 57 species belonging to 26 genera were identified by [Mpawenayo, Mathooko, 2005] on *Cladophora* sampled in various areas of the Niero River in Kenya. Moreover, on *Cladophora* sampled from the Colorado River, there were 78 diatom species representing 20 genera [Hardwick et al., 1992]. On *Cladophora albida* (Nees) Kützing, 1843 in two Black Sea areas, 24 diatom species were recorded [Ryabushko et al., 2013].

As shown in the present study, in Lake Chersonesskoye in July 2017, on *Cladophora* organized in mats, 20 diatom species belonging to 12 genera were identified; in benthic sediments, 13 diatom species representing 10 genera were registered. In the same lake, during the observation period from August 2002 to March 2006, 61 species of unicellular algae belonging to 7 divisions, 10 classes, 22 orders, and 41 genera were found and described in a water column outside the *Cladophora* mat [Senicheva et al., 2008]. The first place in the species number was occupied by dinophytes (19 species); the second place, diatoms (15 species). Out of diatoms, benthic forms prevailed (*Nitzschia tenuirostris* Mereschkowsky, 1902; *Nitzschia* sp.; *Cocconeis scutellum* Ehrenberg, 1838; and *Pleurosigma elongatum* W. Smith, 1852); there were practically no planktonic species, except for individual finds of *C. caspia* and *T. eccentrica*. In Crimean saline lakes, 68 species and 69 intraspecific taxa of bottom diatoms were recorded [Nevrova, Shadrin, 2008]; off the Crimean coast, 465 species, *inter alia* 769 intraspecific taxa, were registered [Nevrova, Petrov, 2008]. To date, more than 1,000 species of all benthic microalgae have been found in the Black Sea, including about 650 species of diatoms [Ryabushko, 2013].

Our study also reveals that epiphytic communities of diatoms in various areas of *Cladophora* mats differ in species composition, total abundance, and biomass, as well as in the significance of certain algal species in the community structure. Most taxa show overlapping distributions in the vertical component of a vegetation mat, while some are found in its specific horizons alone. For example, *Amphora* sp. 1 and *N. provincialis* were registered only in lower layers of the floating mat; *N. sigma*, in bottom sediments alone.

Based on information in literature, we are going to discuss the possible causes of the observed distributions of epiphytic unicellular algae within the *Cladophora* mat.

The upper and lower layers of the floating mat and the algal layer underneath are biotopes with pronounced environmental conditions, both for *Cladophora* and its epiphytes. The floating mat, especially its upper layer, experiences strong daily temperature fluctuations [Prazukin et al., 2008]; moreover, a high level of solar radiation is observed there. According to our previous studies [Prazukin et al., 2018], in the upper thin layer of the floating mat, algae can undergo drying (dehydration); in other cases, a dense layer of salt can be formed on the mat surface. B. Ibelings and L. Mur [1992] found out that the absorption of carbon dioxide and nitrogen by algal cells decreases as those become dehydrated. High levels of ultraviolet radiation can cause photoinhibition, degradation of photosynthetic pigments, and cell death in the upper mat layers [Jiang, Qiu, 2005]; as a consequence, in this part of the mat, there are relatively low values of the intensity of photosynthesis compared to the values in the underlying layer [Prazukin et al., 2019]. In the daytime, oxygen content can be 200% of saturation in the upper mat layer against the backdrop of a lack of oxygen in the lower mat [Shadrin, Anufriieva, 2018]. Insects and their larvae actively develop on the mat surface, and they graze on epiphytic algae [Furey et al., 2012]. Algae of the floating mat may be limited in their access to biogenic elements from bottom sediments, as noted for pelagic phytoplankton populations [Bootsma et al., 2004].

For the communities of unicellular algae in the lower layer of the floating mat and the algal layer of the benthic mat, habitat conditions are completely different from those observed in the upper layer of the floating mat. Thus, even in thin periphyton films of unicellular algae, there is a strong vertical gradient of light [Kühl, Jørgensen, 1992]. In the floating mat of *Pithophora* Wittrock, 1877, only 1% of the incident light reaches a 1-cm depth [O'Neal, Lembi, 1983], while in the *Cladophora* mat, the value is 2% [Eiseltová, Pokorný, 1994]. In dense mats of *Chaetomorpha linum* (O. F. Müller) Kützing, 1845, the light zone is limited to 8 cm [Krause-Jensen et al., 1996]. In turn, the floating mat in relation to the benthic mat is a screen that prevents the passage of light into benthic layers, causing a deterioration in photosynthesis conditions and a decrease in water temperature [Goldsborough, Robinson, 1996; Prazukin, 2015; Prazukin et al., 2008, 2019]. G. Hardwick *et al.* [1992] associate vertical zoning of epiphytic diatoms on *C. glomerata* in the Colorado River (Arizona) (a decrease in cell density) with the weakening of light as the depth increases.

The fact of the mutual metabolic effect of epiphytes and the host plant [Young et al., 2010] cannot be excluded either. This may be reflected in the vertical distribution of epiphytic unicellular algae in the space of *Cladophora* mats.

Conclusion. Each of the factors considered, in varying degrees, can determine the vertical distribution of microalgae within the *Cladophora* mat, but none of them can be called the only determining one. *Cladophora*, forming mats that occupy in some years 80–100% of the surface area of Lake Chersonesskoye, acts here as an ecological engineer. In the space of the mat, a multiplicity of biotic and abiotic gradients is formed, generating a great variety of habitat conditions, which can naturally or accidentally be manifested in time.

Field work, sample processing, data analysis, and this manuscript writing were supported by the Russian Science Foundation (grant No. 18-16-00001 for Aleksander Prazukin and Daria Balycheva). The study of the diatom species composition was carried out within the framework of IBSS state research assignment No. 121041500203-3, 121030300149-0, and 121041400077-1.

Acknowledgement. The authors are grateful to the head of IBSS laboratory of microscopy V. Lishaev for preparing the micrographs.

Supplement s1. Species composition and abundance of diatoms on *Cladophora* threads and in biogenic sediments (Lake Chersonesskoye, 26.07.2017).

Supplement s2. Biomass of diatoms on *Cladophora* threads and in biogenic sediments (Lake Chersonesskoye, 26.07.2017).

REFERENCES

1. *AlgaeBase.* World-wide electronic publication, National University of Ireland, Galway / M. D. Guiry, G. M. Guiry (Eds) : [site], 2020. URL: http://www.algaebase.org [accessed: 29.08.2020].
2. Anufriieva E. V. How can saline and hypersaline lakes contribute to aquaculture development? A review. *Journal of Oceanology and Limnology*, 2018, vol. 36, no. 6, pp. 2002–2009. https://doi.org/10.1007/s00343-018-7306-3
3. Bergey E. A., Boettiger C. A., Resh V. H. Effects of water velocity on the architecture and epiphytes of *Cladophora glomerata* (Chlorophyta). *Journal of Phycology*, 1995, vol. 31, iss. 2, pp. 264–271. https://doi.org/10.1111/j.0022-3646.1995.00264.x
4. Bootsma H. A., Young E. B., Berges J. A. Temporal and spatial patterns of *Cladophora*

biomass and nutrient stoichiometry in Lake Michigan. In: *Cladophora Research and Management in the Great Lakes* : proceedings of a workshop held at the Great Lakes WATER Institute, University of Wisconsin-Milwaukee, December 8, 2004. Milwaukee, Wisconsin, USA : [University of Wisconsin-Milwaukee], 2004, pp. 81–88.

5. *Diatomovyi analiz.* Kniga 2: *Opredelitel' iskopaemykh i sovremennykh diatomovykh vodoroslei. Poryadki Centrales i Mediales.* Moscow : Gosudarstvennoe izdatel'stvo geologicheskoi literatury, 1949, 238 p., [206] p. tabl. (in Russ.)
6. *Diatomovyi analiz.* Kniga 3: *Opredelitel' iskopaemykh i sovremennykh diatomovykh vodoroslei. Poryadok Pennales.* Moscow : Gosudarstvennoe izdatel'stvo geologicheskoi literatury, 1950, 398 p., [220] p. tabl. (in Russ.)
7. *Diatoms of the USSR. Fossils and Modern.* Vol. 2, iss. 2 / I. V. Makarov (Ed.). St. Petersburg : Nauka, 1992, 125 p. (in Russ.)
8. Dodds W. K., Gudder D. A. The ecology of *Cladophora*. *Journal of Phycology*, 1992, vol. 28, iss. 4, pp. 415–427. http://dx.doi.org/10.1111/j.0022-3646.1992.00415.x
9. Eiseltová M., Pokorný J. Filamentous algae in fish ponds of the Třeboň Biosphere Reserve–ecophysiological study. *Vegetatio*, 1994, vol. 113, iss. 2, pp. 155–170. https://doi.org/10.1007/BF00044232
10. Furey P. C., Lowe R. L., Power M. E., Campbell-Craven A. M. Midges, *Cladophora*, and epiphytes: Shifting interactions through succession. *Freshwater Science*, 2012, vol. 31, no. 1, pp. 93–107. http://dx.doi.org/10.1899/11-021.1
11. Goldsborough L. G., Robinson G. G. C. Pattern in wetlands. In: *Algal Ecology: Freshwater Benthic Ecosystems* / R. J. Stevenson, M. L. Bothwell, R. L. Lowe (Eds). San Diego, CA : Academic Press, 1996, pp. 77–117.
12. Gubanov V. I., Bobko N. I. Hydrological and hydrochemical characteristics in the hypersalt Lake Krugloe (Crimea, Cape Hersones). *Morskoj ekologicheskij zhurnal*, 2012, vol. 11, no. 4, pp. 18–26. (in Russ.). https://repository.marine-research.ru/handle/299011/1241
13. Gubelit Yu. I., Berezina N. A. The causes and consequences of algal blooms: The *Cladophora glomerata* bloom and the Neva estuary (eastern Baltic Sea). *Marine Pollution Bulletin*, 2010, vol. 61, iss. 4–6, pp. 183–188. https://doi.org/10.1016/j.marpolbul.2010.02.013
14. Guslyakov N. E., Zakordonets O. A., Gerasimyuk V. P. *Atlas diatomovykh vodoroslei bentosa severo-zapadnoi chasti Chernogo morya i prilegayushchikh vodoemov.* Kyiv : Naukova dumka, 1992, 112 p., [140] p. tabl. (in Russ.)
15. Hardwick G. G., Blinn D. W., Usher H. D. Epiphytic diatoms on *Cladophora glomerata* in the Colorado River, Arizona: Longitudinal and vertical distribution in a regulated river. *The Southwestern Naturalist*, 1992, vol. 37, no. 2, pp. 148–156. https://doi.org/10.2307/3671663
16. Higgins S. N., Malkin S. Y., Todd Howell E., Guildford S. J., Campbell L., Hiriart-Baer V., Hecky R. E. An ecological review of *Cladophora glomerata* (Chlorophyta) in the Laurentian Great Lakes. *Journal of Phycology*, 2008, vol. 44, iss. 4, pp. 839–854. https://doi.org/10.1111/j.1529-8817.2008.00538.x
17. Ibelings B. W., Mur L. R. Microprofiles of photosynthesis and oxygen concentration in *Microcystis* sp. scums. *FEMS Microbiology Letters*, 1992, vol. 86, iss. 3, pp. 195–203. https://doi.org/10.1111/j.1574-6968.1992.tb04810.x
18. Ivanova M. B., Balushkina E. V., Basova S. L. Structural-functional reorganization of ecosystem of hyperhaline Lake Saki (Crimea) at increased salinity. *Russian Journal of Aquatic Ecology*, 1994, vol. 3, no. 2, pp. 111–126. (in Russ.)
19. Jiang H., Qiu B. Photosynthetic adaptation of a bloom-forming cyanobacterium *Microcystis aeruginosa* (Cyanophyceae) to prolonged UV-B exposure. *Journal of Phycology*, 2005, vol. 41, iss. 5, pp. 983–992. https://doi.org/10.1111/j.1529-8817.2005.00126.x
20. Jones C. G., Lawton J. H., Shachak M. Organisms as ecosystem engineers. *Oikos*, 1994, vol. 69, no. 3, pp. 373–386. https://doi.org/10.2307/3545850
21. Kiselev I. A. Metody issledovaniya planktona. In: *Zhizn' presnykh vod SSSR*. Moscow ; Leningrad : Izd-vo AN SSSR, 1956, vol. 4, pt 1, pp. 183–265. (in Russ.)

22. Krause-Jensen D., McGlathery K., Rysgaard S., Christensen P. B. Production within dense mats of the filamentous macroalga *Chaetomorpha linum* in relation to light and nutrient availability. *Marine Ecology Progress Series*, 1996, vol. 134, pp. 207–216. https://doi.org/10.3354/meps134207
23. Kühl M., Jørgensen B. B. Spectral light measurements in microbenthic phototrophic communities with a fiber-optic microprobe coupled to a sensitive diode array detector. *Limnology and Oceanography*, 1992, vol. 37, iss. 8, pp. 1813–1823. https://doi.org/10.4319/lo.1992.37.8.1813
24. Lange-Bertalot H. *Navicula* sensu stricto, 10 genera separated from *Navicula* sensu lato. *Frustulia*. Ruggell : A. R. G. Cantner Verlag K. G., 2001, 526 p. : 140 plts. (Diatoms of Europe: Diatoms of the European Inland Waters and Comparable Habitats / H. Lange-Bertalot (Ed.) ; vol. 2).
25. Malkin S. Y., Sorichetti R. J., Wiklund J. A., Hecky R. E. Seasonal abundance, community composition, and silica content of diatoms epiphytic on *Cladophora glomerata*. *Journal of Great Lakes Research*, 2009, vol. 35, iss. 2, pp. 199–205. https://doi.org/10.1016/j.jglr.2008.12.008
26. Marks J. C., Power M. E. Nutrient induced changes in the species composition of epiphytes on *Cladophora glomerata* Kütz. (Chlorophyta). *Hydrobiologia*, 2001, vol. 450, iss. 1–3, pp. 187–196. https://doi.org/10.1023/A:1017596927664
27. Messyasz B., Leska B., Fabrowska J., Pikosz M., Roj E., Cieslak A., Schroeder G. Biomass of freshwater *Cladophora* as a raw material for agriculture and the cosmetic industry. *Open Chemistry*, 2015, vol. 13, iss. 1, pp. 1108–1118. https://doi.org/10.1515/chem-2015-0124
28. Mpawenayo B., Mathooko J. M. The structure of diatom assemblages associated with *Cladophora* and sediments in a highland stream in Kenya. *Hydrobiologia*, 2005, vol. 544, iss. 1, pp. 55–67. https://doi.org/10.1007/s10750-004-8333-y
29. Mukhanov V. S., Naidanova O. G., Shadrin N. V., Kemp R. B. The spring energy budget of the algal mat community in a Crimean hypersaline lake determined by microcalorimetry. *Aquatic Ecology*, 2004, vol. 38, iss. 3, pp. 375–385. https://doi.org/10.1023/B:AECO.0000035169.08581.10
30. Nevrova E. L., Petrov A. N. Taksonomicheskoe raznoobrazie diatomovykh bentosa Chernogo morya. In: *The Black Sea Microalgae: Problems of Biodiversity Preservation and Biotechnological Usage* / Yu. N. Tokarev, Z. Z. Finenko, N. V. Shadrin (Eds) ; NAS of Ukraine, Institute of Biology of the Southern Seas. Sevastopol : EKOSI-Gidrofizika, 2008, pp. 60–84. (in Russ.). https://repository.marine-research.ru/handle/299011/5521
31. Nevrova E. L., Shadrin N. V. Donnye diatomovye vodorosli gipersolenykh vodoemov Kryma. In: *The Black Sea Microalgae: Problems of Biodiversity Preservation and Biotechnological Usage* / Yu. N. Tokarev, Z. Z. Finenko, N. V. Shadrin (Eds) ; NAS of Ukraine, Institute of Biology of the Southern Seas. Sevastopol : EKOSI-Gidrofizika, 2008, pp. 112–118. (in Russ.). https://repository.marine-research.ru/handle/299011/5521
32. Oxiyuk O. P., Yurchenko V. V. On the weight of the diatomeae algae. *Gidrobiologicheskii zhurnal*, 1971, vol. 7, no. 3, pp. 116–119. (in Russ.)
33. O'Neal S. W., Lembi C. A. Effect of simazine on photosynthesis and growth of filamentous algae. *Weed Science*, 1983, vol. 31, iss. 6, pp. 899–903. https://doi.org/10.1017/S0043174500070958
34. Pavlovskaya T. M., Prazukin A. V., Shadrin N. V. Seasonal phenomena in Infusoria community in hypersaline lake Khersonesskoye (Crimea). *Morskoj ekologicheskij zhurnal*, 2009, vol. 8, no. 2, pp. 53–63. (in Russ.). https://repository.marine-research.ru/handle/299011/1009
35. Prazukin A. V. *Ecological Phytosystemology*. Moscow : "Pero" Publishers, 2015, 375 p. (in Russ.). https://repository.marine-research.ru/handle/299011/1358
36. Prazukin A. V., Anufriieva E. V., Shadrin N. V. *Cladophora* mats in a Crimean hypersaline lake: Structure, dynamics, and inhabiting animals. *Journal of Oceanology and Limnology*, 2018, vol. 36, iss. 6, pp. 1930–1940. https://doi.org/10.1007/s00343-018-7313-4

37. Prazukin A. V., Anufriieva E. V., Shadrin N. V. Photosynthetic activity of green filamentous algae mats in the hypersaline lake Chersonesskoye (Crimea). *Vestnik Tverskogo gosudarstvennogo universiteta. Seriya: biologiya i ekologiya*, 2019, no. 2 (54), pp. 87–102. (in Russ.). https://doi.org/10.26456/vtbio74
38. Prazukin A. V., Anufriieva E. V., Shadrin N. V. Is biomass of filamentous green algae *Cladophora* spp. (Chlorophyta, Ulvophyceae) an unlimited cheap and valuable resource for medicine and pharmacology? A review. *Reviews in Aquaculture*, 2020, vol. 12, iss. 4, pp. 2493–2510. https://doi.org/10.1111/raq.12454
39. Prazukin A. V., Bobkova A. N., Evstigneeva I. K., Tankovska I. N., Shadrin N. V. Structure and seasonal dynamics of the phytocomponent of the bioinert system marine hypersaline lake on cape of Chersonesus (Crimea). *Morskoj ekologicheskij zhurnal*, 2008, vol. 7, no. 1, pp. 61–79. (in Russ.). https://repository.marine-research.ru/handle/299011/945
40. Prazukin A. V., Firsov Yu. K., Gureeva E. V., Kapranov S. V., Zheleznova S. N., Maoka T., Nekhoroshev M. V. Biomass of green filamentous alga *Cladophora* (Chlorophyta) from a hypersaline lake in Crimea as a prospective source of lutein and other pigments. *Algal Research*, 2021a, vol. 54, art. no. 102195 (9 p.). https://doi.org/10.1016/j.algal.2021.102195
41. Prazukin A., Shadrin N., Balycheva D., Firsov Yu., Lee R., Anufriieva E. *Cladophora* spp. (Chlorophyta) modulate environment and create a habitat for microalgae in hypersaline waters. *European Journal of Phycology*, 2021b, vol. 56, iss. 3, pp. 231–243. https://doi.org/10.1080/09670262.2020.1814423
42. Proshkina-Lavrenko A. I. *Diatomovye vodorosli bentosa Chernogo morya.* Moscow ; Leningrad : Nauka, 1963, 243 p. (in Russ.). https://repository.marine-research.ru/handle/299011/12747
43. Ryabushko L. I. *Microphytobenthos of the Black Sea.* Sevastopol : EKOSI-Gidrofizika, 2013, 416 p. (in Russ.). https://repository.marine-research.ru/handle/299011/8301
44. Ryabushko L. I., Balicheva D. S., Strijak A. V. Diatoms epiphyton of some green algae and periphyton of anthropogenic substrates of the Crimean coastal of the Black Sea. *Algologia*, 2013, vol. 23, no. 4, pp. 419–437.
45. Senicheva M. I., Gubelit Yu. I., Prazukin A. V., Shadrin N. V. Fitoplankton gipersolenykh ozer Kryma ; Tablitsa 4. Vidovoi sostav fitoplanktona gipersolenykh ozer Kryma. In: *The Black Sea Microalgae: Problems of Biodiversity Preservation and Biotechnological Usage* / Yu. N. Tokarev, Z. Z. Finenko, N. V. Shadrin (Eds) ; NAS of Ukraine, Institute of Biology of the Southern Seas. Sevastopol : EKOSI-Gidrofizika, 2008, pp. 93–100, 163–165. (in Russ.). https://repository.marine-research.ru/handle/299011/5521
46. Shadrin N. V., Anufriieva E. V. Ecosystems of hypersaline waters: Structure and trophic relations. *Zhurnal obshchei biologii*, 2018, vol. 79, no. 6, pp. 418–427. (in Russ.). https://doi.org/10.1134/S0044459618060076
47. Shadrin N. V., Anufriieva E. V., Belyakov V. P., Bazhora A. I. Chironomidae larvae in hypersaline waters of the Crimea: Diversity, distribution, abundance and production. *The European Zoological Journal*, 2017, vol. 84, iss. 1, pp. 61–72. https://doi.org/10.1080/11250003.2016.1273974
48. Shadrin N. V., Mikhodyuk O. S., Naidanova O. G., Voloshko L. N., Gerasimenko L. M. Donnye tsianobakterii gipersolenykh ozer Kryma. In: *The Black Sea Microalgae: Problems of Biodiversity Preservation and Biotechnological Usage* / Yu. N. Tokarev, Z. Z. Finenko, N. V. Shadrin (Eds) ; NAS of Ukraine, Institute of Biology of the Southern Seas. Sevastopol : EKOSI-Gidrofizika, 2008, pp. 100–112. (in Russ.). https://repository.marine-research.ru/handle/299011/5521
49. Stevenson R. J., Stoermer E. F. Seasonal abundance patterns of diatoms on *Cladophora* in Lake Huron. *Journal of Great Lakes Research*, 1982, vol. 8, iss. 2, pp. 169–183. https://doi.org/10.1016/S0380-1330(82)71955-0

50. Semkin B. I. On the relation between mean values of two measures of inclusion and measures of similarity. *Byulleten' Botanicheskogo sada DVO RAN*, 2009, iss. 3, pp. 91–101. (in Russ.)
51. *Vodorosli* : spravochnik / S. P. Vasser (Ed.). Kyiv : Naukova dumka, 1989, 608 p. (in Russ.)
52. Witkowski A., Lange-Bertalot H., Metzeltin D. *Diatom Flora of Marine Coasts. 1*. Ruggell ; Königstein : Gantner Verlag : Koeltz Scientific Books, 2000, 925 p. (Iconographia Diatomologica : Annotated Diatom Micrographs ; vol. 7: Diversity-Taxonomy-Identification / H. Lange-Bertalot (Ed.))
53. Young E. B., Tucker R. C., Pansch L. A. Alkaline phosphatase in freshwater *Cladophora*-epiphyte assemblages: Regulation in response to phosphorus supply and localization. *Journal of Phycology*, 2010, vol. 46, iss. 1, pp. 93–101. https://doi.org/10.1111/j.1529-8817.2009.00782.x
54. Zulkifly S. B., Graham J. M., Young E. B., Mayer R. J., Piotrowski M. J., Smith I., Graham L. E. The genus *Cladophora* Kützing (Ulvophyceae) as a globally distributed ecological engineer. *Journal of Phycology*, 2013, vol. 49, iss. 1, pp. 1–17. https://doi.org/10.1111/jpy.12025
55. Zulkifly S., Hanshew A., Young E. B., Lee Ph., Graham M. E., Graham M. E., Piotrowski M., Graham L. E. The epiphytic microbiota of the globally widespread macroalga *Cladophora glomerata* (Chlorophyta, Cladophorales). *American Journal of Botany*, 2012, vol. 99, iss. 9, pp. 1541–1552. https://doi.org/10.3732/ajb.1200161

CLADOPHORA (CHLOROPHYTA) КАК «ИНЖЕНЕР-ЭКОЛОГ» В ГИПЕРСОЛЁНОМ ОЗЕРЕ ХЕРСОНЕССКОМ: РАСПРЕДЕЛЕНИЕ ДИАТОМОВЫХ ВОДОРОСЛЕЙ В СТРУКТУРИРОВАННОМ ПРОСТРАНСТВЕ РАСТИТЕЛЬНЫХ МАТОВ

А. В. Празукин, Р. И. Ли, Д. С. Балычева, Ю. К. Фирсов, В. В. Холодов

ФГБУН ФИЦ «Институт биологии южных морей имени А. О. Ковалевского РАН»,
Севастополь, Российская Федерация
E-mail: *prazukin@mail.ru*

Род *Cladophora* — один из крупнейших родов зелёных водорослей, представители которого встречаются во всех водоёмах мира. Кладофора организует среду обитания для разных групп организмов, в том числе для эпифитных одноклеточных водорослей. Цель работы — изучить вертикальное распределение диатомей в структурированном пространстве матов *Cladophora* и в донных отложениях гиперсолёного озера в Крыму. В вертикальном строении мата кладофоры различали плавучий и донный маты, каждый из которых имел характерную структуру. Всего в ходе данного исследования зарегистрированы 20 видов диатомовых водорослей из 12 родов. Общая численность диатомей и их биомасса на *Cladophora* (в расчёте на единицу сухой биомассы) и в донных отложениях (в расчёте на единицу сухой массы) варьировали в широком диапазоне. На кладофоре численность изменялась от $1{,}85 \times 10^6$ до $69{,}52 \times 10^6$ кл.·г$^{-1}$, а биомасса — от 7,77 до 157,43 мг·г$^{-1}$. В донных осадках численность варьировала от $6{,}05 \times 10^6$ до $16{,}87 \times 10^6$ кл.·г$^{-1}$, биомасса — от 7,76 до 36,39 мг·г$^{-1}$. Доля биомассы диатомовых водорослей в сырой массе всего мата *Cladophora* в среднем составила 1,06 %.

Ключевые слова: диатомовые водоросли, эпибионты, нитчатые зелёные водоросли, плавучие маты, гиперсолёное озеро

Supplement 1. Species composition and abundance of diatoms on *Cladophora* threads and in biogenic sediments (Lake Chersonesskoye, 26.07.2017)

Species	Sampling station and position in the *Cladophora* mats and bottom biogenic sediments													*FO*, %
	D1			*D2*			*E3*			*E4*				
	α	δ	ε	α	δ	η	α + δ	ε	η	α	δ	ε	η	
	Abundance *per* unit of *Cladophora* dry biomass and bottom biogenic sediments, $\times 10^4$ cells·g^{-1}													
Kingdom Chromista Phylum Ochrophyta Class Bacillariophyceae														
Achnanthes brevipes	–	–	6	–	–	–	–	–	3	–	–	–	–	15
Achnanthes longipes	–	–	–	–	–	–	–	–	–	2	–	4	7	23
Amphora sp. 1	–	5	–	–	–	–	–	–	–	–	–	–	–	8
Cocconeis kujalnitzkensis	1,039	6,506	1,970	731	3,882	1,187	1,982	910	19	37	421	195	435	100
Cyclotella caspia	–	–	–	–	248	46	–	–	–	–	–	–	7	23
Cylindrotheca closterium	6	–	70	–	–	65	–	–	–	–	–	–	–	23
Halamphora coffeiformis	10	20	70	54	175	–	–	15	74	10	3	7	3	85
Halamphora hyalina	–	–	122	86	769	122	–	–	–	–	–	–	4	38
Mastogloia braunii	–	–	96	17	180	91	53	53	45	125	349	100	189	85
Mastogloia lanceolata	–	–	–	–	116	–	–	–	–	–	–	–	1	15
Navicula cancellata	–	–	–	29	146	–	–	–	–	–	–	–	–	15
Navicula pennata var. *pontica*	–	–	–	123	96	26	–	–	–	–	–	–	–	23
Navicula ramosissima	–	36	141	51	589	150	–	–	–	–	–	–	–	38
Neosynedra provincialis	–	–	–	–	26	–	–	–	–	–	–	–	–	8
Nitzschia inconspicua	22	29	531	30	474	–	21	35	462	11	5	4	5	92
Nitzschia pusilla	–	–	–	177	–	–	–	–	–	–	1	–	–	15
Nitzschia sigma	–	–	–	–	–	–	–	–	2	–	–	–	–	8
Nitzschia tenuirostris	11	–	23	81	126	–	–	–	–	–	–	–	–	31
Parlibellus delognei	5	46	62	18	125	–	–	–	–	–	–	–	–	38
Thalassiosira eccentrica	11	–	–	–	–	–	–	–	–	–	–	–	–	8
Species number in a sample	7	6	10	11	13	7	3	4	6	5	5	5	8	–
Total abundance of diatoms in a sample, $\times 10^6$ cells·g^{-1}	11.05	66.43	30.91	13.98	69.52	16.87	20.56	10.12	6.05	1.85	7.79	3.11	6.52	–

Note: α, the upper layer of the floating mat; δ, the lower layer of the floating mat; ε, the algal layer under the floating mat; η, layer of bottom biogenic sediments; and *FO*, frequency of occurrence.

Supplement 2. Biomass of diatoms on *Cladophora* threads and in biogenic sediments (Lake Chersonesskoye, 26.07.2017)

Species	Sampling station and position in the *Cladophora* mats and bottom biogenic sediments												
	D1			*D2*			*E3*			*E4*			
	α	δ	ε	α	δ	η	α + δ	ε	η	α	δ	ε	η
	Biomass *per* unit of *Cladophora* dry biomass and bottom biogenic sediments, mg·g^{-1} (wet mass)												
Kingdom Chromista Phylum Ochrophyta Class Bacillariophyceae													
Achnanthes brevipes	–	–	0.27	–	–	–	–	–	0.11	–	–	–	–
Achnanthes longipes	–	–	–	–	–	–	–	–	–	0.05	–	0.38	0.42
Amphora sp. 1	–	0.23	–	–	–	–	–	–	–	–	–	–	–
Cocconeis kujalnitzkensis	20.88	155.94	58.20	16.47	93.52	24.15	42.50	17.18	0.39	0.50	7.09	3.97	8.22
Cyclotella caspia	–	–	–	–	0.28	0.43	–	–	–	–	–	–	0.03
Cylindrotheca closterium	0.006	–	0.12	–	–	0.07	–	–	–	–	–	–	–
Halamphora coffeiformis	0.06	0.08	0.28	0.18	0.83	–	–	0.70	3.17	0.37	0.11	0.27	0.05
Halamphora hyalina	–	–	4.34	3.21	26.56	4.70	–	–	–	–	–	–	0.18
Mastogloia braunii	–	–	7.32	1.15	10.73	6.09	3.28	3.83	3.35	6.82	32.28	5.69	12.62
Mastogloia lanceolata	–	–	–	–	10.76	–	–	–	–	–	–	–	0.11
Navicula cancellata	–	–	–	0.12	0.72	–	–	–	–	–	–	–	–
Navicula pennata var. *pontica*	–	–	–	0.47	0.43	0.60	–	–	–	–	–	–	–
Navicula ramosissima	–	0.10	0.36	0.06	1.67	0.35	–	–	–	–	–	–	–
Neosynedra provincialis	–	–	–	–	0.06	–	–	–	–	–	–	–	–
Nitzschia inconspicua	0.04	0.04	1.00	0.07	1.05	–	0.03	0.05	0.60	0.03	0.01	0.005	0.01
Nitzschia pusilla	–	–	–	0.23	–	–	–	–	–	–	0.001	–	–
Nitzschia sigma	–	–	–	–	–	–	–	–	0.15	–	–	–	–
Nitzschia tenuirostris	0.01	–	0.04	0.16	0.30	–	–	–	–	–	–	–	–
Parlibellus delognei	0.06	1.04	1.33	0.48	1.36	–	–	–	–	–	–	–	–
Thalassiosira eccentrica	0.18	–	–	–	–	–	–	–	–	–	–	–	–
Total biomass of diatoms, mg·g^{-1}	21.24	157.43	73.26	22.61	148.25	36.39	45.80	21.75	7.76	7.77	39.50	10.32	21.64

Note: α, the upper layer of the floating mat; δ, the lower layer of the floating mat; ε, the algal layer under the floating mat; and η, layer of bottom biogenic sediments.

1871
ИнБЮМ – IBSS

Морской биологический журнал
Marine Biological Journal
2023, vol. 8, no. 3, pp. 87–96
https://marine-biology.ru

UDC [551.351:577.121.2](262.5)

RELATIONSHIP OF THE PROCESSES OF AEROBIC OXIDATION AND ANAEROBIC DESTRUCTION OF ORGANIC MATTER IN THE BOTTOM SEDIMENTS OF COASTAL WATERS OF CRIMEA (BLACK SEA)

© 2023 **V. P. Chekalov**

A. O. Kovalevsky Institute of Biology of the Southern Seas of RAS, Sevastopol, Russian Federation

Received by the Editor 25.02.2021; after reviewing 11.06.2021;
accepted for publication 04.08.2023; published online 21.09.2023.
E-mail: *valch@mail.ru*

The relationship between water masses and bottom sediments is obvious. This primarily refers to the formation of oxygen regime and self-purification of water bodies. Stoichiometric ratios allow assessing certain parameters of energy metabolism associated with oxygen consumption. The aim of this work is to determine the possible contribution of aerobic and anaerobic processes to the destruction of organic matter in bottom sediments of various areas of the Crimean coast by interpreting the data on oxygen consumption. The total oxygen consumption rate was measured using a respirometry camera hermetically connected to an HQ40D oxygen sensor with LDO oximeter. To suppress bacterial activity and reveal the rate of oxidation of reduced anaerobiotic products, the antibiotic streptomycin was used. Vertical sounding of the bottom sediment strata in the Belbek River paleochannel showed an increase with depth of oxidative potential and a subsurface peak of anaerobic activity. Due to the limited diffusion of oxygen, the rate of hydrogen sulfide oxidation in the surface layer was comparable to the rate of its formation in the underlying sediment layer. A higher level of aerobic oxygen consumption and content of reduced compounds was observed in the bottom sediments of the Chernaya River paleochannel in contrast to its slopes. Increased concentration of hydrogen sulfide is due to the higher rate of its formation at relatively low rates of oxidation. In the Sevastopol Bay, the experimentally measured oxygen consumption by a unit of the bottom surface in the 0.6-cm sediment layer averaged 2.18 $\mu g \cdot cm^{-2} \cdot h^{-1}$. In the Kruglaya Bay, certain differences in the dynamics of reduced compounds (H_2S) were registered between the oxidized background areas and the zones of reduced bottom sediments (sulfurettes). In sulfurettes, the calculated values for concentration, oxidation rate, and formation of hydrogen sulfide were higher by 32, 29, and 57%, respectively. The maximum rate of organic matter decomposition, up to 4.05 $\mu g \cdot cm^{-3} \cdot h^{-1}$, was recorded in the Sevastopol Bay and the adjacent water areas, with the anaerobic component accounting for a larger share. The share turned out to be quite high in the Kruglaya Bay as well, but there, aerobic destruction prevailed. This is due to differences in both the targeted use of the bays and the granulometric composition of bottom sediments. In sulfurette sediments, against the backdrop of the rate of oxidation of organic substances equal to that of the background area, anaerobic utilization occurred more than 2 times more intensive. Its absolute value corresponded to the level characteristic of the open-sea coastal areas, in particular, the Belbek River paleochannel.

Keywords: bottom sediments, oxygen consumption, destruction of organic matter, Black Sea

When assessing the state of the environment, including the Black Sea bottom sediments, data are usually given on the content of both organic matter and its possible oxidizers [Gorshkova, 1974; Orekhova, 2010]. Specifically, it was reported that the share of the organic component in sediments of the Heracles Peninsula bays varied within 0.51–5.41% [Orekhova et al., 2018]. Oxygen concentration fluctuates over a wide range as well. Thus, almost complete absence of oxygen was recorded in the Sevastopol Bay sediments during the warm season: its content in the bottom water layer could drop to 30 μmol·L^{-1}, which is 10 times lower than the value characteristic for the winter period [Orekhova, Konovalov, 2018a]. Regular monitoring in the Sevastopol Bay [Ignat'eva et al., 2008; Moiseenko, Orekhova, 2011; Osadchaya et al., 2003] allows identifying certain trends, but single measurements in other water areas only make it possible to ascertain levels of the substances at a given time. However, their content often results from multidirectional processes, the intensity of which can shift the balance in one direction or another. Therefore, the study of such dynamic characteristics allows for both short-term and long-term forecasting. In this regard, a key role is played by the rate of oxygen consumption, the calculation of which in the form of certain derived parameters provides an integral picture of the processes occurring in biocenoses. On the one hand, these are the formation of environmental conditions and self-purification; on the other hand, these are the state and stability of constituent elements. Based on stoichiometric formulas, patterns for determining possible coefficients were proposed for the transition between various indicators of the biological activity of the community [Sapozhnikov, Metrevely, 2015]. By shifts in one parameter, a whole range of characteristics can be tracked. In order to study the relationship between possible rates of aerobic and anaerobic utilization of organic matter in various areas of the Crimean coast, an attempt was made to analyze the data obtained by the author on oxygen consumption by bottom sediments.

MATERIAL AND METHODS

In most of the surveyed water areas (the Dvuyakornaya Bay, the Chernaya River paleochannel, the Sevastopol Bay, and the Balaklava Bay), sampling was carried out with a Petersen grab. The material for the study was a surface 2-cm layer of bottom sediments. Containers for transportation were filled to the top to prevent air penetration. In the Kruglaya Bay, material was sampled from the same layer directly from the sulfurette and the background area by a diver using syringe tubes. In the clean coastal zone of the Cape Martyan nature reserve and in the Belbek River paleochannel, samples were taken from a 4–6-m depth with a Rumalot-type tubular sampler equipped with a transparent acrylic tube, 54 mm in diameter and 30 cm in height, with a shut-off valve at the opposite end and a weight with fastening fittings. As a rule, lifted bottom sediment cores retained an undisturbed structure, which made it possible to study them layer by layer. The coordinates of sampling points and the dates of field works are given in Table 1.

Oxygen content and redox potential were measured using sensors HQ40D and Sension 1 (Hach, the USA) with LDO oximeter. The accuracy of dissolved oxygen determination was ±0.1 mg·L^{-1} within a range of 0.1–8.0 mg·L^{-1}. To stabilize the readings of the redox potential, the sensor was immersed in a sample for 10 min; then, the result was recorded. The total oxygen consumption rate (hereinafter TOC) was determined in a 60-mL respirometry chamber filled with seawater and hermetically connected to an oxygen sensor. Initial oxygen concentration in water was about 7–8 mg·L^{-1}. A test 0.2-cm^3 sample was introduced into the chamber; there, it was distributed over an area of 20 cm^2, which corresponded to a layer of about 0.01 cm. The results were registered at 1-h intervals automatically for 20–24 h. Based on the data obtained, mean TOC was subsequently calculated.

From the bottom sediments of the Cape Martyan area, samples were taken from the horizons of 0–2 and 3–5 cm, while in the Belbek River paleochannel, from 0–2, 2–4, and 4–6 cm. For each layer, a unified scheme for TOC calculating was applied. It involved measurements under conditions of oxygen maximum availability in the 0.01-cm surface layer, followed by extrapolation to a thickness of 0.6 cm, with the features in diffusion of oxygen into bottom sediments taken into account [Chekalov, 2016].

The rate of oxygen neutralization of reduced compounds (hereinafter ONRC) was determined in a similar way, after suppressing the vital activity of bacteria. It was achieved by adding streptomycin to a measuring container at a final concentration of 0.1 mg·mL^{-1} and then incubating it at +8…+10 °C for the entire measurement period. This was also facilitated by lowering pH to 5 (using a 0.1N solution of sulfuric acid) in order to shift the ratio of sulfur compounds in water (S^{2-}, HS^{-}, H_2S) towards the prevalence of the most actively oxidized hydrogen sulfide. Oxygen content was determined every hour. Based on the data obtained, the mean rate of hydrogen sulfide oxidation was calculated, taking into account that in aqueous solutions, hydrogen sulfide is usually oxidized to sulfur and water:

$$2H_2S + O_2 \rightarrow 2H_2O + 2S\ .$$

The rate of aerobic oxygen consumption (hereinafter AOC) was obtained by subtracting ONRC values from the corresponding levels of total oxygen consumption. The data for AOC and ONRC are given as mean values with a confidence interval ($p = 0.95$).

To establish the rate of enrichment (production) with reduced compounds, immediately after sampling, ONRC was determined under laboratory conditions until the curve of oxygen content change reached a plateau, *i. e.*, until the readings stabilized at approximately the same level for more than 3 measurements. Based on the volume of oxygen consumed in this case, possible hydrogen sulfide content was calculated. In parallel, a part of samples, avoiding oxygen penetration, was placed in sealed containers, which were kept under conditions close to natural. The duration of incubation was determined experimentally. Usually, incubation lasted for 30–60 days, and then ONRC was determined again. The difference between the initial value and the repeated measurement, taking into account the time interval, allowed calculating the rate of formation of reduced compounds.

The results on aerobic oxygen consumption and the dynamics of reduced compounds (H_2S) according to stoichiometric formulas [Orekhova, Konovalov, 2018a; Sapozhnikov, Metrevely, 2015] were expressed as the utilization rate of organic matter:

$$(CH_2O)_{106}(NH_3)_{16}H_3PO_4 + 138O_2 = 106CO_2 + 122H_2O + 16HNO_3 + H_3PO_4\ ,$$

$$(CH_2O)_{106}(NH_3)_{16}H_3PO_4 + 53H_2SO_4 = 106CO_2 + 16NH_3 + H_3PO_4 + 53H_2S + 106H_2O\ .$$

Organic matter concentration in bottom sediments was determined by the gravimetric method after drying of samples at +105 °C and their further calcination at +500 °C [Gorshkova, 1974; PND F 16.2.2:2.3:3.32-02, 2002].

RESULTS AND DISCUSSION

In terms of the degree of isolation of the water areas studied, the sampling points can be united into two groups: those located within relatively closed bays and those located in the coastal zones of open sea areas. The first group includes stations in the Sevastopol, Kruglaya, and Balaklava bays,

which are characterized by a large-scale influx of suspended matter into bottom sediments. Thus, in the Sevastopol Bay, the sedimentation rate was 2.4 mm·year^{-1}, while in coastal waters of Crimea, the value was only 0.35 mm·year^{-1} [Denisov, 1998]. Accordingly, in the first group, TOC obtained by us varied in the range of 2.63–4.36 μg·cm^{-3}·h^{-1}. In the second group, which included stations in the Dvuyakornaya Bay, in the Cape Martyan area, and in the Belbek River paleochannel, the values did not exceed 2.90 μg·cm^{-3}·h^{-1} (Table 1).

Table 1. Oxygen consumption and derived data on the dynamics of reduced compounds (H_2S) in the bottom sediments of coastal waters of Crimea

Coordinates of sampling points, date	Layer, cm	Redox potential, mV	O_2, μg·cm^{-3}·h^{-1}		Reduced compounds (H_2S)		
			AOC	ONRC	Concentration, μg·cm^{-3}	Oxidation, μg·cm^{-3}·h^{-1}	Production, μg·cm^{-3}·h^{-1}
Dvuyakornaya Bay, 44.990°N, 35.36°E, 07.07.2012	0–0.6	−182	2.20 ± 1.00	0.70 ± 0.20	38	1.49	0.77
Cape Martyan, 44.509°N, 34.256°E, 13.08.2014	0–0.6	14	2.40 ± 0.19	0.27 ± 0.23	574	0.57	0.17
	3–3.6	−199	3.36 ± 1.07	0.35 ± 0.28	567	0.74	0.62
Belbek River paleochannel, 44.631°N, 33.418°E, 21.05.2013	0–0.6	−193	1.27 ± 0.52	0.61 ± 0.13	609	1.30	0.34
	2–2.6	−176	2.46 ± 0.86	0.84 ± 0.60	777	1.79	0.54
	4–4.6	−184	9.43 ± 5.48	1.35 ± 0.99	1,011	2.87	0.17
Chernaya River paleochannel, 44.618°N, 33.474°E, 26.05.2013	Riverbed, 0–0.6	−68	2.41 ± 0.78	0.28 ± 0.09	1,320	0.60	1.07
	Slope, 0–0.6	−140	1.25 ± 0.43	0.43 ± 0.15	797	0.91	0.71
Sevastopol Bay, 44.615°N, 33.520°E, 12.06.2012	0–0.6	–	2.00 ± 0.59	0.63 ± 0.19	1,345	1.34	1.00
Kruglaya Bay, 44.602°N, 33.441°E, 27.07.2020	Background, 0–0.6	30	3.39 ± 0.49	0.35 ± 0.18	750	0.75	0.15
	Sulfurette, 0–0.6	−72	3.14 ± 0.25	0.50 ± 0.21	1,097	1.06	0.35
Balaklava Bay, 44.496°N, 33.595°E, 23.10.2008	0–0.6	−209	3.98 ± 0.78	0.38 ± 0.03	703	0.81	–

Note: AOC, aerobic oxygen consumption; ONRC, oxygen neutralization of reduced compounds.

The formation of sediments in the Chernaya River paleochannel is affected by significant anthropogenic load on the Sevastopol Bay [Orekhova et al., 2013]. Apparently, it explains the similarity of these sampling points in several parameters, which does not allow us to attribute the paleochannel area to any group. As a specific object, paleochannels in Sevastopol vicinity are analyzed in the paper [Gulin, Kovalenko, 2010]. Bottom sediments in both groups were represented by slightly silty sands and finely dispersed silts. Silty sediments were characteristic of the Sevastopol and Balaklava bays

and paleochannels of the Chernaya and Belbek rivers. Other samples were represented by sands with minor traces of siltation. In most samples, negative values of the redox potential were recorded, and this evidenced for reduced environmental conditions.

Bottom sediments of the Cape Martyan (a protected area) and the Belbek River paleochannel differed in granulometric characteristics, anthropogenic load, and, accordingly, concentration of organic compounds. At the same time, vertical sounding of bottom sediment strata at these sampling points revealed an increase with depth of oxidative potential and a subsurface peak of anaerobic activity (see Table 1).

In 2008, we determined several parameters in the bottom sediments of the central Kruglaya Bay, *inter alia* TOC. Repeated studies of TOC and organic matter content, which were carried out in the course of this work, did not reveal significant changes in the values over time. TOC varied within 3.25–3.66 $\mu g \cdot cm^{-3} \cdot h^{-1}$, and organic matter concentration was about 33 $mg \cdot g^{-1}$.

The rates of formation of reduced compounds depended, among other things, on the granulometric composition of bottom sediments: in silts, those were 1.5–2 times higher than in sands. The maximum values, more than 1 $\mu g\, H_2S \cdot cm^{-3} \cdot h^{-1}$, were obtained in the silty sediments of the Sevastopol Bay. In general, a higher level of hydrogen sulfide concentration was registered in the bays, up to 1.4 $mg \cdot cm^{-3}$. In the samples from the coastal zones of open sea areas, H_2S content did not exceed 0.6 $mg \cdot cm^{-3}$ in the surface layer, and the formation rate was 0.77 $\mu g\, H_2S \cdot cm^{-3} \cdot h^{-1}$. The bottom sediments in the Chernaya River paleochannel were the exception, and this can be explained by the effect of the Sevastopol Bay. Specifically, the intensity of sulfate reduction in the surface sediment layer in the bays of Sevastopol reached 93 $\mu M \cdot dm^{-3} \cdot day^{-1}$, or 0.132 $\mu g \cdot cm^{-3} \cdot h^{-1}$ [Egorov et al., 2012]. The values of bacterial sulfate reduction in the sediments of the Black Sea northwestern shelf ranged from 28.3 to 427.0 $mg\, H_2S \cdot kg^{-1}$ of wet sediment *per* day [Karnachuk, 1989].

Hydrological features of relatively closed bays, which are associated with limited water exchange, weakened wave action, and, as a rule, significant influx of organic and biogenic substances, contribute to intensive sedimentation [Lomakin, Popov, 2014; Orekhova et al., 2013]. With sufficient aeration, this ultimately results in increased activity of biochemical processes in the surface sediment layer.

Oxygen supply to the reduced sediment layer also initiates oxidative processes, the intensity of which can be even higher than for the surface sediment layer. Thus, in the sediment core from the Belbek River paleochannel, AOC rose from 1.27 $\mu g\, O_2 \cdot cm^{-3} \cdot h^{-1}$ at the surface to 9.43 $\mu g\, O_2 \cdot cm^{-3} \cdot h^{-1}$ at a 4-cm depth. Apparently, a subsurface peak of activity of reduced compounds, mentioned above, is related to the activation of sulfate reduction. Compared to the surface horizon, it increases by 1.5–3.5 times. At the same time, the oxidation of anaerobiosis products in the sediments of the paleochannel due to insufficient diffusion of oxygen into the silts is limited by the surface layer alone. Therefore, the layer-by-layer sum of the rates of H_2S formation and its oxidation rate in the surface layer turn out to be quite comparable. In the Cape Martyan area, in more aerated sandy sediments, the layer of oxidation of reduced compounds is slightly thicker; in general, the scale of this process prevails over the scale of their production, which determines positive values of the redox potential.

As already mentioned, the formation of the bottom sediments in the Chernaya River paleochannel is affected by the proximity of the Sevastopol Bay mouth [Orekhova et al., 2013]. Directly in the mouth, the sediments differed from those on the slope by a higher maximum level of aerobic oxygen consumption, as well as by the content of reduced compounds, which can be explained by a higher rate of their formation at relatively low rates of oxidation.

In the 0.01-cm sediment layer of the Sevastopol Bay, experimentally measured TOC averaged 0.96 μg·cm^{-2}·h^{-1} [Chekalov, 2016]. Considering the assumed depth of oxygen penetration (0.6 cm), this corresponds to 2.18 μg·cm^{-2}·h^{-1}. As reported earlier [Orekhova, Konovalov, 2018a], the value of the oxygen flux through the surface of the bottom sediments in the bay, calculated according to Fick's first law, varied insignificantly during the cold season, averaging 2 mol·m^{-2}·year^{-1}. This value corresponds to 0.73 μg·cm^{-2}·h^{-1}, which is slightly lower than that obtained by us. However, the authors point out that several geophysical factors and the high rate of biochemical processes were not taken into account. In another paper [Orekhova, Konovalov, 2018b], the values of the oxygen flux calculated for the Crimean shelf increased from 2.85 M·m^{-2}·year^{-1} in the western area to 3.55 M·m^{-2}·year^{-1} on the southern coast and to 4.26 M·m^{-2}·year^{-1} in the eastern water area, which corresponds to 1.05, 1.31, and 1.56 μg O_2·cm^{-2}·h^{-1}.

The agreement between the given and previously obtained values of the total oxygen consumption by bottom sediments in the Kruglaya Bay allows us to assume a balanced state of this system. Despite rather intensive recreational use of the bay, the key role seems to be played by the hydrochemical regime and loose composition of sandy sediments, which ensure free oxygen penetration into their core. In general, unlike water masses, bottom sediments are a more conservative environment, and its inertness is smoothed by both seasonal and interannual fluctuations in hydrochemical parameters. In the bay, zones of reduced sediments with negative values of the redox potential (sulfurettes) were revealed. We recorded certain differences in the dynamics of reduced compounds (H_2S) between sediments of sulfurettes and adjacent oxidized areas. In sulfurettes, the calculated data on concentration, rate of oxidation, and formation of hydrogen sulfide were higher by 32, 29, and 57%, respectively.

Based on the experimentally obtained data on TOC, including that during oxidation of reduced compounds, we calculated possible rates of destruction of organic matter (Table 2). The sum of aerobic and anaerobic utilization of organic compounds turned out to be maximum, up to 4.05 μg·cm^{-3}·h^{-1}, in the Sevastopol Bay and the adjacent water area, with the anaerobic component accounting for a larger share. The share turned out to be quite high in the Kruglaya Bay as well, but there, aerobic destruction prevailed. This is due to differences in both the targeted use of the bays and the granulometric composition of bottom sediments. Loose sediments are usually more aerated, which determines the prevalence of the oxidative metabolism. Even in sulfurettes of sandy sediments in the Kruglaya Bay, the level of aerobic oxidation turned out to be as high as in the background point. At the same time, the intensity of anaerobic utilization of organic matter differed twofold, although its absolute values remained closer to the level characteristic of the coastal zones of open sea areas, in particular, the Belbek River paleochannel.

During vertical sounding of the sediment strata in the Cape Martyan area and in the Belbek River paleochannel, a rise was recorded in the ability to both aerobic and anaerobic destruction with depth, which naturally repeated the oxygen profile. Thus, in the Cape Martyan area, the values increased in the 0–3-cm layer from 1.93 to 2.70 and from 0.34 to 1.22 μg·cm^{-3}·h^{-1}, respectively. Absolute values of the oxidation rates of organic matter in the sediments of the Belbek River paleochannel were slightly lower, 1.02–1.98 μg·cm^{-3}·h^{-1}. Decomposition of organic matter due to sulfate reduction in the surface horizon turned out to be twice higher there; the value, forming a peak of 1.06 μg·cm^{-3}·h^{-1} at a depth of 2 cm, dropped to 0.34 μg·cm^{-3}·h^{-1}. In the bottom sediments of the Sevastopol Bay, already in the surface layer, the rates of anaerobic destruction exceeded aerobic utilization of organic matter, reaching 1.97 *vs.* 1.61 μg·cm^{-3}·h^{-1}. So, larger variability is characteristic of the anaerobic component.

Oxygen penetration into the sediment layer deeper than 1 cm is usually very insignificant; in particular, in the Sevastopol Bay, the value is no more than 0.5 cm [Orekhova et al., 2013]. In this case, in the lack of oxygen, aerobic destruction of organic matter, in contrast to anaerobic one, almost stops in underlying sediment layers. Therefore, taking into account the intensity of anaerobic processes in the sediment core, we obtain an approximately equal, and sometimes even higher contribution of anaerobiosis to total destruction of organic matter. Sulfate reduction was found to contribute up to 50% of organic carbon mineralization in marine sediments [Jørgensen, 1982]. At the same time, it decomposes up to 99% of organic carbon consumed for sulfate reduction and methanogenesis [Karnachuk, 1989]. All this evidences the significance of the participation of sulfate reducers both in the global sulfur cycle and the carbon cycle.

Table 2. Content of organic matter and calculated rates of its aerobic and anaerobic destruction in the bottom sediments of coastal waters of Crimea

Sampling point	T, °C	Layer, cm	Organic matter, mg·cm^{-3}	Destruction of organic matter, μg·cm^{-3}·h^{-1}	
				aerobic	anaerobic
Dvuyakornaya Bay	+24	0–0.6	25	1.77	1.52
Cape Martyan	+24	0–0.6	17	1.93	0.34
		3–3.6	24	2.70	1.22
Belbek River paleochannel	+21	0–0.6	45	1.02	0.67
		2–2.6	54	1.98	1.06
		4–4.6	46	7.58	0.34
Chernaya River paleochannel	+20	Riverbed, 0–0.6	68	1.94	2.11
		Slope, 0–0.6	51	1.01	1.40
Sevastopol Bay	+21	0–0.6	60	1.61	1.97
Kruglaya Bay	+25	Background, 0–0.6	41	2.73	0.30
		Sulfurette, 0–0.6	34	2.52	0.69
Balaklava Bay	+19	0–0.6	61	3.18	–

Conclusion. Certain differences were registered between relatively closed bays and open sea areas in terms of the rate of oxygen consumption and, accordingly, the utilization of organic matter in bottom sediments. First of all, this results from the features in hydrology, sedimentation, and intensity of anthropogenic use of water areas. Specifically, depending on the level of anthropogenic load and the composition of bottom sediments, either aerobic destruction of organic matter prevails (as in the Kruglaya Bay), or anaerobic destruction (this is typical for the sediments of the Sevastopol Bay). In the Chernaya River paleochannel, a higher level of aerobic oxygen consumption and content of reduced compounds was revealed in contrast to its slopes. This can be explained by the prevalence of the processes of their formation over oxidation. Differences were recorded in the dynamics of reduced compounds (H_2S) between areas of reduced sediments (sulfurettes) and oxidized background ones. The calculated data on concentration, oxidation rate, and formation of hydrogen sulfide in sulfurette were higher by 32, 29, and 57%, respectively. In sulfurette, anaerobic destruction of organic matter is more than twice as intense, while there are no differences in the rate of oxidation. In the sediment core in the Cape Martyan area and in the Belbek River paleochannel, an increase with depth in the oxidative potential and a subsurface peak of anaerobic activity were established. At the same time, due to the limited diffusion of oxygen, the rate of hydrogen sulfide oxidation in the surface horizon and the layer-by-layer sum of the rates of its formation

for the sediment core turned out to be comparable. For the same reason, the contribution of anaerobiosis processes to the destruction of organic matter is often equal to, and sometimes higher than the contribution of the aerobic pathway.

This work was carried out within the framework of IBSS state research assignment "Functional, metabolic, and toxicological aspects of hydrobionts and their populations existence in biotopes with different physical and chemical regimes" (No. 121041400077-1).

REFERENCES

1. Gorshkova T. I. Biogeochemistry of modern marine sediments and their biological significance. *Trudy VNIRO*, 1974, vol. 48, iss. 1, pt 2, pp. 135–144. (in Russ.)
2. GOST 26213-91. *Pochvy. Metody opredeleniya organicheskogo veshchestva* : vzamen GOST 26213-84; vved. 1993-07-01. Moscow : Izdatel'stvo standartov, 1992, 8 p. (in Russ.)
3. Gulin M. B., Kovalenko M. V. Paleo-rivers Chernaya and Belbek at the continental shelf of southwestern Crimea – new object of ecological researches. *Morskoj ekologicheskij zhurnal*, 2010, vol. 9, no. 1, pp. 23–31. (in Russ.). https://repository.marine-research.ru/handle/299011/1051
4. Denisov V. I. *Zakonomernosti obrazovaniya vzveshennogo materiala na shel'fe Chernogo morya*. [dissertation]. Rostov-on-Don, 1998, 299 p. (in Russ.)
5. Egorov V. N., Pimenov N. V., Malakhova T. V., Artemov Yu. G., Kanapatsky T. A., Malakhova L. V. Biogeochemical characteristics of methane distribution in sediment and water at the gas seepage site of Sevastopol bays. *Morskoj ekologicheskij zhurnal*, 2012, vol. 11, no. 3, pp. 41–52. (in Russ.). https://repository.marine-research.ru/handle/299011/1230
6. Ignat'eva O. G., Ovsyanyi E. I., Romanov A. S., Konovalov S. K., Orekhova N. A. Analysis of state of the carbonate system of waters and variations of the content of organic carbon in bottom sediments of the Sevastopol Bay in 1998–2005. *Morskoi gidrofizicheskii zhurnal*, 2008, no. 2, pp. 57–67. (in Russ.)
7. Karnachuk O. V. *Bakterial'naya sul'fatreduktsiya v pribrezhnykh morskikh osadkakh* : avtoref. dis. … kand. biol. nauk : 03.00.07. Abovyan, 1989, 23 p. (in Russ.)
8. Lomakin P. D., Popov M. A. Otsenka stepeni zagryazneniya i perspektiva ekologicheskikh issledovanii vod Balaklavskoi bukhty. *Ekologicheskaya bezopasnost' pribrezhnoi i shel'fovoi zon i kompleksnoe ispol'zovanie resursov shel'fa*, 2014, iss. 28, pp. 195–213. (in Russ.)
9. Moiseenko O. G., Orekhova N. A. Investigation of the mechanism of the long-term evolution of the carbon cycle in the ecosystem of the Sevastopol Bay. *Morskoi gidrofizicheskii zhurnal*, 2011, no. 2, pp. 72–83. (in Russ.)
10. Orekhova N. A. Gipoksiya i anoksiya v donnykh osadkakh krymskogo poberezh'ya. In: *Heohrafiia ta turyzm* : naukovyi zbirnyk / Ya. B. Oliinyk (Ed.). Kyiv : Al'terpres, 2010, iss. 4, pp. 146–152. (in Russ.)
11. Orekhova N. A., Moiseenko O. G., Konovalov S. K. Study of the Sevastopol Bay geochemical features. *Current Fishery and Environmental Problems of the Azov and Black Seas Region* : materials of VIII International Conference. Kerch, 26–27 June, 2013. Kerch : YugNIRO Publishers, pp. 55–58. (in Russ.)
12. Orekhova N. A., Konovalov S. K. Oxygen and sulfides in bottom sediments of the coastal Sevastopol region of Crimea. *Okeanologiya*, 2018a, vol. 58, no. 5, pp. 739–750. (in Russ.). https://doi.org/10.1134/S0030157418050106
13. Orekhova N. A., Konovalov S. K. Kislorod i sul'fidy v verkhnem sloe donnykh otlozhenii Chernogo morya. In: *Sistema Chernogo morya* / A. P. Lisitsyn (Ed.). Moscow : Nauchnyi mir, 2018b, pp. 542–559. (in Russ.)

14. Orekhova N. A., Ovsyany E. I., Gurov K. I., Popov M. A. Organic matter and grain-size distribution of the modern bottom sediments in the Balaklava Bay (the Black Sea). *Morskoi gidrofizicheskii zhurnal*, 2018, no. 6, pp. 523–533. (in Russ.). https://doi.org/10.22449/0233-7584-2018-6-523-533
15. PND F 16.2.2:2.3:3.32-02. *Kolichestvennyi khimicheskii analiz pochv. Metodika vypolneniya izmerenii soderzhaniya sukhogo i prokalennogo ostatka v tverdykh i zhidkikh otkhodakh proizvodstva i potrebleniya, osadkakh, shlamakh, aktivnom ile, donnykh otlozheniyakh gravimetricheskim metodom* / Gosudarstvennyi komitet RF po okhrane okruzhayushchei sredy. Moscow, 2002, 15 p. (in Russ.)
16. Sapozhnikov V. V., Metrevely M. P. Organic matter stoichiometry as a basis for quantitative studies of production and destruction processes in the oceans. *Trudy VNIRO*, 2015, vol. 155, pp. 137–141. (in Russ.)
17. Chekalov V. P. Oxygen absorption in the oxidation of organic compounds in the coastal sediments of Sevastopol (the Black Sea). *Morskoj biologicheskij zhurnal*, 2016, vol. 1, no. 4, pp. 44–52. (in Russ.). https://doi.org/10.21072/mbj.2016.01.4.06
18. Jørgensen B. B. Mineralization of organic matter in the sea bed–the role of sulphate reduction. *Nature*, 1982, vol. 296, pp. 643–645. https://doi.org/10.1038/296643a0
19. Osadchaya T. S., Ovsyaniy E. I., Kemp R., Romanov A. S., Ignatieva O. G. Organic carbon and oil hydrocarbons in bottom sediments of Sevastopol Bay (the Black Sea). *Morskoj ekologicheskij zhurnal*, 2003, vol. 2, no. 2, pp. 94–101. https://repository.marine-research.ru/handle/299011/711

СООТНОШЕНИЕ ПРОЦЕССОВ АЭРОБНОЙ И АНАЭРОБНОЙ ДЕСТРУКЦИИ ОРГАНИЧЕСКОГО ВЕЩЕСТВА В ДОННЫХ ОТЛОЖЕНИЯХ ПРИБРЕЖНЫХ АКВАТОРИЙ КРЫМА (ЧЁРНОЕ МОРЕ)

В. П. Чекалов

ФГБУН ФИЦ «Институт биологии южных морей имени А. О. Ковалевского РАН»,
Севастополь, Российская Федерация
E-mail: *valch@mail.ru*

Взаимосвязь водных масс с донными отложениями является очевидной, в первую очередь в вопросах формирования кислородного режима и, как следствие, самоочищения водоёмов. Зная скорость потребления кислорода, с помощью стехиометрических соотношений можно оценить ряд сопряжённых параметров энергетического обмена. Цель настоящей работы — посредством интерпретации данных кислородного потребления рассчитать возможный вклад аэробных и анаэробных процессов в деструкцию органических веществ в донных осадках различных районов крымского прибрежья Чёрного моря. Измерение суммарной скорости потребления кислорода проводили с помощью респирометрической камеры, герметично соединённой с кислородным датчиком LDO-оксиметра HQ40D. Для подавления бактериальной активности и выявления темпов окисления восстановленных продуктов анаэробиоза использовали антибиотик стрептомицин. Вертикальное зондирование толщи грунта в палеорусле реки Бельбек показало рост с глубиной окислительного потенциала и подповерхностный пик анаэробной активности. Вследствие ограниченной диффузии кислорода, скорость окисления сероводорода в поверхностном слое была сопоставима с темпами его образования в нижележащей толще грунта. Непосредственно на участке палеорусла реки Чёрная, прилегающем к устью Севастопольской бухты, донные отложения отличались от грунтов на склоне бóльшим уровнем аэробного потребления кислорода, а также содержанием восстановленных соединений, которое обусловлено более высокой скоростью их образования при относительно низких темпах окисления.

Поглощение кислорода единицей донной поверхности в 0,6-см слое осадков Севастопольской бухты в среднем составляло 2,18 мкг·см$^{-2}$·ч$^{-1}$. В бухте Круглая наблюдали различия по динамике восстановленных соединений (H_2S) между окисленными фоновыми участками и зонами восстановленных грунтов (сульфурет). В сульфуретах расчётные данные концентрации, темпов окисления и образования сероводорода выше на 32, 29 и 57 % соответственно. Максимальной, до 4,05 мкг·см$^{-3}$·ч$^{-1}$, скорость утилизации органического вещества была в Севастопольской бухте и в прилегающей к ней акватории. Бóльшая доля приходилась на анаэробную составляющую. Достаточно высокой она оказалась и в бухте Круглая, но здесь преобладала аэробная деструкция. Это связано с различиями как в целевом использовании бухт, так и в гранулометрическом составе донных осадков. В грунтах сульфуреты при скорости окисления органических веществ, равной таковой фонового участка, анаэробная утилизация протекала более чем в 2 раза интенсивнее. Её абсолютное значение было ближе к уровню, характерному для прибрежных участков открытого моря, в частности для палеорусла реки Бельбек.

Ключевые слова: донные отложения, потребление кислорода, деструкция органического вещества, Чёрное море

1871
ИнБЮМ – IBSS

Морской биологический журнал
Marine Biological Journal
2023, vol. 8, no. 3, pp. 97–101
https://marine-biology.ru

UDC 593.933.7-045.35(262.5.04:560)

FIRST FIND OF THE STARFISH, *ASTERIAS RUBENS* LINNAEUS, 1758, OFF THE ANATOLIAN COAST OF THE BLACK SEA (SINOP)

© 2023 **E. Aydemir-Çil[1], Z. Birinci-Özdemir[2], and S. Özdemir[3]**

[1]Environmental Engineering Department, Faculty of Engineering and Architecture of Sinop University, Sinop, Turkey
[2]Marine Biology Department, Fisheries Faculty of Sinop University, Sinop, Turkey
[3]Fishing Technology Department, Fisheries Faculty of Sinop University, Sinop, Turkey
E-mail: *eylemaydemir@sinop.edu.tr*

Received by the Editor 08.07.2022; after reviewing 25.01.2023;
accepted for publication 04.08.2023; published online 21.09.2023.

Starfish *Asterias rubens* was found as the first record from the Anatolian coast of the Black Sea (Sinop). This alien starfish was reported in 1996 in the Bosporus Strait (the Marmara Sea). In 2009, *A. rubens* was registered off Karasu and Sakarya coasts in the Western Black Sea. *A. rubens* (8 cm in diameter; wet weight 12.970 g) was sampled by a commercial demersal trawl on the sandy-mud bottom at 85.5-m depth on 12 February, 2022, on the Anatolian coast of the Black Sea, which indicates further expansion of its areal in the sea.

Keywords: starfish, *Asterias rubens*, alien species, Black Sea, Turkey

Asterias rubens Linnaeus, 1758 is a fairly common species in the northeastern Atlantic Ocean [Budd, 2008]. Most of the species in the Black Sea are migrants of Atlantic origin that reached the Pontiac basin with the reopening of the Bosporus 7,000–10,000 years ago [Öztürk B., Öztürk A., 1996]. Some of the migrant species [such as *Rapana venosa* (Valenciennes, 1846), *Mnemiopsis leidyi* A. Agassiz, 1865, *Beroe ovata* Bruguière, 1789, and *Anadara inaequivalvis* (Bruguière, 1789)] have arrived with ship ballast waters. The Bosporus Strait of Istanbul provided the connection between the Mediterranean Sea and the Atlantic Ocean, as well as the Black Sea. Mediterranean migrants are the largest community of organisms in the Black Sea biota and account for 80% of the total number of species [Exotic Species, 2001].

Although the Black Sea has a great habitat diversity, species diversity is low due to low salinity. This provides favorable conditions for the spread of alien species [CIESM, 2010]. The phylum Echinodermata is represented by approximately 7,000 living species [Pawson, 2007]. Species of this phylum have been recorded in the Sea of Marmara since 1990 [Albayrak, 1996; Karhan et al., 2007; Yüce, Sadler, 2000].

The release of ballast waters from ships facilitates the inter-sea migration of planktotrophic larvae of non-native species. It is thought that *A. rubens* was transported to the Sea of Marmara that way [Zibrowius, 2002]. Nevertheless, it should be considered that current systems affect the dynamics of the spread of alien species [Jaspers et al., 2018].

The aim of this article is to report the Atlantic starfish *Asterias rubens* on Turkish Black Sea coast, which can be considered an indicator of the spread of this species along the coast of the Black Sea from Marmara. It is the first record of this alien species from the Anatolian coast of the Black Sea.

MATERIAL AND METHODS

A single specimen of *A. rubens* (8 cm in diameter; weight 12.970 g) (Fig. 1) was sampled by a commercial demersal trawl (codend mesh size 40 mm) off İnceburun (42°08′765″N, 34°51′895″E) and Sarıkum (42°06′886″N, 34°52′274″E), Sinop area of the Anatolian Turkey coast (Fig. 2), on the sandy-mud bottom, at average depth 85.5 m and temperature +8.4 °C, on 12 February, 2022. The sample was preserved in 96% ethanol.

The analysis of morphological characteristics and description of the starfish were carried out in the Laboratory of the Fisheries Faculty of Sinop University.

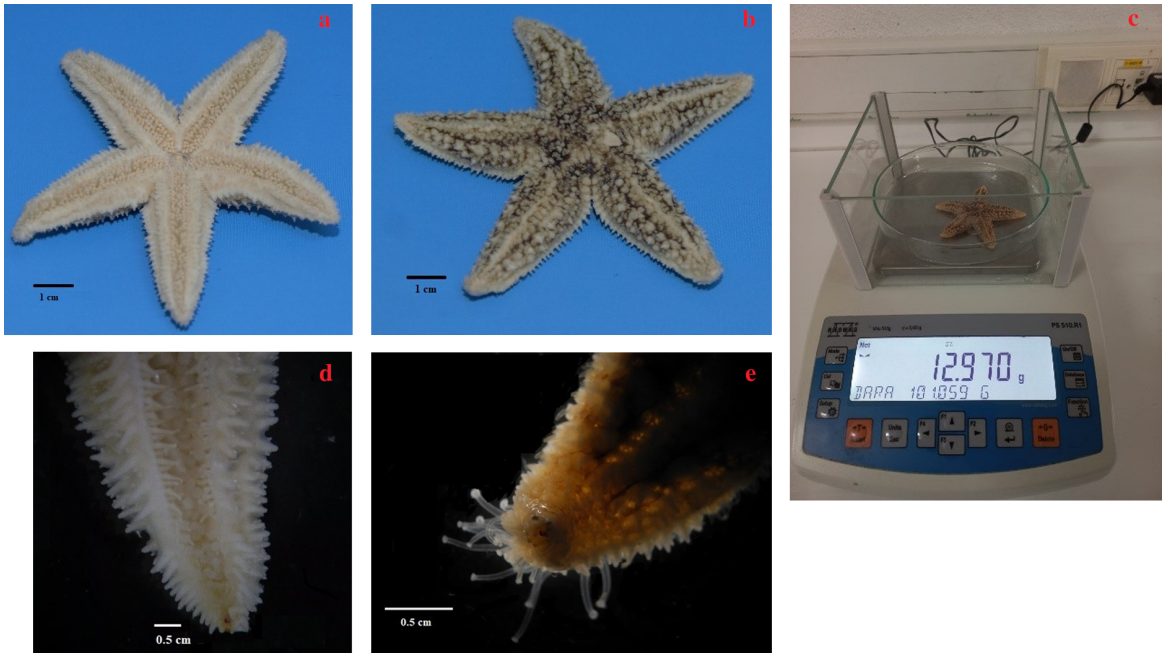

Fig. 1. *Asterias rubens* (8 cm in diameter) captured at Sinop, the Black Sea (original photos)

Body of the starfish is generally small and disc-shaped. The five arms begin to narrow at the base; the average diameter is 35 mm. On the aboral side, there are small cream spots at the base of the spines, while the arms are cream-colored, with a brown spot at the tips. The body wall is soft and flexible. There are numerous papules on the surface [Müller, Troschel, 1842].

The bottom of the starfish is covered with hundreds of tube feet that are used to walk, cling to rocks, and catch prey. With these tiny legs, *A. rubens* moves at speeds of 30 cm *per* minute, or 60 feet *per* hour [Dale, 1997].

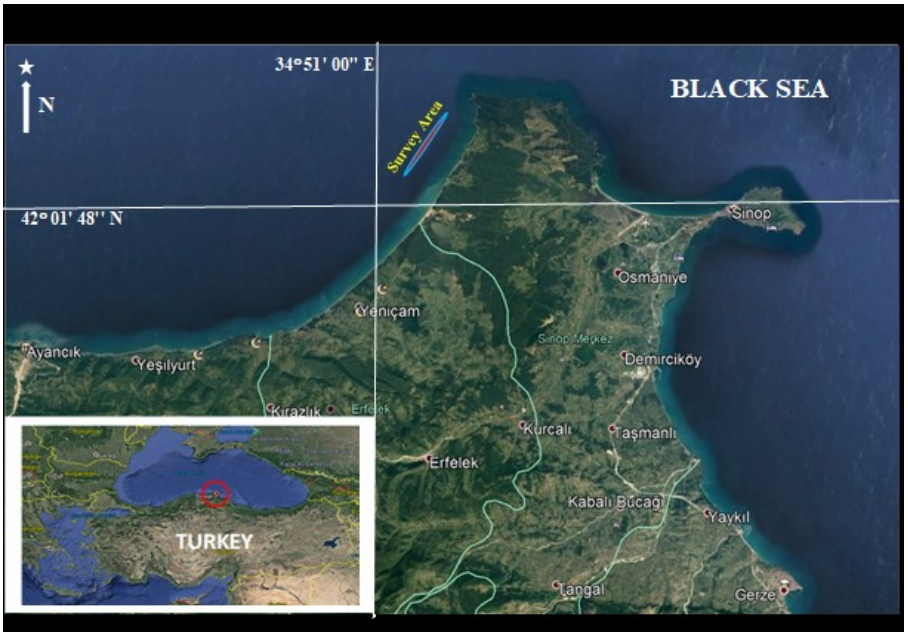

Fig. 2. Location of the survey area

RESULTS AND DISCUSSION

Habitat. *Asterias* species are found on hard, rocky, sandy, or soft substrates, with most species preferring rocky sea bottoms. In winter, *A. rubens* activity is confined to the bottom. Sea stars are able to attach to hard surfaces and move well [Hennebert et al., 2010], but the movement and attachment systems are dysfunctional on non-adhesive, *i. e.* soft, substrates [Anger et al., 1977]. Physical parameters significantly constrain species abundance, physical activity, and predation rates [Hancock, 1955].

It is known that environmental conditions, such as temperature, salinity, and hydrodynamic regime, affect distribution, life cycle, nutrition, abundance, and performance of *A. rubens* [Menge et al., 1994].

In a study conducted by Y. Ceylan and S. Gül [2021], based on current *A. rubens* distribution, it was reported that temperature is the most restrictive environmental variable.

Feeding. *A. rubens* feeds on a wide range of living organisms and carcasses, most of which are composed of macroinvertebrates, including molluscs, polychaetes, and other echinoderms. Sometimes, small crustaceans are caught by suction discs of tube feet. *A. rubens* feeds mainly on molluscs, especially bivalves and snails. Digestive enzymes enter the hunt along with the everted stomach lining to further aid digestion. The starfish can also use its tube feet to open a bivalve [Pearse et al., 1987]. However, their food seems to consist largely of bivalve molluscs [Budd, 2008; Chadwick, 1923]. Therefore, there is no problem for this species to find food in the Black Sea, because *Mytilus galloprovincialis* Lamarck, 1819, a mytilid bivalve, forms very large populations on the coast of this sea [Hancock, 1958]. *M. galloprovincialis* is a species of high economic significance which is cultivated in countries bordering the Black Sea, and it is important in terms of creating habitats for many hydrobionts [Zaitsev, Mamaev, 1997].

While the spread of *A. rubens* has been reported around Marmara and in the Bosporus system for more than 20 years, it is detected for the first time in the current research area.

As a result, new studies are needed to understand the current state of *A. rubens* in the Black Sea and its effects on the ecosystem. For the Black Sea, which responses quickly to changes in the ecosystem, the existence and spread of the species is important. The spread of *A. rubens* to the shores of Karasu

and Sakarya in the Sea of Marmara, the Bosporus system, and the Western Black Sea has been reported for more than two decades [Albayrak, 1996; Ceylan, Gül, 2021; Dalgıç et al., 2009; Karhan et al., 2007; Öztoprak et al., 2014; Yüce, Sadler, 2000], and it was detected for the first time on the shores of Sinop in this study. As a result of this research, it has been proved that this species has spread to the Anatolian coast of the Black Sea region.

REFERENCES

1. Albayrak S. Echinoderm fauna of the Bosphorus (Turkey). *Oebalia: International Journal of Marine Biology and Oceanography*, 1996, vol. 22, pp. 25–32.
2. Anger K., Rogal U., Schriever G., Valentin C. *In-situ* investigations on the echinoderm *Asterias rubens* as a predator of softbottom communities in the Western Baltic Sea. *Helgoländer wissenschaftliche Meeresuntersuchungen*, 1977, vol. 29, pp. 439–459. https://doi.org/10.1007/BF01609982
3. Budd G. C. *Asterias rubens*. Common starfish. In: Tyler-Walters H. *Marine Life Information Network: Biology and Sensitivity Key Information Reviews* : [site]. Plymouth : Marine Biological Association of the United Kingdom, 2008. URL: https://www.marlin.ac.uk/species/detail/1194 [accessed: 07.03.2022].
4. Chadwick H. C. Asterias. In: *L. M. B. C. Memoirs on Typical British Marine Plants and Animals*, 1923, vol. 25, 63 p.
5. Ceylan Y., Gül S. Potential habitats of an alien species (*Asterias rubens* Linnaeus, 1758) in the Black Sea: Its current and future distribution patterns. *Environmental Science and Pollution Research*, 2021, vol. 29, pp. 19563–19571. https://doi.org/10.1007/s11356-021-17171-5
6. *CIESM, 2010. Climate Forcing and Its Impacts on the Black Sea Marine Biota.* Monaco : CIESM Publisher, 2010, 152 p. (CIESM Workshop Monographs / [F. Briand (Ed.)] ; no. 39).
7. Dale J. *How Starfish Move – And the Water Vascular System* : [site], 1997. URL: http://www.madreporite.com/science/movement.htm [accessed: 07.04.2000].
8. Dalgıç G., Ceylan Y., Şahin C. The Atlantic starfish, *Asterias rubens* Linnaeus, 1758 (Echinodermata: Asteroidea: Asteriidae) spreads in the Black Sea. *Aquatic Invasions*, 2009, vol. 4, iss. 3, pp. 485–486. https://doi.org/10.3391/ai.2009.4.3.7
9. *Exotic Species in the Aegean, Marmara, Black, Azov and Caspian Seas* / Y. Zaitsev, B. Öztürk (Eds). Istanbul, Turkey : Turkish Marine Research Foundation, 2001, 267 p.
10. Hancock D. A. The feeding behavior of starfish on Essex oyster beds. *Journal of the Marine Biological Association of the United Kingdom*, 1955, vol. 34, iss. 2, pp. 313–331. https://doi.org/10.1017/S0025315400027685
11. Hancock D. A. Notes on starfish on an Essex oyster bed. *Journal of the Marine Biological Association of the United Kingdom*, 1958, vol. 37, iss. 3, pp. 565–589. https://doi.org/10.1017/S0025315400005622
12. Hennebert E. D., Haesaerts P., Dubois P., Flammang P. Evaluation of the different forces brought into play during tube foot activities in sea stars. *Journal of Experimental Biology*, 2010, vol. 213, iss. 7, pp. 1162–1174. https://doi.org/10.1242/jeb.037903
13. Jaspers C., Huwer B., Antajan E., Hosia A., Hinrichsen H.-H., Biastoch A., Angel D., Asmus R., Augustin Ch., Bagheri S., Beggs S. E., Balsby Th. J. S., Boersma M., Bonnet D., Christensen J. T., Dänhardt A., Delpy F., Falkenhaug T., Finenko G., Fleming N. E. C., Fuentes V., Galil B., Gittenberger A., Griffin D. C., Haslob H., Javidpour J., Kamburska L., Kube S., Langenberg V. T., Lehtiniemi M., Lombard F., Malzahn A., Marambio M., Mihneva V., Møller L. F., Niermann U., Okyar M. I., Özdemir Z. B., Pitois S., Reusch Th. B. H., Robbens J., Stefanova K., Thibault D., van der Veer H. W., Vansteenbrugge L., van Walraven L., Woźniczka A. Ocean current connectivity

propelling the secondary spread of a marine invasive comb jelly across western Eurasia. *Global Ecology and Biogeography*, 2018, vol. 27, iss. 7, pp. 814–827. https://doi.org/10.1111/geb.12742

14. Karhan S. Ü., Kalkan E., Yokeş B. First record of the Atlantic starfish, *Asterias rubens* (Echinodermata: Asteroidea) from the Black Sea. *Marine Biodiversity Records*, 2007, vol. 1, article no. 63 (3 p.).
15. Menge B. A., Berlow E. L., Blanchette C. A., Navarrete S. A., Yamada S. B. The keystone species concept: Variation in interaction strength in a rocky intertidal habitat. *Ecological Monographs*, 1994, vol. 64, iss. 3, pp. 249–286. http://dx.doi.org/10.2307/2937163
16. Müller J., Troschel F. H. *System der Asteriden, 1. Asteriae, 2. Ophiuridae.* Braunschweig : F. Vieweg und Sohn, 1842, 134 p., 12 pls. https://doi.org/10.5962/bhl.title.11715
17. Öztürk B., Öztürk A. A. On the biology of the Turkish straits system. In: *Dynamics of Mediterranean Straits and Channels* / F. Briand (Ed.). Monaco : Musée océanographique, 1996, pp. 205–221. (CIESM Science Series ; no. 2). (Bulletin de l'Institut oceanographique ; no. special 17). https://ciesm.org/online/monographs/CSS-2/CSS_2_205_221.pdf
18. Öztoprak B., Doğan A., Dağlı E. Checklist of Echinodermata from the coasts of Turkey. *Turkish Journal of Zoology*, 2014, vol. 38, no. 6, pp. 892–900. https://doi.org/10.3906/zoo-1405-82
19. Pawson D. L. Phylum Echinodermata. *Zootaxa*, 2007, vol. 1668, no. 1, pp. 749–764. https://doi.org/10.11646/zootaxa.1668.1.31
20. Pearse V., Pearse J., Buchsbaum M., Buchsbaum R. *Living Invertebrates.* Boston, Massachusetts : Blackwell Scientific Publications, 1987, 848 p.
21. Yüce Ö., Sadler K. C. Boğaz ve Marmara'da bulunan iki baskın denizyıldızı türünün üreme periodlarının saptanması. In: *Proceedings of SBT, 4th National Meeting of Underwater Science and Technology* / S. Hamarat, V. Evrin (Eds). İstanbul, Turkey, 2000, pp. 45–49. (in Turkish).
22. Zaitsev Y., Mamaev V. *Marine Biological Diversity in the Black Sea: A Study of Change and Decline.* New York : United Nations Publications, 1997, 208 p.
23. Zibrowius H. Assessing scale and impact of ship-transported alien fauna in the Mediterranean. In: CIESM, 2002. *Alien Marine Organisms Introduced by Ships in the Mediterranean and Black Sea.* Monaco : CIESM Publisher, 2002, pp. 63–68. (CIESM Workshop Monographs ; no. 20).

ПЕРВАЯ НАХОДКА МОРСКОЙ ЗВЕЗДЫ *ASTERIAS RUBENS* LINNAEUS, 1758 У АНАТОЛИЙСКОГО ПОБЕРЕЖЬЯ ЧЁРНОГО МОРЯ (ГОРОД СИНОП)

Е. Айдемир-Чиль[1], З. Биринчи-Оздемир[2], С. Оздемир[3]

[1]Кафедра инженерной защиты окружающей среды, инженерно-архитектурный факультет Синопского университета, Синоп, Турция

[2]Кафедра морской биологии, факультет рыболовства Синопского университета, Синоп, Турция

[3]Кафедра технологии рыболовства, факультет рыболовства Синопского университета, Синоп, Турция

E-mail: *eylemaydemir@sinop.edu.tr*

Атлантическая морская звезда *Asterias rubens* впервые обнаружена у Анатолийского побережья Чёрного моря (город Синоп). В 1996 г. этот вид-вселенец был найден в проливе Босфор (Мраморное море). В 2009 г. морская звезда зарегистрирована у берегов Карасу и Сакарья в западной части Чёрного моря. Особь *A. rubens* (диаметр — 8 см; сырой вес — 12,97 г) поймана 12 февраля 2022 г. донным тралом на песчано-илистом дне на глубине 85,5 м у Анатолийского побережья Чёрного моря. Это свидетельствует о дальнейшем расширении ареала морской звезды в море.

Ключевые слова: морская звезда, *Asterias rubens*, виды-вселенцы, Чёрное море, Турция

1871
ИнБЮМ – IBSS

Морской биологический журнал
Marine Biological Journal
2023, vol. 8, no. 3, pp. 102–107
https://marine-biology.ru

NOTES

UDC 593.1-14:[57.044:546.47]

DISCOORDINATION OF *HOILUNGIA HONGKONGENSIS* (PLACOZOA) MOVEMENTS IN THE PRESENCE OF Zn^{2+} IONS

© 2023 **A. V. Kuznetsov and N. I. Bobko**
A. O. Kovalevsky Institute of Biology of the Southern Seas of RAS, Sevastopol, Russian Federation
E-mail: *kuznet61@gmail.com*

Received by the Editor 24.05.2021; after reviewing 26.06.2023;
accepted for publication 04.08.2023; published online 21.09.2023.

Placozoa are the simplest multicellular organisms with a dynamic body plan. Calcium ions play a significant role in maintaining the integrity of these animals. We studied the effect of zinc ions on the interaction of *Hoilungia hongkongensis* cells. The coordination of amoeboid movement was disrupted by the addition of 20–25 μM Zn^{2+} ions, which led to the formation of "branched" forms of animals. Locomotor ciliated cells moved without coordination and independently of each other. Experimental research showed that the contact interaction of *H. hongkongensis* cells is important for coordinated movements of the organism, whereas zinc ions can compete with calcium ions, disrupting the regulation and destroying the connection between cells.

Keywords: Placozoa, locomotion, calcium and zinc ions

Trace elements may have played a key role as catalysts for the emergence of life on Earth. The change in trace element composition in the oceans over geological time suggests how their availability in the marine environment affected the early stages of biological evolution [Dupont et al., 2006]. Especially in the Archean Eon the excess of Fe, Co, and Cu ensured their widespread utilization by prokaryotes. In the Paleoproterozoic–Mesoproterozoic, there was a rise in Mo content in the ocean and a notable drop in Fe, Co, and Cu, which contributed to the appearance of alternative metabolic pathways and the birth of eukaryotes. In the Neoproterozoic and Cambrian, the general gain in Mo, Zn, Ni, and Cu concentration was favorable for the complexity and diversification of ancient biota [Robbins et al., 2016]. It has been suggested that the emergence of the first Placozoa organisms was associated with the ratio of Mg^{2+} and Ca^{2+} ions concentrations in the aragonite ocean during the Ediacaran or Cryogenian [Erwin, 2015; Mayorova et al., 2018].

Hoilungia hongkongensis Eitel, Schierwater & Wörheide, 2018 (haplotype H13), the same as *Trichoplax adhaerens* Schulze, 1883 (haplotype H1), is the simplest multicellular organism up to 1–2 mm in size, which consists of about 50,000 cells that form a three-layer plate [Smith et al., 2014]. The movement of this animal is performed due to the beating of the cilia of the ventral epithelium and the contraction of the plate [Armon et al., 2018]. As believed, the organism's integrity is maintained by Ca^{2+} bridges since trichoplax is destroyed by chelating agents that bind calcium ions [Ruthmann, Terwelp, 1979].

It is well known that metal ions compete for binding sites with proteins, according to the Irving–Williams order of stability of bivalent transition metal complexes as $Mg^{2+} / Ca^{2+} < Mn^{2+} < Fe^{2+} < Co^{2+} < Ni^{2+} < Cu^{2+} \sim Zn^{2+}$ [Rosenzweig, 2002], while Zn^{2+} ions replace Ca^{2+} ions during adsorption [Zachara et al., 1988]. A previous study [Kuznetsov et al., 2021] showed that Zn^{2+} ions, the same as Ca^{2+} ions, are located in specific binding sites of cadherin cell adhesion molecules and, thus, destroy calcium bridges that leads to the dissociation of the trichoplax body into individual cells. In this paper, the emphasis is on the analysis of a violation of the interaction between *H. hongkongensis* cells under the effect of zinc ions.

The aim of this work is to study morphological changes in *Hoilungia hongkongensis* when Zn^{2+} ions are added.

MATERIAL AND METHODS

H. hongkongensis was cultivated in 90-mm glass Petri dishes on mats of the unicellular green microalga *Tetraselmis marina* (Cienkowski) R. E. Norris, Hori & Chihara, 1980. The dishes were kept in a thermostat at +25 °C. Animals were transferred to a fresh mat every three weeks, and artificial seawater (ASW) with a salinity of 35 ‰ was changed once a week [Kuznetsov et al., 2021, 2022]. At least 20 *H. hongkongensis* organisms were picked up for each experiment. More than 500 animals were used in a series of 3 experiments. For adaptation, *H. hongkongensis* were transferred into plastic Petri dishes with ASW without algae 30–45 min before the beginning of the experiment. $ZnCl_2$ solution was added to the individuals that were kept in 50 mL of ASW, so that Zn^{2+} ions final concentration was raised by 10–25 μM, and the animals were then investigated for different time intervals: 15 and 30 min, as well as 1, 2, 4, and 24 h. The studies were carried out at magnification from ×40 to ×400 under light microscopes Zeiss Stemi 305 (Germany) and Nikon Eclipse Ts2R (Japan) equipped with digital cameras.

RESULTS AND DISCUSSION

H. hongkongensis incubation for 2 h after the addition of 15–25 μM Zn^{2+} ions caused an alteration in the structure and shape of the body plate, which manifested itself in its thickening and the appearance of multiple “branched” structures resembling tentacles in some animals. These “tentacles” did not move, while the organism body moved forward. The animals retained the vortex motions of cell groups in the center of the plate and were able to move forward.

Further exposure of *H. hongkongensis* for 24 h with additional 15 μM Zn^{2+} ions in ASW caused an elevation in the share of organisms with the “branched” structure (68.1%) or partially decomposed animals (2.8%). Interestingly, the parts of the disintegrated individuals continued to move without coordination and independently of each other due to the beating of the cilia of the ventral epithelium cells (Fig. 1b, d). The addition of 25 μM zinc ions resulted in a gradual increase in the proportion of “branched” and destroyed animals to 77.1 and 16.3%, respectively (Fig. 2).

There are such mechanisms of zinc toxicity as copper displacement from intracellular proteins [Plum et al., 2010], superoxide generation [Ninsontia et al., 2016], and binding to thiol groups [Gazaryan et al., 2002]. Zn^{2+} ions can interact with Ca^{2+} binding sites on cadherin and calmodulin [Kuznetsov et al., 2021]. It is worth noting that with a gradual rising in the concentration of Zn^{2+} ions capable of replacing Ca^{2+} ions, the share of “branched” and decaying animals increased proportionally. Apparently, the described morphological alterations are due to initial disruption of signaling between individual

cells [Jékely, 2021; Senatore et al., 2017; Varoqueaux et al., 2018] and the consequent destruction of direct physical contacts between them [Ruthmann, Terwelp, 1979], since Ca^{2+} ions are involved in the transmission of signals into the cell in addition to cell adhesion [Berridge et al., 2003].

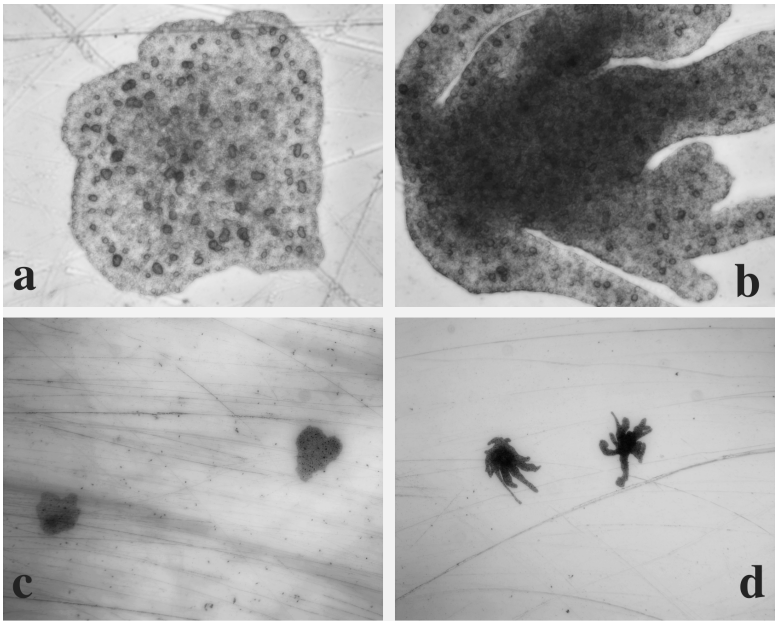

Fig. 1. *Hoilungia hongkongensis* morphological changes following a day of incubation with zinc ions: a, c, control without reagents; b, d, 20 μM Zn^{2+}. Magnification: a, b, 400 times; c, d, 40 times

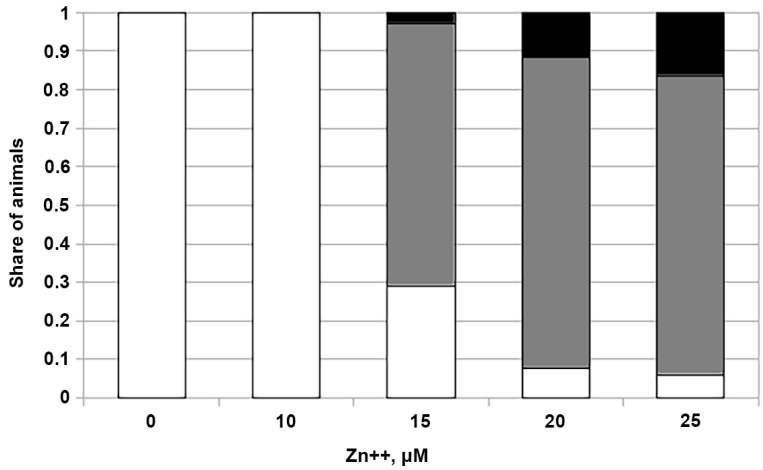

Fig. 2. Quantitative examination of abnormalities that occurred when *Hoilungia hongkongensis* was incubated with zinc ions at various doses for a day. Intact individuals are shown in white color; "branched" individuals are shown in gray; motionless, damaged, or completely destroyed individuals are shown in black. There were 245 animals used in the experiment

Let us pay attention to zinc toxicity for the freshwater sponge *Ephydatia fluviatilis* (Linnaeus, 1759) at a concentration exceeding 0.1 μM [John, Harrison, 1988]. This is comparable to data from our experiments on Placozoa organisms, as well as to data for two *Hydra* species, *Hydra vulgaris* Pallas, 1766 and *Hydra viridissima* Pallas, 1766, for which 96-h LD_{50} values are about 35 and 14 mM, respectively [Holdway et al., 2001]. As shown, the starlet sea anemone *Nematostella vectensis* Stephenson, 1935 activates the genes for early transcription factors Egr1, AP1, and NF-κB already an hour after exposure to Hg, Cu, Cd, and Zn ions. This is followed by the expression of stress response genes, including *Hsp*,

ABC, and *CYP* [Elran et al., 2014], which can compensate for the toxic effect of heavy metal ions. It is known that *Trichoplax* sp. H2, whose genome is well annotated [Kamm et al., 2018], contains orthologous proteins, such as Egr1 (RDD41957.1), NF-κB (RDD44621.1), and Hsp (RDD46759.1). Perhaps, a similar defense systems exist in *H. hongkongensis*.

Thus, experimental exposure to Zn^{2+} ions leads to a discoordination of amoeboid movement in *H. hongkongensis*, which is observed in the emergence of uncontrolled "tentacles." This is consistent with the results of experiments on *Trichoplax* sp. H2 [Kuznetsov et al., 2021]. Some areas of *H. hongkongensis* plate begin to move without coordination and independently of each other. Later, the animal body dissociates into separate cells, which may be the result of Zn^{2+} ions interference in the regulation of two fundamental processes by Ca^{2+} ions: 1) coordinating the joint cell functioning and 2) maintaining the integrity of the animal body structure.

This work was carried out within the framework of IBSS state research assignment "Investigation of mechanisms of controlling production processes in biotechnological complexes with the aim of developing scientific foundations for production of biologically active substances and technical products of marine genesis" (No. 121030300149-0).

Acknowledgement. The authors are grateful to Prof. A. Igamberdiev for valuable recommendations during the work, as well as Iu. Baiandina, A. Pirkova, E. Chelebieva, O. Krivenko, S. Kapranov, and V. Ryabushko for helpful advice in preparing the manuscript.

REFERENCES

1. Kuznetsov A. V., Vainer V. I., Volkova Yu. M., Tsygankova V. M., Bochko D. N., Mukhanov V. S. *Trichoplax* sp. H2 cultivation and regeneration from body fragments and dissociated cell aggregates: Outlook for genetic modification. *Morskoj biologicheskij zhurnal*, 2022, vol. 7, no. 3, pp. 60–79. (in Russ.). https://marine-biology.ru/mbj/article/view/353
2. Armon S., Bull M. S., Aranda-Diaz A., Prakash M. Ultrafast epithelial contractions provide insights into contraction speed limits and tissue integrity. *Proceedings of the National Academy of Sciences*, 2018, vol. 115, no. 44, pp. E10333–E10341. https://doi.org/10.1073/pnas.1802934115
3. Berridge M. J., Bootman M. D., Roderick H. L. Calcium signalling: Dynamics, homeostasis and remodelling. *Nature Reviews Molecular Cell Biology*, 2003, vol. 4, iss. 7, pp. 517–529. https://doi.org/10.1038/nrm1155
4. Dupont C. L., Yang S., Palenik B., Bourne P. E. Modern proteomes contain putative imprints of ancient shifts in trace metal geochemistry. *The Proceedings of the National Academy of Sciences*, 2006, vol. 103, no. 47, pp. 17822–17827. https://doi.org/10.1073/pnas.0605798103
5. Elran R., Raam M., Kraus R., Brekhman V., Sher N., Plaschkes I., Chalifa-Caspi V., Lotan T. Early and late response of *Nematostella vectensis* transcriptome to heavy metals. *Molecular Ecology*, 2014, vol. 23, iss. 19, pp. 4722–4736. https://doi.org/10.1111/mec.12891
6. Erwin D. H. Early metazoan life: Divergence, environment and ecology. *Philosophical Transactions of the Royal Society B. Biological Sciences*, 2015, vol. 370, iss. 1684, art. no. 20150036 (7 p.). https://doi.org/10.1098/rstb.2015.0036
7. Gazaryan I. G., Krasnikov B. F., Ashby G. A., Thorneley R. N., Kristal B. S., Brown A. M. Zinc is a potent inhibitor of thiol oxidoreductase activity and stimulates reactive oxygen species production by lipoamide dehydrogenase. *Journal of Biological Chemistry*, 2002, vol. 277, iss. 12, pp. 10064–10072. https://doi.org/10.1074/jbc.M108264200
8. Holdway D. A., Lok K., Semaan M. The acute and chronic toxicity of cadmium and zinc to two hydra species. *Environmental Toxicology*, 2001, vol. 16, iss. 6, pp. 557–565. https://doi.org/10.1002/tox.10017

9. Jékely G. The chemical brain hypothesis for the origin of nervous systems. *Philosophical Transactions of the Royal Society B. Biological Sciences*, 2021, vol. 376, iss. 1821, art. no. 20190761 (13 p.). https://doi.org/10.1098/rstb.2019.0761
10. John C. F., Harrison F. W. Copper and zinc toxicity in *Ephydatia fluviatilis* (Porifera: Spongillidae). *Transactions of the American Microscopical Society*, 1988, vol. 107, no. 1, pp. 67–78. https://doi.org/10.2307/3226409
11. Kamm K., Osigus H. J., Stadler P. F., DeSalle R., Schierwater B. *Trichoplax* genomes reveal profound admixture and suggest stable wild populations without bisexual reproduction. *Scientific Reports*, 2018, vol. 8, iss. 1, art. no. 11168 (11 p.). https://doi.org/10.1038/s41598-018-29400-y
12. Kuznetsov A. V., Vainer V. I., Volkova Yu. M., Kartashov L. E. Motility disorders and disintegration into separate cells of *Trichoplax* sp. H2 in the presence of Zn^{2+} ions and L-cysteine molecules: A systems approach. *BioSystems*, 2021, vol. 206, art. no. 104444 (11 p.). https://doi.org/10.1016/j.biosystems.2021.104444
13. Mayorova T. D., Smith C. L., Hammar K., Winters C. A., Pivovarova N. B., Aronova M. A., Leapman R. D., Reese T. S. Cells containing aragonite crystals mediate responses to gravity in *Trichoplax adhaerens* (Placozoa), an animal lacking neurons and synapses. *PLoS One*, 2018, vol. 13, iss. 1, art. no. e0190905 (20 p.). https://doi.org/10.1371/journal.pone.0190905
14. Ninsontia Ch., Phiboonchaiyanan P. P., Chanvorachote P. Zinc induces epithelial to mesenchymal transition in human lung cancer H460 cells via superoxide anion-dependent mechanism. *Cancer Cell International*, 2016, vol. 16, art. no. 48 (16 p.). https://doi.org/10.1186/s12935-016-0323-4
15. Plum L. M., Rink L., Haase H. The essential toxin: Impact of zinc on human health. *International Journal of Environmental Research and Public Health*, 2010, vol. 7, iss. 4, pp. 1342–1365. https://doi.org/10.3390/ijerph7041342
16. Robbins L. J., Lalonde S. V., Planavsky N. J., Partin C. A., Reinhard Ch. T., Kendall B., Scott C., Hardisty D. S., Gill B. C., Alessi D. S., Dupont Ch. L., Saito M. A., Crowe S. A., Poulton S. W., Bekker A., Lyons T. W., Konhauser K. O. Trace elements at the intersection of marine biological and geochemical evolution. *Earth-Science Reviews*, 2016, vol. 163, pp. 323–348. https://doi.org/10.1016/j.earscirev.2016.10.013
17. Rosenzweig A. C. Metallochaperones: Bind and deliver. *Chemistry & Biology*, 2002, vol. 9, iss. 6, pp. 673–677. https://doi.org/10.1016/s1074-5521(02)00156-4
18. Ruthmann A., Terwelp U. Disaggregation and reaggregation of cells of the primitive metazoan *Trichoplax adhaerens*. *Differentiation*, 1979, vol. 13, iss. 3, pp. 185–198. https://doi.org/10.1111/j.1432-0436.1979.tb01581.x
19. Senatore A., Reese T. S., Smith C. L. Neuropeptidergic integration of behavior in *Trichoplax adhaerens*, an animal without synapses. *Journal of Experimental Biology*, 2017, vol. 220, iss. 18, pp. 3381–3390. https://doi.org/10.1242/jeb.162396
20. Smith C. L., Varoqueaux F., Kittelmann M., Azzam R. N., Cooper B., Winters C. A., Eitel M., Fasshauer D., Reese T. S. Novel cell types, neurosecretory cells, and body plan of the early-diverging metazoan *Trichoplax adhaerens*. *Current Biology*, 2014, vol. 24, iss. 14, pp. 1565–1572. https://doi.org/10.1016/j.cub.2014.05.046
21. Varoqueaux F., Williams E. A., Grandemange S., Truscello L., Kamm K., Schierwater B., Jékely G., Fasshauer D. High cell diversity and complex peptidergic signaling underlie placozoan behavior. *Current Biology*, 2018, vol. 28, iss. 21, pp. 3495–3501. https://doi.org/10.1016/j.cub.2018.08.067
22. Zachara J. M., Kittrick J. A., Harsh J. B. The mechanism of Zn^{2+} adsorption on calcite. *Geochimica et Cosmochimica Acta*, 1988, vol. 52, iss. 9, pp. 2281–2291. https://doi.org/10.1016/0016-7037(88)90130-5

НАРУШЕНИЕ КООРДИНАЦИИ ДВИЖЕНИЙ *HOILUNGIA HONGKONGENSIS* (PLACOZOA) В ПРИСУТСТВИИ ИОНОВ Zn^{2+}

А. В. Кузнецов, Н. И. Бобко

ФГБУН ФИЦ «Институт биологии южных морей имени А. О. Ковалевского РАН»,
Севастополь, Российская Федерация
E-mail: *kuznet61@gmail.com*

Hoilungia hongkongensis принадлежит к типу пластинчатые (Placozoa) — простейшим многоклеточным организмам с динамическим планом строения тела. В поддержании целостности этих животных важную роль играют ионы кальция. В настоящей работе экспериментально изучено влияние ионов цинка на взаимодействие клеток *H. hongkongensis*. При увеличении концентрации ионов Zn^{2+} на 20–25 мкМ нарушается согласованность амёбоидного движения, что приводит к образованию «ветвистых» форм животного. Локомоторные реснитчатые клетки двигаются хаотично и независимо друг от друга. Эксперименты показали, что контактное взаимодействие клеток *H. hongkongensis* важно для скоординированных движений организма, в то время как ионы цинка могут конкурировать с ионами кальция, нарушая регуляцию и разрушая связь между клетками.

Ключевые слова: пластинчатые, локомоция, ионы кальция и цинка

1871
ИнБЮМ – IBSS

Морской биологический журнал
Marine Biological Journal
2023, vol. 8, no. 3, pp. 108–110
https://marine-biology.ru

UDC 581.526.323(262.5-751.2)

FLORISTIC FINDS IN THE COASTAL MARINE WATER AREA OF THE NATURE RESERVE "CAPE MARTYAN" (CRIMEA, BLACK SEA)

© 2023 **S. Ye. Sadogurskiy, T. V. Belich, and S. A. Sadogurskaya**

Nikitsky Botanical Gardens – National Scientific Center of RAS, Yalta, Russian Federation
E-mail: *ssadogurskij@yandex.ru*

Received by the Editor 27.07.2023; after reviewing 02.08.2023;
accepted for publication 04.08.2023; published online 21.09.2023.

Based on the samples of 2020 and 2023, three new species of marine macroalgae are indicated for the flora of the territorial-aquatic nature reserve "Cape Martyan," located on the Southern Coast of Crimea (SCC): *Punctaria latifolia* Grev., *Compsothamnion gracillimum* De Toni, and *Dasya hutchinsiae* Harv. (the last one is recorded for the Black Sea hydrobotanical area "SCC" for the first time). The list of macrophytes of the reserve now includes 163 species, or 37% of the total number of taxa known for the Black Sea. The obtained results expand the understanding of the level of natural phytodiversity of the reserve, hydrobotanical area, and the region as a whole.

Keywords: macrophytobenthos, floristic finds, nature reserve "Cape Martyan", Black Sea

The specially protected natural area (hereinafter SPNA) "Cape Martyan" is located on the Southern Coast of Crimea (SCC), which is washed by waters of the Black Sea hydrobotanical area (hereinafter HBA) "SCC" [Kalugina-Gutnik, 1975]. Since its creation (since 1973, as a state reserve; now, in the status of a natural park), hydrobotanical monitoring is carried out there. Its aim is to clarify understanding of the composition and structure of macrophytobenthos of the territorial-aquatic SPNA in connection with the optimization of environmental management within the boundaries of protected and recreational areas on the SCC.

Macrophytobenthos was sampled along two profiles in the depth range (h) of 0–8 m at a distance (l) of up to 200 m from the coast, off Cape Martyan (26.02.2020; 44°30′20.3″N, 34°14′40.4″E) and off Cape Montedor (22.06.2023; 44°30′14.7″N, 34°13′59.0″E), during solo dives in accordance to the generally accepted hydrobotanical technique [Kalugina-Gutnik, 1975]. Nomenclature, taxonomy, and general distribution of macrophytes are given according to [AlgaeBase, 2020]; ecological and floristic characteristics, according to [Kalugina-Gutnik, 1975]. In the samples, regionally rare macroalgal species were revealed that were not previously noted for the flora of the nature reserve.

Punctaria latifolia Greville, 1830 (Ectocarpales Bessey, 1907, Acinetosporaceae G. Hamel ex J. Feldmann, 1937). In the sublittoral zone near Cape Martyan; h = 3 m; l = 60…70 m. Epiphytic on thalli of *Cystoseira* s. l. representatives. Seasonal winter, wide-boreal, oligosaprobic, marine. General distribution: the Atlantic Ocean coast, including subpolar regions and islands; seas of the Mediterranean

and the Baltic Sea; the northern and southern Pacific Ocean. Off the coast of Crimea, it is recorded relatively rarely (7 localities in HBA No. 3, 6–8) in small abundance [Evstigneeva, Tankovskaya, 2010, 2015, 2018; Evstigneeva et al., 2015; Kostenko et al., 2004; Mironova, Pankeeva, 2021].

Compsothamnion gracillimum De Toni, 1903 (Ceramiales Nägeli, 1847, Wrangeliaceae J. Agardh, 1851). In the sublittoral zone near Cape Martyan; h = 8 m; l = 200 m. Epiphytic on leaves of *Zostera noltei* Hornemann, 1832. Annual, low-boreal, mesosaprobic, brackish-marine. General distribution: the Atlantic Ocean coast from Scandinavia to Morocco, including islands; seas of the Mediterranean and the Baltic Sea. Off the coast of Crimea, it is rare (3 localities in HBA No. 6–7) and is noted in small abundance [Kalugina-Gutnik, 1975; Kostenko et al., 2004].

Dasya hutchinsiae Harvey, 1833 (Ceramiales Nägeli, 1847, Delesseriaceae Bory, 1828). In the sublittoral zone near Cape Montedor; h = 4.5 m; l = 30 m. Epiphytic on thalli of *Cladostephus hirsutus* (Linnaeus) Boudouresque & M. Perret-Boudouresque ex Heesch et al., 2020 and *Cystoseira* s. l. Seasonal summer, low-boreal, oligosaprobic, marine. General distribution: the Atlantic Ocean coast, including islands; seas of the Mediterranean. Off the coast of Crimea, it is rare (3 localities in HBA No. 3, 6–7) and registered in small abundance [Evstigneeva, Tankovskaya, 2010; Kalugina-Gutnik, 1975]. For the HBA “SCC,” the species is indicated for the first time.

As a result, the flora of marine macrophytes of the SPNA “Cape Martyan” now includes 163 species, which is about 37% of the total number known for the Black Sea [Minicheva et al., 2014]. Obtained data expand the understanding of the level of natural phytodiversity of the SPNA, HBA “SCC,” and the region in general.

This work was carried out within the framework of NBG–NSC state research assignment No. 1023042800079-0-1.6.11;1.5.8.

REFERENCES

1. Evstigneeva I. K., Grintsov V. A., Lisitskaja E. V., Makarov M. V., Tankovskaya I. N. Biodiversity of macrophytes communities Kasachia Bay. *Byulleten’ Moskovskogo obshchestva ispytatelei prirody. Otdel biologicheskii*, 2015, vol. 120, iss. 6, pp. 51–64. (in Russ.)
2. Evstigneeva I. K., Tankovskaya I. N. Macrophytobenthos and macrophytoperiphython of reserve “Swan Islands” (Black Sea, Ukraine). *Algologia*, 2010, vol. 20, no. 2, pp. 176–191. (in Russ.)
3. Evstigneeva I. K., Tankovskaya I. N. Algocenoses of artificial and natural substrates in coastal zone of Feodosiya Bay (Black Sea). In: *100 Years of the T. I. Vyazemsky Karadag Scientific Station* : issue of scientific papers / A. V. Gaevskaya, A. L. Morozova (Eds). Simferopol : N.Orianda, 2015, pp. 493–506. (in Russ.)
4. Evstigneeva I. K., Tankovskaya I. N. Macrophytobenthos of the Batiliman seashore region (Black Sea, “Cape Ajja” reserve). *Vestnik Tverskogo gosudarstvennogo universiteta. Seriya: Biologiya i ekologiya*, 2018, no. 4, pp. 100–117. (in Russ.). https://doi.org/10.26456/vtbio31
5. Kalugina-Gutnik A. A. *Fitobentos Chernogo morya.* Kyiv : Naukova dumka, 1975, 248 p. (in Russ.). https://repository.marine-research.ru/handle/299011/5645
6. Kostenko N. S., Evstigneeva I. K., Dikii E. A. In: *Karadag. Gidrobiologicheskie issledovaniya* : sbornik nauchnykh trudov, posvyashchennyi 90-letiyu Karadagskoi nauchnoi stantsii imeni T. I. Vyazemskogo i 25-letiyu Karadagskogo prirodnogo zapovednika NAN Ukrainy / A. L. Morozova, V. F. Gnyubkin (Eds). Simferopol : SONAT, 2004, pp. 275–307. (in Russ.)
7. Mironova N. V., Pankeeva T. V. Spatial-temporal changes of macrophytobenthos in the coastal zone of the reserve “Karan’sky” (Sevastopol city,

Black Sea). *Povolzhskii ekologicheskii zhurnal*, 2021, no. 1, pp. 47–63. (in Russ.). https://doi.org/10.35885/1684-7318-2021-1-47-63

8. *AlgaeBase*. World-wide electronic publication, National University of Ireland, Galway / M. D. Guiry, G. M. Guiry (Eds) : [site], 2020. URL: http://www.algaebase.org [accessed: 26.07.2023].
9. Minicheva G., Afanasyev D., Kurakin A. *Black Sea Monitoring Guidelines. Macrophytobenthos*. [S. l. : s. n.], 2014, 92 p. URL: https://emblasproject.org/wp-content/uploads/2013/12/Manual_macrophytes_EMBLAS_ann.pdf [accessed: 26.07.2023].

ФЛОРИСТИЧЕСКИЕ НАХОДКИ В ПРИБРЕЖНОЙ АКВАТОРИИ ЗАПОВЕДНИКА «МЫС МАРТЬЯН» (КРЫМ, ЧЁРНОЕ МОРЕ)

С. Е. Садогурский, Т. В. Белич, С. А. Садогурская

ФГБУН «Никитский ботанический сад — Национальный научный центр РАН»,
Ялта, Российская Федерация
E-mail: *ssadogurskij@yandex.ru*

Для флоры территориально-аквального заповедника «Мыс Мартьян», расположенного на Южном берегу Крыма (ЮБК), по материалам 2020 и 2023 гг. указаны три новых вида морских макроводорослей: *Punctaria latifolia* Grev., *Compsothamnion gracillimum* De Toni и *Dasya hutchinsiae* Harv. (последний — впервые для гидроботанического района Чёрного моря «ЮБК»). Список макрофитов заповедника теперь включает 163 вида, или около 37 % общего количества, известного для Чёрного моря. Полученные результаты расширяют представления об уровне природного фиторазнообразия заповедника, гидроботанического района и региона в целом.

Ключевые слова: макрофитобентос, флористические находки, заповедник «Мыс Мартьян», Чёрное море

1871
ИнБЮМ – IBSS

Морской биологический журнал
Marine Biological Journal
2023, vol. 8, no. 3, pp. 111–112
https://marine-biology.ru

CRHONICLE AND INFORMATION

IN MEMORIAM: ALEXANDER TRAPEZNIKOV (29.01.1951 – 29.06.2023)

On 29 June, 2023, the outstanding radioecologist Alexander Trapeznikov passed away – D. Sc., Professor, head of the Continental Radioecology Department at the Institute of Plant and Animal Ecology of the Ural Branch of the Russian Academy of Sciences (IPAE UB RAS) in Yekaterinburg, and head of the Biophysical Station in Zarechny town, Sverdlovsk Oblast.

A. Trapeznikov was born on 29 January, 1951, in Perm. In 1973, he graduated from the Faculty of Biology of the Perm State University. Since 1974, he worked at the Biophysical Station of IPAE UB RAS, and since 1993, he headed this station. In 1990, he defended his PhD thesis *Accumulation, Distribution, and Migration of ^{60}Co in Freshwater Ecosystem Components*; in 2001, he defended his dissertation *Radioecology of Freshwater Ecosystems (on the Example of Ural)*. The main areas of his 50-year scientific activity were as follows: radioecology of freshwater ecosystems exposed to nuclear fuel cycle enterprises; study of ^{3}H, ^{60}Co, ^{90}Sr, ^{137}Cs, and ^{239,240}Pu migration in river and lake ecosystems and reservoirs; and construction of migration models of technogenic radionuclides in large river ecosystems. The works authored by Alexander Trapeznikov are of great fundamental and applied significance for radioecology. His scientific, organizational, and educational activities made the Continental Radioecology Department of IPAE UB RAS in Yekaterinburg and the Biophysical Station in Zarechny a recognized international scientific radioecological center.

A. Trapeznikov became the author of more than 460 scientific publications, *inter alia* 14 monographs and 10 patents. Out of his works, fundamental monographs are worth noting: *Freshwater Radioecology* (2012) and a 3-volume *Radioecological Monitoring of Freshwater Ecosystems* (2014, 2016, and 2018).

Alexander Trapeznikov was a member of the Bureau of RAS Scientific Councils on Radiobiology. He was awarded the title of Honored Ecologist of the Russian Federation. Moreover, he was awarded the medal in the name of N. Timofeeff-Ressovsky (UB RAS), the prize of the I International Competition of Scientific Papers in Radioecology named after V. Klechkovsky, and the medal named after academician E. Avrorin (UB RAS).

For many years, A. Trapeznikov served on the editorial board of *Marine Biological Journal*.

The IBSS Radiation and Chemical Biology Department successfully and fruitfully cooperated with the Continental Radioecology Department headed by Alexander Trapeznikov. Within the framework of the IAEA project and the RFBR grant, joint studies were carried out, and internships of young researchers were organized. The results of these investigations were reported at international conferences and seminars and reflected in collective scientific publications. Colleagues will always remember A. Trapeznikov not only as an outstanding scientist, a talented organizer, and a great leader, but also as a kind-hearted, sincere, and understanding person and a wonderful family man.

IBSS staff deeply mourns and expresses its sincere condolences and support to colleagues and relatives of Alexander Trapeznikov.

Colleagues from the IBSS Radiation and Chemical Biology Department

ПАМЯТИ АЛЕКСАНДРА ВИКТОРОВИЧА ТРАПЕЗНИКОВА (29.01.1951 – 29.06.2023)

29 июня 2023 г. ушёл из жизни выдающийся радиоэколог Александр Викторович Трапезников — доктор биологических наук, профессор, лауреат медали имени академика Е. Н. Аврорина УрО РАН. А. В. Трапезников — автор более чем 460 научных работ, среди которых фундаментальная монография «Радиоэкологический мониторинг пресноводных экосистем» в трёх томах.

ISSN 2499-9768
23003
9 772499 976005 >

Вниманию читателей!

Институт биологии южных морей имени А. О. Ковалевского РАН, Зоологический институт РАН

издают научный журнал

Морской биологический журнал
Marine Biological Journal

- МБЖ — периодическое издание открытого доступа. Подаваемые материалы проходят независимое двойное слепое рецензирование. Журнал публикует обзорные и оригинальные научные статьи, краткие сообщения и заметки, содержащие новые данные теоретических и экспериментальных исследований в области морской биологии, материалы по разнообразию морских организмов, их популяций и сообществ, закономерностям распределения живых организмов в Мировом океане, результаты комплексного изучения морских и океанических экосистем, антропогенного воздействия на морские организмы и экосистемы.
- Целевая аудитория: биологи, экологи, биофизики, гидро- и радиобиологи, океанологи, географы, учёные других смежных специальностей, аспиранты и студенты соответствующих научных и отраслевых профилей.
- Статьи публикуются на русском и английском языках.
- Периодичность — четыре раза в год.
- Подписной индекс в каталоге «Пресса России» — Е38872. Цена свободная.

Заказать журнал

можно в научно-информационном отделе ИнБЮМ. Адрес: ФГБУН ФИЦ «Институт биологии южных морей имени А. О. Ковалевского РАН», пр-т Нахимова, 2, г. Севастополь, 299011, Российская Федерация.
Тел.: +7 8692 54-06-49.
E-mail: *mbj@imbr-ras.ru*.

A. O. Kovalevsky Institute of Biology of the Southern Seas of RAS, Zoological Institute of RAS

publish scientific journal

Морской биологический журнал
Marine Biological Journal

- MBJ is an open access, peer reviewed (double-blind) journal. The journal publishes original articles as well as reviews and brief reports and notes focused on new data of theoretical and experimental research in the fields of marine biology, diversity of marine organisms and their populations and communities, patterns of distribution of animals and plants in the World Ocean, the results of a comprehensive studies of marine and oceanic ecosystems, anthropogenic impact on marine organisms and on the ecosystems.
- Intended audience: biologists, ecologists, biophysicists, hydrobiologists, radiobiologists, oceanologists, geographers, scientists of other related specialties, graduate students, and students of relevant scientific profiles.
- The articles are published in Russian and English.
- The journal is published four times a year.
- The subscription index in the “Russian Press” catalogue is E38872. The price is free.

You may order the journal

in the scientific information department of IBSS. Address: A. O. Kovalevsky Institute of Biology of the Southern Seas of RAS, 2 Nakhimov avenue, Sevastopol, 299011, Russian Federation.
Tel.: +7 8692 54-06-49.
E-mail: *mbj@imbr-ras.ru*.